APPENDIX A

BACKGROUND WATER QUALITY IN THE ALLUVIAL MATERIALS AT THE QMC FACILITY, AMBROSIA LAKE, NEW MEXICO

January 2001

Prepared for
Rio Algom Mining Company

Prepared by

Maxim Technologies, Inc.
10601 Lomas NE
Albuquerque, New Mexico 87112

BACKGROUND WATER QUALITY IN THE ALLUVIAL MATERIALS AT THE QMC FACILITY, AMBROSIA LAKE, NEW MEXICO

Table of Contents

List of Tables

List of Figures

BACKGROUND WATER QUALITY IN THE ALLUVIAL MATERIALS AT THE QMC FACILITY, AMBROSIA LAKE, NEW MEXICO

1. INTRODUCTION

This document provides an evaluation of background water quality in the alluvial materials at the QMC Mill Facility in Ambrosia Lake, New Mexico (QMC Facility). According to U.S. Nuclear Regulatory Commission (NRC) Guidance (1996), background water quality at sites regulated under the Uranium Mill Tailings Radiation Control Act is defined as the quality of groundwater that would exist if QMC's uranium-milling activities had not occurred. Sources other than QMC's milling activities have caused widespread ambient groundwater contamination that is unrelated to, but inseparable from impacts related to milling at the QMC Facility. Therefore, these ambient conditions are defined as background for the purposes of this report.

Data on background groundwater quality as established by the Uranium Recovery Field Office in License Condition 34 is limited to one monitor well in each geologic unit at the facility. According to NRC Materials License SUA-1473, alluvial background groundwater quality for this facility is recognized in Monitor Well 5-03. It is theorized that this well was chosen as background because it had the lowest concentrations of mill derived constituents.

Spatial variability in groundwater quality is commonly much greater than temporal variability seen in groundwater collected from one monitor well. Therefore, it is unlikely that this one background monitor well in the Alluvium adequately represents the true variability of alluvial groundwater at the QMC Facility. Concentrations of constituents reported in Monitor Well 5-03 do not reflect all of the sources of constituents in the vicinity of Ambrosia Lake (Figure 1). Additional sources of molybdenum, nickel, lead, selenium, radium thorium and uranium, which are unrelated to milling impacts, include the following:

- Mine Pumping and Discharge

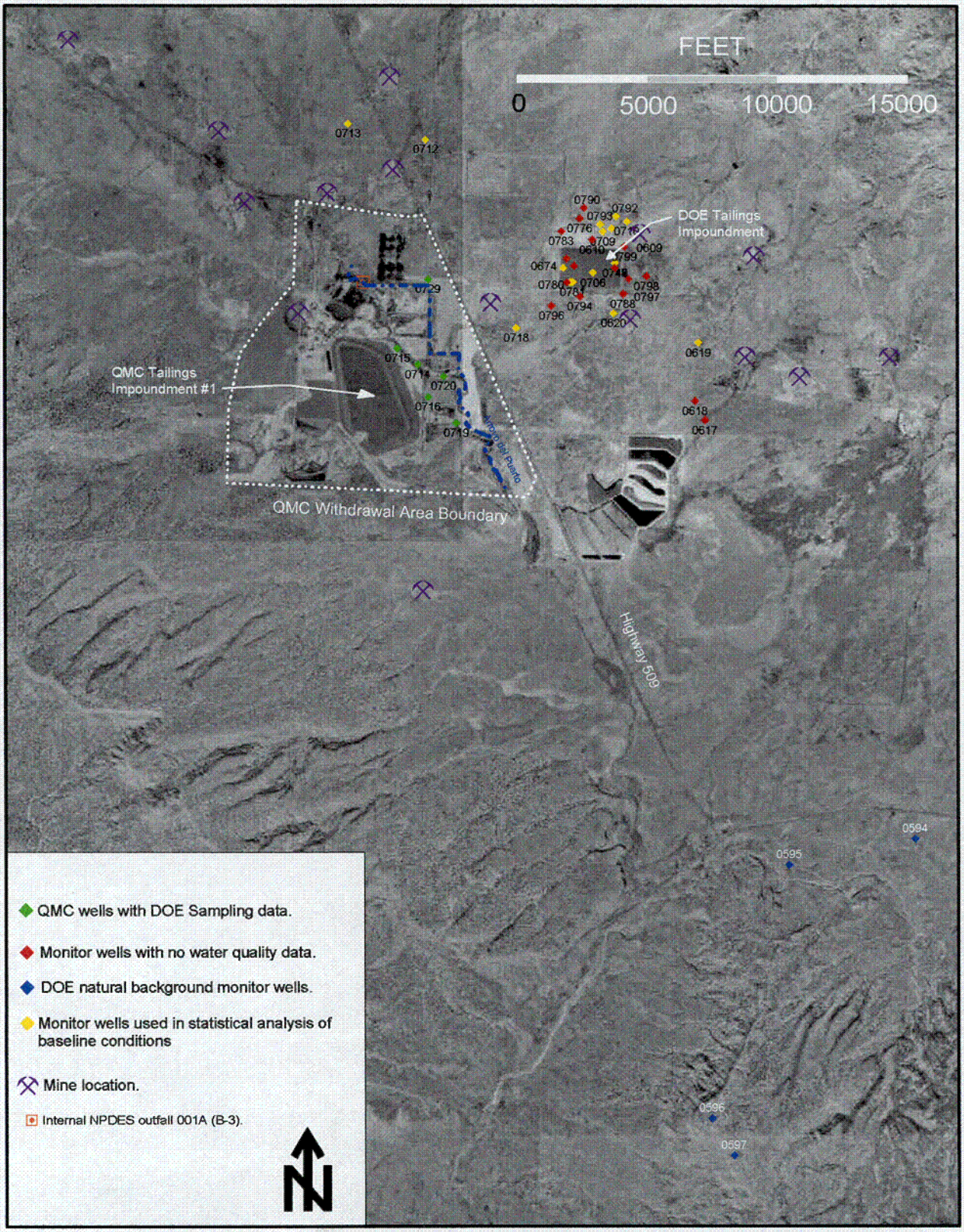

Monitor Wells Included in DOE Data from the DOE Site, Locations of Mines Near the QMC Site, and Location of Internal NPDES Outfall 001A (B-3)
FIGURE 1

C01

- Seepage from the nearby UMTRA Title I Tailings Facility (DOE Facility)
- Runoff and Erosion from Abandoned Mine Spoils and Ore Piles.

The influence of these and any other sources of constituents must be evaluated to determine realistic cleanup standards that consider the range of background conditions. The current groundwater cleanup standards for the QMC facility, based on water quality from the single Monitor Well 5-03, are not achievable due to high ambient concentrations of constituents at the facility. The wide variety of sources and hydrogeochemical processes that are known to have operated in the Ambrosia Lake Valley have resulted in higher levels of uranium ore-related constituents in groundwater than are observed in Well 5-03.

1.1. Mine Pumping and Discharge

The alluvial materials were unsaturated before mining began in the Ambrosia Lake Valley (Bostick, 1985). Mine-dewatering discharges from underlying geologic units created saturated conditions during the development of numerous mines in the vicinity. The quality of mine discharge water is dependent on site-specific mine conditions, and mining processes. Mine discharge has not, historically, been regulated by the NRC and has been considered unrelated to regulated milling activities. As of December, 2000, this position has been changed to consider all discharges related to licensed activities as byproduct material based on NRC Staff interpretation.

Current mine discharge water typically exceeds Alluvial Groundwater Protection Standards (GPS) for uranium, molybdenum, and selenium (Table 1). It is important to note that while mine discharge water is the primary source of groundwater in Monitor Well 5-03, low concentrations of constituents measured in groundwater at that location are likely due to the natural attenuation capacity of the alluvial materials as mine water infiltrates and travels through the Alluvium. The natural attenuation capacity of the alluvial materials removes constituents from groundwater along its flowpath, resulting in low concentrations of constituents in alluvial groundwater in areas away from constituent sources.

Table 1. Comparison of treated mine water discharge (B-3) with current Alluvial Groundwater Protection Standards.			
	B-3 Ave	B-3 Max	GPS (NRC)
Molybdenum (mg/L)	0.23	0.29	0.06
Nickel (mg/L)			0.06
Lead-210 (pCi/L)			4.9
Radium-226+228 (pCi/L)	2.84	12	5
Selenium (mg/L)	0.14	0.24	0.05
Sulfate (mg/L)	1325	1750	
TDS (mg/L)	2940	3710	
Thorium-230 (pCi/L)			3.1
Natural Uranium (mg/L)	1.44	2.6	0.06

B-3 = Sampling point on Arroyo del Puerto adjacent to QMC Internal NPDES Outfall 001A.

mg/L = milligrams per Liter.

pCi/L = picocuries per Liter

1.2. Seepage from the DOE Facility

Seepage from the nearby DOE Facility (Figure 2) is unrelated to milling activity at the QMC Facility, although it does contribute to saturation and constituent mass in the Alluvium within the confines of QMC's land withdrawal area. Figure 2 shows contours of uranium concentrations using 1986 DOE data from the DOE Facility. The 1986 data were used as they represent the most complete sampling event in the DOE database. QMC uranium data are also contoured at the same contour interval and for the same time period. These contour plots strongly suggest that, at least until 1986, the DOE Facility seepage was the primary contributor to uranium concentrations in alluvial groundwater on the east side of Highway 509.

Flow directions in the Alluvium are toward and along a paleochannel incised into older bedrock units. The axis of the paleochannel is roughly parallel to the current axis of the Arroyo del Puerto (Figure 3) but is located to the east of that feature, near the current location of Highway 509. QMC has employed a hydrologic barrier using the redirected waterway between tailings seepage and the paleochannel since mining began, and a seepage collection system since 1983. Any flow from the QMC Facility is first to the

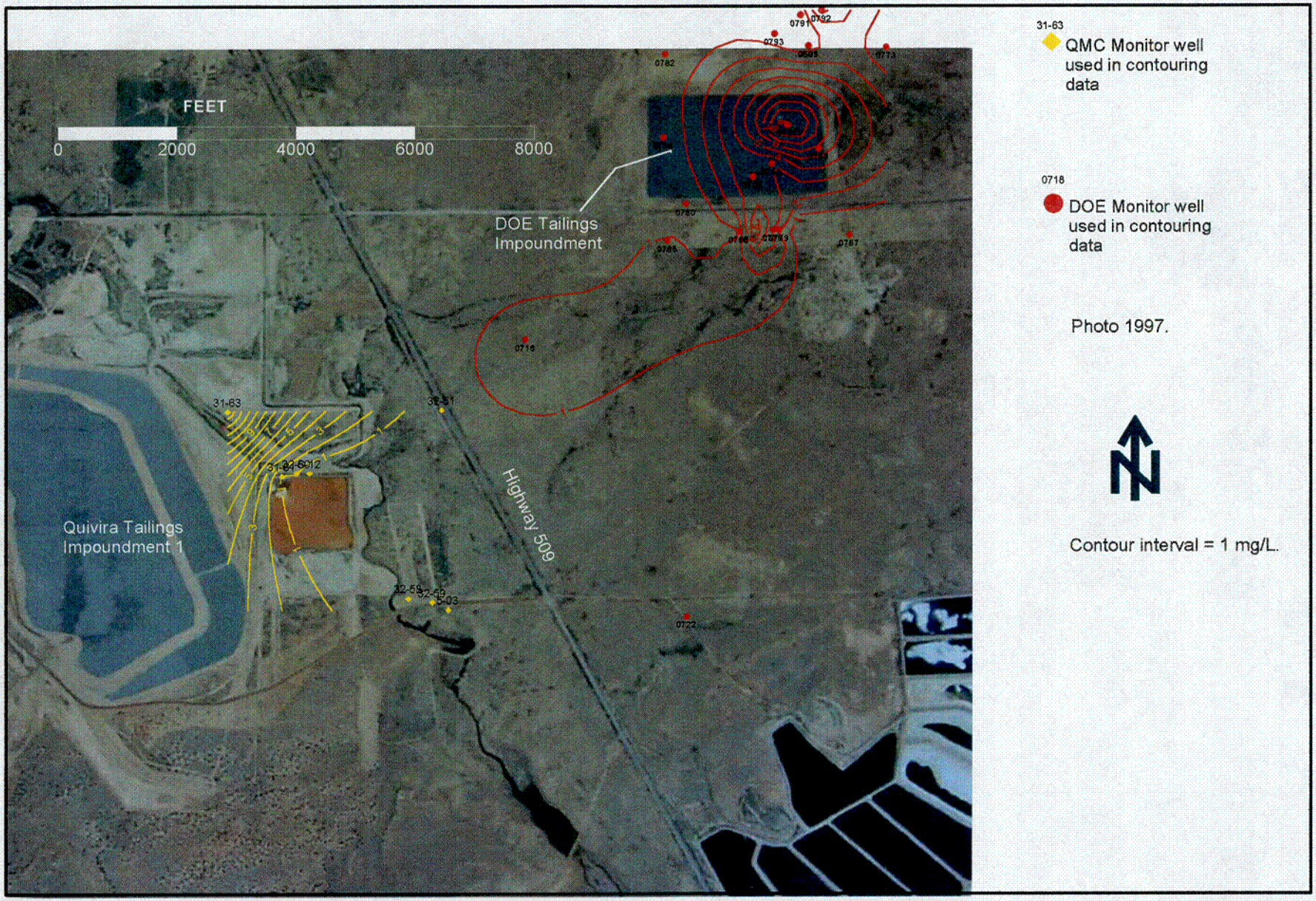

Uranium Concentrations Using 1986 QMC data and 1986 DOE data.
FIGURE 2

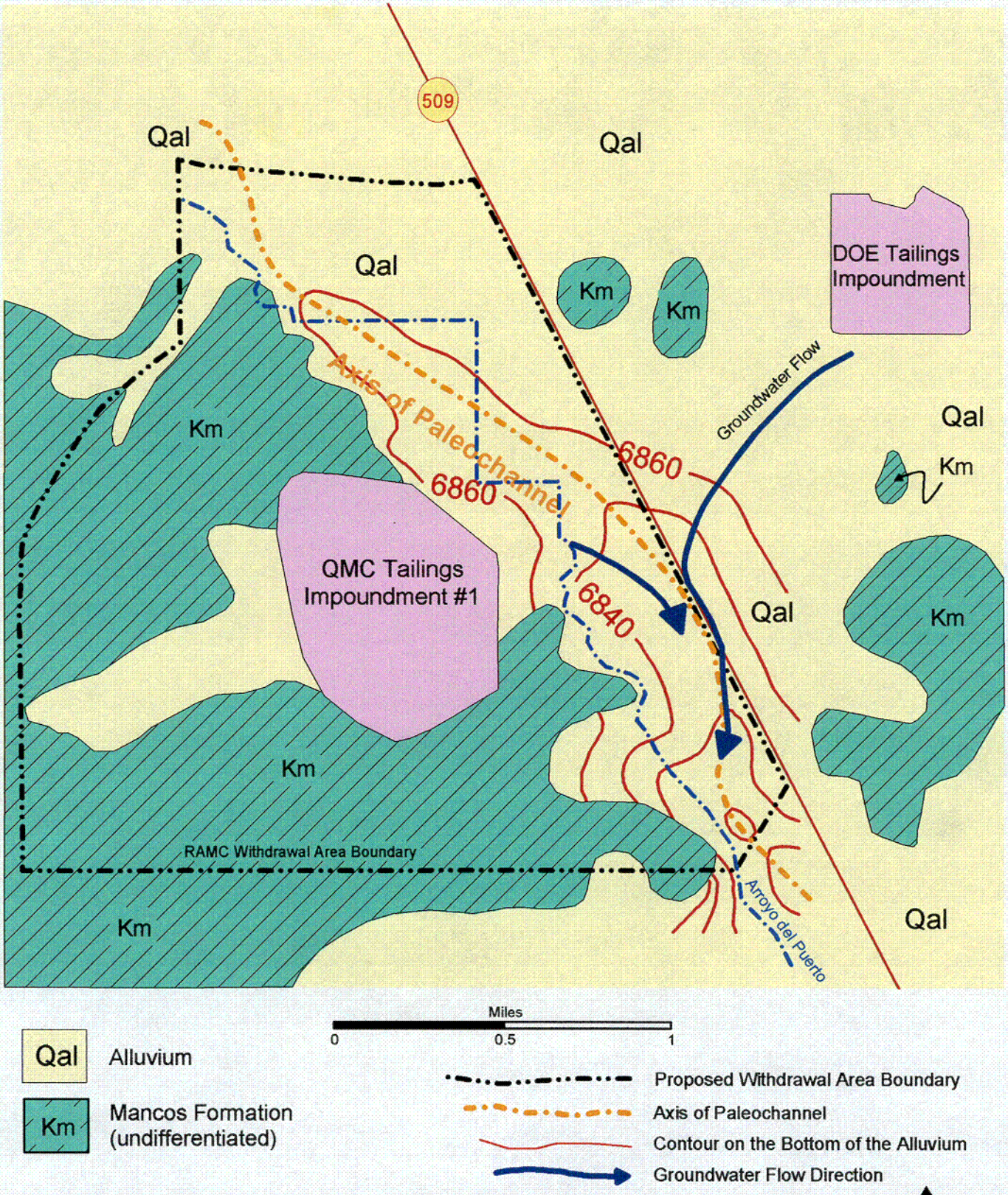

Figure 3. Simplified geologic map of the QMC Site showing contours on the bottom of the alluvium and the trace of the axis of the paleochannel.

C03

east toward the paleochannel and then south along the axis of the paleochannel. Flow from the DOE Facility, which has never employed a barrier or seepage collection system, is west toward the paleochannel, where it joins with flow from the QMC Facility and moves south into the QMC land withdrawal area.

The effect of seepage from the DOE Facility can be clearly identified in analyses of groundwater from monitor wells on the eastern side of the QMC Facility. Figure 4 shows contours of TDS/chloride ratios in groundwater from monitor wells completed in the alluvium between Tailings Impoundment #1 and the DOE Facility Tailings Impoundment. The TDS/chloride ratio found in seepage from a uranium mill tailings impoundment is related to the milling process, and can serve to fingerprint the source of the seepage. The milling at the QMC Facility was an acid leach process that used sodium chlorate as an oxidizer, resulting in high chloride concentrations, while milling at the DOE Facility was an alkaline leach process (DOE, 1985) that did not use sodium chlorate.

Groundwater collected near to the tailing impoundment at the QMC Facility has a TDS/chloride ratio between 5 and 15 (Figure 4). As seepage from Tailings Impoundment #1 moves along its flowpath, the natural geochemical attenuation capacity of alluvial materials removes various constituents from solution, thus lowering the TDS of resulting groundwater. In contrast, chloride is a conservative constituent that typically does not react with alluvial material. Therefore, its concentration in groundwater would be expected to remain constant along a flowpath.

If groundwater TDS/chloride ratios in the alluvial material were only affected by seepage from Tailings Impoundment #1, the ratio could be expected to decrease from the 5-15 range as groundwater moves away from the impoundment. This is because the numerator (TDS) would be constantly getting smaller through natural geochemical processes, while the denominator (chloride) remains the same. Mine discharge water would have little effect on the ratio because it has both low TDS and low chloride relative to tailings seepage, so that it would dilute both equally. However, analytical data indicate that TDS/chloride ratios *increase* dramatically to the east away from Tailings Impoundment #1 (Figure 4), indicating another source of water for the samples characterized by the elevated TDS/chloride ratios in the eastern portion of the facility. These TDS/chloride

Contours of Total Dissolved Solids (TDS)/Chloride Ratios in Groundwater from QMC Site Monitor Wells Completed in the Alluvium.
FIGURE 4

C04

ratios are consistent with alkaline leach milling processes such as those employed at the DOE Facility (DOE, 1985).

1.3. Runoff and Erosion from Mine Spoils and Ore Piles

Figure 1 shows numerous mines in locations that drain to Arroyo del Puerto in the Ambrosia Lake Valley. QMC has documented one incident in 1997 when a storm mobilized stockpiled uranium ore and spoils at the Coppin Mine, directly south of the QMC Facility (QMC, 1997). Storm runoff transported this material to the vicinity of stock ponds north of the QMC NPDES Outfall, resulting in a discharge with elevated levels of uranium and selenium at the NPDES Outfall.

While this is the only documented incident, it is likely that mining related sediments have been transported from similar sources to Arroyo Del Puerto in the past. Such sources undoubtedly contribute constituents to surface water during storm events and to groundwater through infiltration. There is also a potential to concentrate mining related constituents by evaporation of standing water in the wake of storm events. These residual ponds would be an extended source of infiltration to groundwater.

2. BACKGROUND EVALUATION METHODS

2.1. Mine Pumping and Discharge Data

Water from mine pumping is discharged to Arroyo del Puerto through NPDES internal outfall 001A. Prior to discharge, the mine water is treated to remove uranium and radium to meet NPDES discharge limits. Samples are taken from Arroyo del Puerto at monitoring location B-3 located at the 001A outfall (Figure 1). Data collected between March 1994 and June 2000 were used for this evaluation of the effects of mine pumping on background groundwater quality.

Constituents measured in the discharge water include pH, arsenic, chloride, molybdenum, selenium, TDS, sulfate, radium-226 (dissolved), radium-226 (total), and uranium (total). Molybdenum, selenium, radium-226 (total), and uranium (total) have GPS in the

Alluvium. Therefore, these parameters were evaluated statistically to distinguish between the constituent sources.

2.2. DOE Facility Data

QMC requested DOE groundwater data from the DOE Facility and received groundwater quality data collected between 1980 and 1996 from 44 alluvial monitor wells. Figure 1 shows the monitor wells that exist in the DOE database.

Monitor wells 0594, 0595, 0596, and 0597 are located four to six miles south of both QMC and the DOE Facility (Figure 1). These wells are so far off gradient that they could not be impacted by constituents from either the DOE Facility or the QMC facility and were likely sampled by the DOE to provide natural background in the Ambrosia Lake area. These wells have been evaluated separately from the other DOE wells and are discussed in the section on statistical analysis. They provide a useful comparison for Well 5-03.

Some monitor wells in the DOE database had no water quality data associated with them. These wells are shown in red on Figure 1. Some monitor wells in the DOE database are QMC wells that the DOE had sampled (shown in green on Figure 1). These alluvial wells are located across the paleochannel beneath the Alluvium from the DOE Facility and, therefore are unlikely to represent seepage from the DOE Facility. Data from all these wells are not included in the statistical analysis of DOE Alluvial wells.

Monitor wells that were used in the statistical evaluation of DOE Alluvial data are shown in Table 2 and in yellow on Figure 1. Also included in Table 2 are the number of sampling events completed for each well, and the years during which sampling occurred. Most wells have only one complete set of data available, and the bulk of those sampling events occurred in the early 1980's. Only four monitor wells have more than five sampling events worth of data available, and those were all located immediately adjacent to the DOE tailings impoundment. These wells typically have data available for the years between 1986 and 1996. In order to obtain a broad view of groundwater quality, and ensure a conservative estimate of background values, all data shown in Table 2 was used.

This approach results in lower estimates of background water concentrations contributed by the DOE Facility than an approach using only those wells adjacent to the tailings impoundment.

Table 2. Information for monitor wells used in the statistical evaluation of DOE Alluvial data, the number of sampling rounds available, and the years during which sampling occurred.

Monitor Well ID	Dates Sampled	Sampling Rounds Available
594	1980	1
595	1981	1
596	1982	1
597	1982	1
609	1985-86	2
619	1985	1
620	1985-91	7
650	1986-87	2
674	1989-96	8
706	1982-87	4
709	1982	1
710	1982	1
712	1980	1
713	1980	1
718	1980-86	3
747	1985	1
748	1986	1
749	1986	1
780	1985-87	3
781	1985	1
792	1986-96	8
793	1986-96	10

2.3. Runoff and Erosion from Abandoned Mine Spoils and Ore Piles Data

The contribution of runoff and erosion from abandoned mine spoils and ore piles to groundwater quality is difficult to quantify because it is widespread and variable, depending upon pile location and local geology. In an effort to qualitatively describe this source, samples of surface soils were collected in November 2000 by Daniel W. Erskine, Ph.D. of Maxim Technologies, Inc., from three mine sites located in the vicinity of the

QMC Facility, which are not owned by QMC. These included the Homestake New Mexico Partners Mine directly across State Highway 509 from QMC Offices; the Section 27 Mine approximately one mile east of the Homestake Mine; and the Coppin Mine, approximately one mile south of the QMC Tailings Impoundment. As mentioned earlier, material from the Coppin Mine was transported to stock ponds north of the QMC NPDES Outfall during a storm runoff event, causing a discharge at the NPDES Outfall (QMC, 1997).

2.4. Sampling Methodology

Two samples were collected by hand from the top four inches of soil at visible ore or waste piles at each site with the exception of the Homestake Mine site. At the Homestake Mine site, no piles were visible, so samples were taken from near the center of the graded area. Samples were sent to ACZ Analytical Laboratories in Steamboat Springs Colorado for SPLP extraction by EPA Method 1312 and analysis of the leachate for lead, molybdenum, nickel, selenium, thorium, uranium, and radium-226. The SPLP test is appropriate for prediction of potential metals removal from mining overburden (EPA, 1999).

One sample from the Homestake Mine site and one sample from the Section 27 Mine were sent back unanalyzed because they exceeded the Laboratory Radioactivity License (600 μR/hr and 2100 μR/hr respectively). Summary statistics for the remaining four samples are presented in the section on statistical analysis.

2.5. Treatment of Below Detection Limit and Negative Radionuclide Values

Some constituents in the data set include a fraction of concentrations below method detection limits. The calculation of summary statistics for constituents which include below detection limit values was performed by substituting the below detection limit value with one-half the detection limit.

Due to the random nature of radioactive decay, low activity samples may have a decay rate that is lower than the decay rate determined for ambient background. In this case, a negative activity is reported. Calculation of summary statistics for constituents that include negative values was performed by substituting a value of 0.1 for the negative values.

Substitution for negative values was necessary to avoid divide-by-zero errors in subsequent calculations and to minimize the influence of these values on standard deviation calculations when examining log normal distributions. Large standard deviations in lognormal data lead to high upper tolerance limit values for a data set. Therefore, substitution of 0.1, rather than 0.01 or 0.001, for negative values leads to lower, more conservative estimates of constituents in groundwater from sources that QMC does not control.

2.6. Distribution Analysis

Most statistical tests assume that data represent a normal distribution. However, EPA Guidance (1992) suggests that a lognormal distribution is a more appropriate default statistical model for most groundwater data (EPA, 1992). It is important to identify the distribution of the data because data that do not fit assumptions made in designing statistical operations can lead to false conclusions.

Therefore, following EPA guidance for statistical analysis of groundwater monitoring data (EPA, 1992), data sets represented herein were first tested for Lognormality and then, if the assumption of Lognormality failed, tested for Normality. Data were tested using both Coefficient of Skewness and the Shapiro-Wilk Tests of Normality. Skewness Coefficients of less than one are consistent with assumptions of Normality. In addition, if the Shapiro-Wilk statistic (W) is less than the 5 percent critical value for the sample size, the assumption of Normality can be rejected. Data that do not meet the assumptions of Normality or Lognormality are evaluated using non-parametric statistics.

Attachment A shows histograms for each constituent, produced using the software program *Statistica* (manufactured by Statsoft). Also shown in each figure in Attachment

A are the Skewness Coefficient, the W for each constituent, and the decision to either accept or reject the hypothesis that data are normally distributed.

3. STATISTICAL ANALYSIS

Data from DOE natural background monitor wells and the results of SPLP leaching of mine spoil and ore pile samples are presented in Tables 3 and 4, respectively. These data help to provide a qualitative understanding of these specific source terms and their resultant impact to groundwater. DOE natural background data indicate naturally occurring levels of molybdenum and uranium that exceed QMC's GPS (Table 3). A quantitative assessment of constituents contributed to groundwater from runoff from abandoned mine spoils and ore piles may not even be possible due to the large number of confounding variables affecting groundwater concentrations. However, metal mobility was evaluated using the EPA Method 1312 Synthetic Precipitation Leachability Procedure (SPLP). The SPLP test is appropriate for prediction of potential metals removal from mining overburden (US EPA, 1999) and data from Table 4 indicate potential mobility of molybdenum, selenium, thorium, uranium, and radium.

Table 3. Data from DOE natural background monitor wells.

Location ID	Date	Molybdenum (mg/L)	Selenium (mg/L)	Uranium (mg/L)
0594	Jun-80	0.159	0.022	0.178
	Jul-81	-	-	0.22
0595	Jul-81	0.155	0.028	-
0596	Jan-82	0.01	0.005	-
0597	Jan-82	0.012	0.005	-

Table 4. Results of EPA Method 1312, Synthetic Precipitation Leaching Procedure on mine spoil and ore pile soil samples.

Location ID	Lead (mg/L)	Molyb-denum (mg/L)	Nickel (mg/L)	Selenium (mg/L)	Thorium (mg/L)	Uranium (mg/L)	Radium-226 (pCi/L)
Q109001	0.02 U	0.19	0.005 U	0.018	0.0002	0.143	7.9
Q109003	0.02 U	0.16	0.005 U	0.015	0.00005 U	0.219	52
Q109005	0.02 U	0.005 U	0.005 U	0.027	0.00005 U	0.0137	13
Q109006	0.02 U	0.005 U	0.005 U	0.002	0.0002	0.106	4.2
MIN	0.02 U	0.005 U	0.005 U	0.002	0.00005 U	0.0137	4.2
MEAN	0.02 U	0.09	0.005 U	0.0155	0.000125	0.120425	19.275
MAX	0.02 U	0.19	0.005 U	0.027	0.0002	0.219	52

U = Analyte was analysed for but not detected at the applicible Method Detection Limit (MDL). The calculation of summary statistics for constituents which include below detection limit values was performed by substituting the MDL with one-half the detection limit.

mg/L = milligrams per Liter.

pCi/L = picocuries per Liter.

Descriptive statistics were calculated for mine water samples from the B-3 sampling point on Arroyo del Puerto and for DOE data from the DOE Facility. Mine discharge represents a higher volume of water than DOE Facility seepage, but DOE Facility seepage is just as likely as QMC Tailings seepage to contribute constituents to the paleochannel in the Alluvium. Therefore, DOE Facility seepage is just as likely to contribute constituents to groundwater at QMC's point of exposure (Figure 3).

Table 5 contains descriptive statistics and whether or not the assumption of Normality or Lognormality could be rejected for each constituent of mine water (B-3) data. Table 5 also contains the calculated 95 percent upper tolerance intervals (UTLs) for each constituent. EPA (1992) recommends that a UTL be constructed on background data when comparing a compliance well to background concentrations. If the concentration in the compliance well exceeds the background UTL, then contamination is deemed to be

present in the compliance well. The UTL is the upper end of a tolerance interval that contains 95 percent of all background values and therefore represents background for the QMC Facility. Table 6 presents information similar to that provided in Table 5 for each constituent of DOE Facility data.

Table 5. Descriptive statistics and 95% Upper Tolerance Intervals for Mine Water (B-3) data.

	*n	Mean	Std Dev	Min	Median	Max	**UTL	Normality Rejected
Mo (mg/L)	25	0.23	0.03	0.17	0.23	0.29	**0.29**	**No**
Ln Mo		-1.47	0.13	-1.77	-1.47	-1.24	-1.23	
EXP Ln Mo		0.23	1.14	0.17	0.23	0.29	0.29	No
Se (mg/L)	25	0.14	0.06	0.03	0.14	0.24	**0.24**	**No**
LN Se		-2.07	0.52	-3.58	-1.96	-1.41	-1.17	
EXP LN Se		0.13	1.68	0.03	0.14	0.24	0.31	No
Ra226(d) (pCi/L)	25	2.84	2.25	0.50	2.70	12.0	6.77	Yes
LN Ra226		0.81	0.72	-0.69	0.99	2.48	2.06	
EXP LN Ra226		2.24	2.05	0.50	2.70	12.0	**7.85**	**No**
U(t) (mg/L)	25	1.44	0.33	1.01	1.40	2.60	2.03	Yes
LN U(t)		0.35	0.21	0.01	0.34	0.96	0.71	
EXP LN U (t)		1.41	1.23	1.01	1.40	2.60	**2.03**	**No**

*n = number of samples

* *UTL (95 Percent Upper Tolerance Limit) = Mean + (Tolerance Factor (k)) * (Standard Deviation)

Where:

$k = t_{n-1, 0.05}(1+1/n)^{1/2}$

$t_{n-1, 0.05}$ = 95 percent upper percentile of the Student t-distribution

n-1 = degrees of freedom

Ln = natural log

EXP Ln = inverse of the natural log

(d) = filtered sample

(t) = unfiltered sample

Table 6. Descriptive statistics and 95% Upper Tolerance Intervals for DOE data.

	*n	Mean	Std Dev	Min	Median	Max	**UTL	Normality Rejected
Mo (mg/L)	54	16.9	51.7	0.001	1.26	225	104	Yes
LN Mo		-0.04	2.64	-6.91	0.23	5.42	4.42	
EXP LN Mo		0.96	14.1	0.001	1.25	225	**83.2**	**No**
Ni (mg/L)	31	0.04	0.04	0.002	0.020	**0.140**	0.11	Yes
LN Ni		-3.72	1.09	-6.50	-3.91	-1.97	-1.85	
EXP LN Ni		0.02	2.96	0.002	0.020	0.140	0.16	Yes
Se (mg/L)	54	0.73	0.87	0.00	0.15	**3.10**	2.20	Yes
Ln Se		-1.95	2.43	-5.99	-1.90	1.13	2.15	
EXP Ln Se		0.14	11.4	0.00	0.15	3.10	8.61	Yes
GA (pCi/L)	31	2066	3012	3.20	1110	15000	7260	Yes
LN GA		6.61	1.81	1.16	7.01	9.62	10	
EXP LN GA		741	6.09	3.20	1110	15000	**16726**	**No**
Ra-226 (pCi/L)	40	15.5	42.5	0.10	0.75	**190**	87.9	Yes
Ln		0.17	2.14	-2.30	-0.29	5.25	3.81	
EXP		1.19	8.46	0.10	0.75	190	45.4	Yes
Ra-228 (pCi/L)	29	0.74	1.18	0.10	0.40	**6.10**	2.78	Yes
Ln Ra-226		-1.02	1.17	-2.30	-0.92	1.81	1.02	
EXP LN Ra-226		0.36	3.24	0.10	0.40	6.10	2.77	Yes
Th-230 (pCi/L)	24	1.04	1.53	0.10	0.50	**5.25**	3.72	Yes
LN Th-230		-0.78	1.28	-2.30	-0.71	1.66	1.46	
EXP LN Th-230		0.46	3.60	0.10	0.49	5.25	4.30	Yes
U (mg/L)	52	2.56	2.77	0.001	2.19	**11.1**	7.26	Yes
LN U		-0.22	2.13	-7.42	0.78	2.41	3.38	
EXP LN U		0.80	8.41	0.001	2.18	11.1	29.5	Yes
Pb-210 (pCi/L)	15	9.05	26.3	0.08	0.50	102	56.8	Yes
LN Pb-210		-0.31	2.15	-2.50	-0.69	4.62	3.61	
EXP LN Pb-210		0.74	8.61	0.08	0.50	102	**36.9**	**No**

*n = number of samples

* *UTL (95 Percent Upper Tolerance Limit) = Mean + (Tolerance Factor (k)) * (Standard Deviation)

Where:

$k = t_{n-1,0.05}(1+1/n)^{1/2}$

$t_{n-1,0.05}$ = 95 percent upper percentile of the Student t-distribution

n-1 = degrees of freedom

Ln = natural log

this guidance, DOE data sets that failed the tests for Normal and Lognormal distribution were assigned the highest observed value in a data set as the UTL.

In Summary, background values for the QMC Facility were determined by calculation of a UTL for constituent data sets that were either Normally or Lognormally distributed, or assigned the highest observed value as the UTL in data sets that were not Normally or Lognormally distributed.

4. CONCLUSIONS

Background concentrations established for constituents in the Alluvium near the QMC Facility are shown in Table 7. The current GPS set forth in License SUA-1473 are also presented in Table 7, along with risk-based standards calculated for the groundwater at the QMC Facility (AVM, 2000).

The following points indicate that seepage from the DOE Facility, mine pumping and discharge, and the runoff and erosion from abandoned mine spoils and ore piles have caused widespread ambient groundwater contamination that is unrelated to, but inseparable from impacts related to milling at the QMC Facility:

- DOE natural background data evaluated by the statistical analysis suggest that levels of some constituents (e.g. uranium and molybdenum) occur naturally at levels that are an order of magnitude higher than current GPS.

- SPLP leaching results for mine spoil and ore pile soil samples indicates that there is a potential for these sources to contribute concentrations of uranium ore related constituents to groundwater.

- Seepage from the DOE Title I tailings has contributed solutions with high concentrations of constituents to alluvial materials. These solutions will ultimately arrive at the QMC Point of Exposure (POE).

- QMC has no control over the sources of constituents other than those they have contributed to groundwater. Constituents from the DOE Facility are just as likely to arrive at the QMC point of exposure as constituents from the QMC Facility.

A number of sources, specifically mine pumping and discharge, seepage from the nearby DOE Facility and runoff/erosion from abandoned mine spoils and ore piles, have contributed constituents to the alluvial groundwater. As a result background groundwater in the alluvial materials is of low quality and, therefore, of limited use. The current GPS, based on water quality from a single monitor well completed in the Alluvium, are unrealistic due to high ambient concentrations of constituents at the facility.

Table 7. Background UTL Values.

	Background (UTL_{95}) Concentration	NRC GPS	Risk-Based Protection Value
Mo (mg/L)	83	0.06	0.2
Ni (mg/L)	0.14	0.06	0.1
Se (mg/L)	3.1	0.05	0.1
GA (pCi/L)	16726	57	
Ra-226 (pCi/L)	190		
Ra-228 (pCi/L)	6.1		
Ra-226 + Ra-228 (pCi/L)		5*	41**
Th-230 (pCi/L)	5	3	139
U (mg/L)	11.1	0.06	0.2
Pb-210 (pCi/L)	36	4.9	13

* NRC GPS for Radium is Ra-226+Ra-228 = 5 pCi/L.

** Risk Based Protection Value for Radium is Ra-226+Ra-228 = 41 pCi/L.

5. REFERENCES

AVM (AVM Environmental Services, Inc and Applied Hydrology Associates, Inc.,) 2000, Corrective Action Program and Alternate Concentration Limits Petition for Upper Most Bedrock Units Ambrosia Lake Uranium Mill Facility Near Grants, New Mexico. Prepared for QMC Mining Company USNRC License No. SUA-1473, Docket No. 40-8905

Bostick, K., 1985, Ground-Water Discharge Plan Analysis for Kerr-McGee Nuclear Corporation Ambrosia Lake Uranium Mill, QMC Mining Company. New Mexico Environmental Improvement Division Unpublished Report, 86p.

DOE (U.S. Department of Energy), 1985, Remedial Action Plan and Site Conceptual Design for Stabilization of the Inactive Uranium Mill Tailings at Ambrosia Lake, New Mexico. DOE/AL50516.0000. Prepared by the U.S. Department of Energy, UMTRA Project Office, Albuquerque Operations Office, Albuquerque, New Mexico.

EPA (U.S. Environmental Protection Agency), 1992, Statistical Analysis of Groundwater Monitoring Data at RCRA Facilities, Addendum to Interim Final Guidance. Office of Solid Waste, Permits and State Programs Division, U.S. Environmental Protection Agency, Washington, D.C., July 1980.

EPA (U.S. Environmental Protection Agency), 1999, Draft EPA and Hard Rock Mining: A Source Book for Industry in the Northwest and Alaska. EPA 910-R-99-016, November 1999.

NRC (U.S. Nuclear Regulatory Commission). 1996. *Staff Technical Position, Alternate Concentration Limits for Title II Uranium Mills. Standard Format and Content Guide, and Standard Review Plan for Alternate Concentration Limit Applications.* January 1996. 31 pp.

QMC (Quivira Mining Company), 1997, NPDES Permit No. NM0020532 Outfall 001 Report. Submitted to USEPA October 21, 1997.

Attachment A

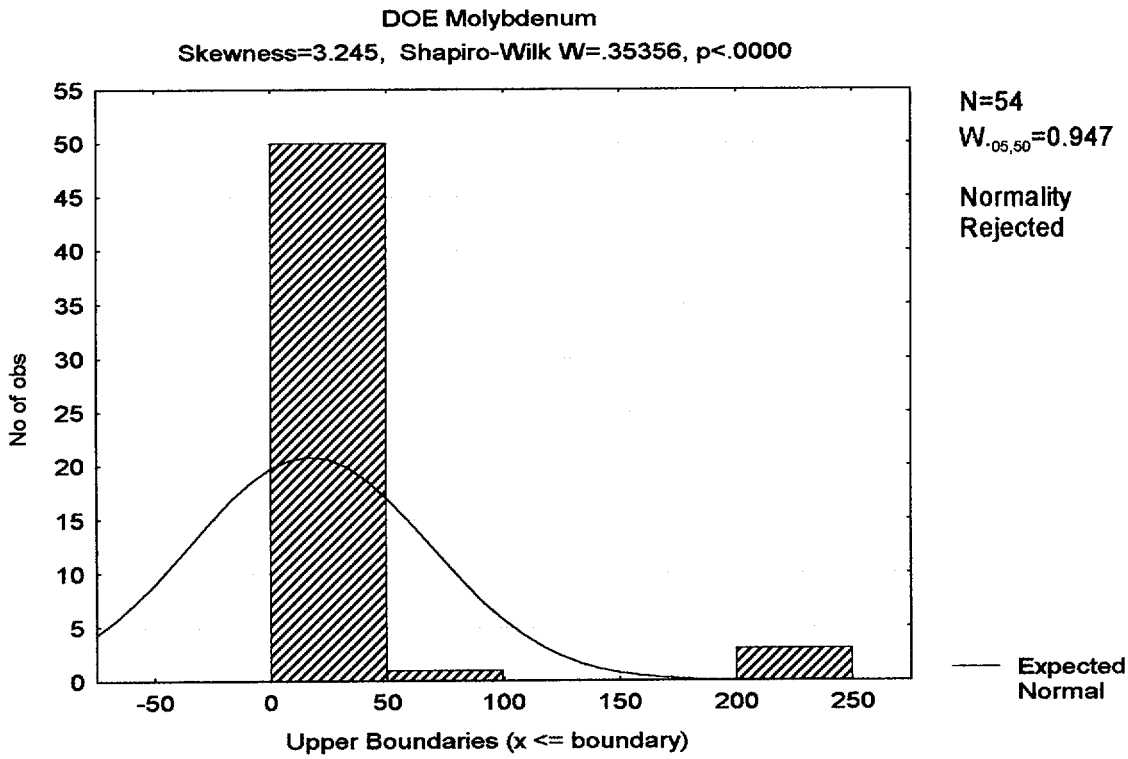

Figure A-1. Test for normal distribution of DOE Molybdenum data.

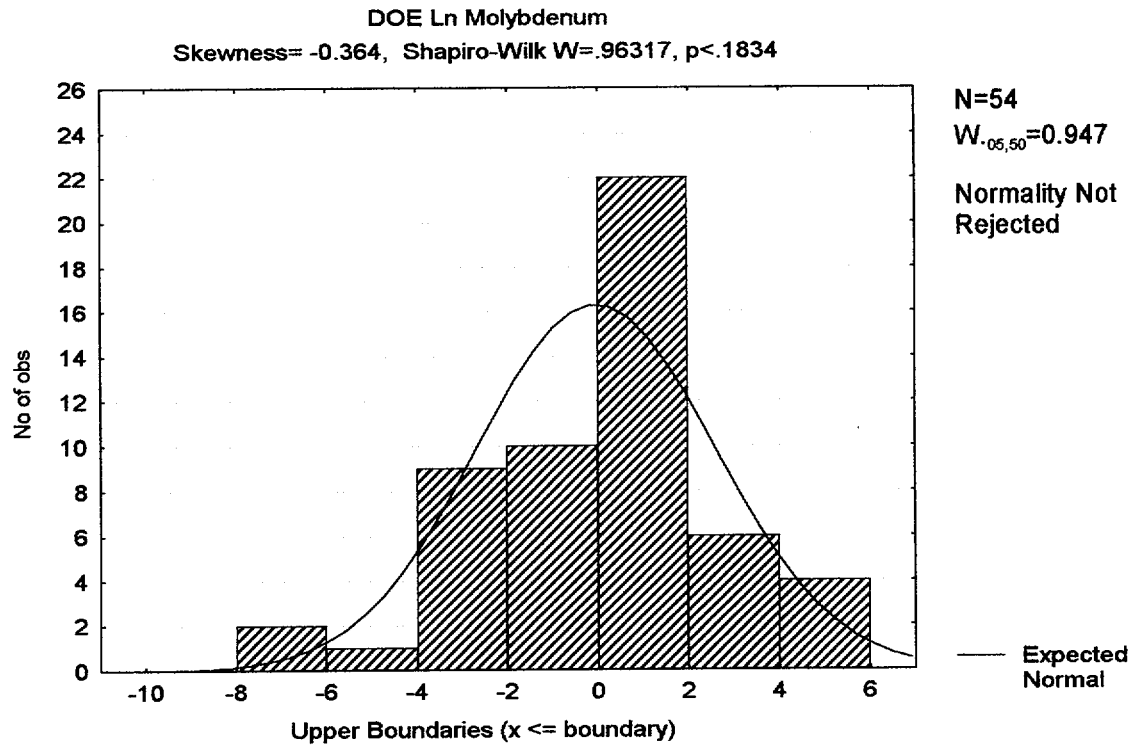

Figure A-2. Test for normal distribution of the natural log of DOE Molybdenum data.

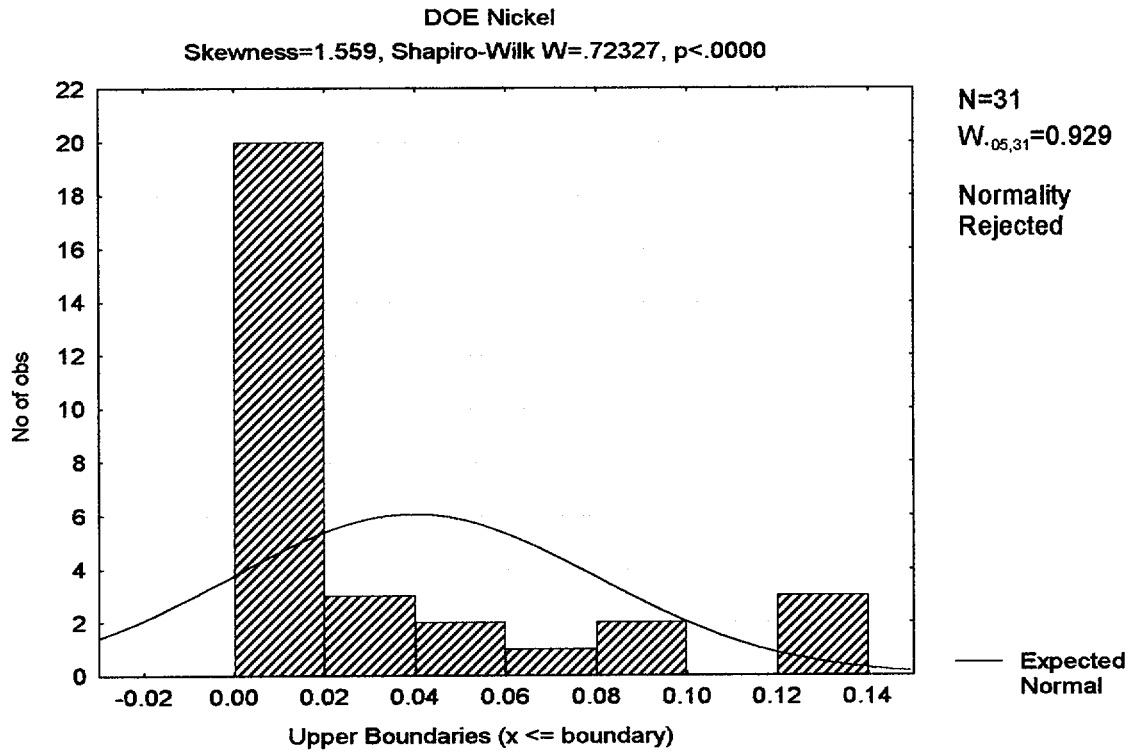

Figure A-3. Test for normal distribution of DOE Nickel data.

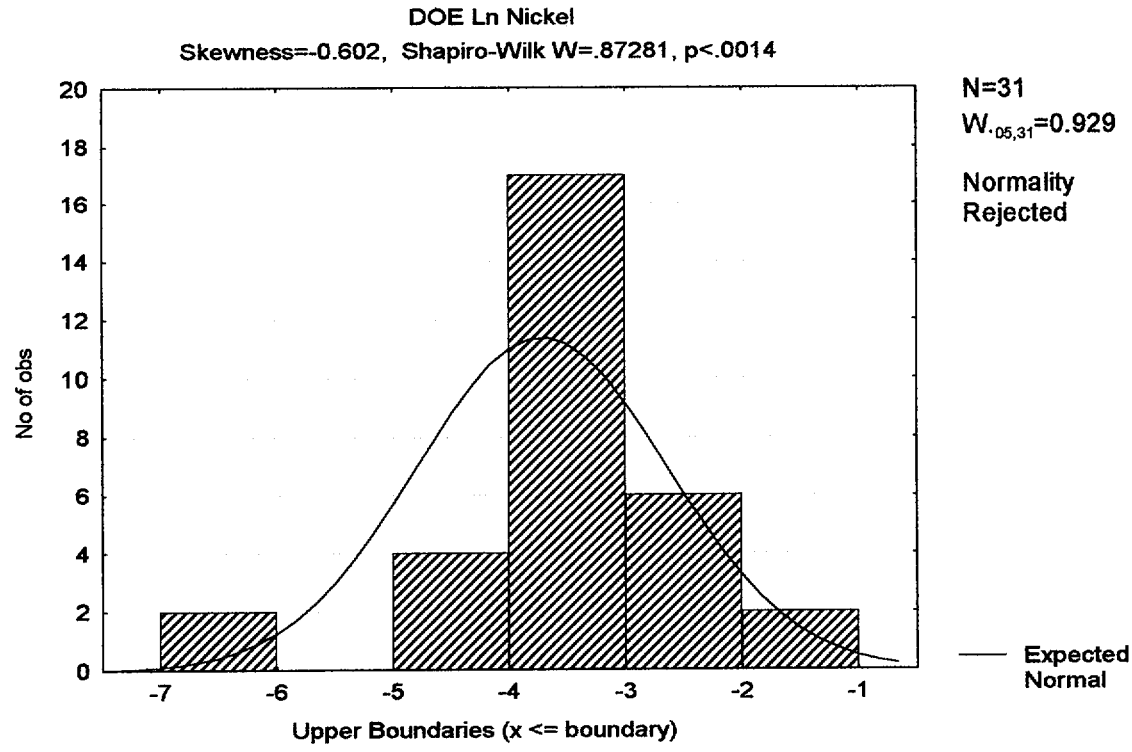

Figure A-4. Test for normal distribution of the natural log of DOE Nickel data.

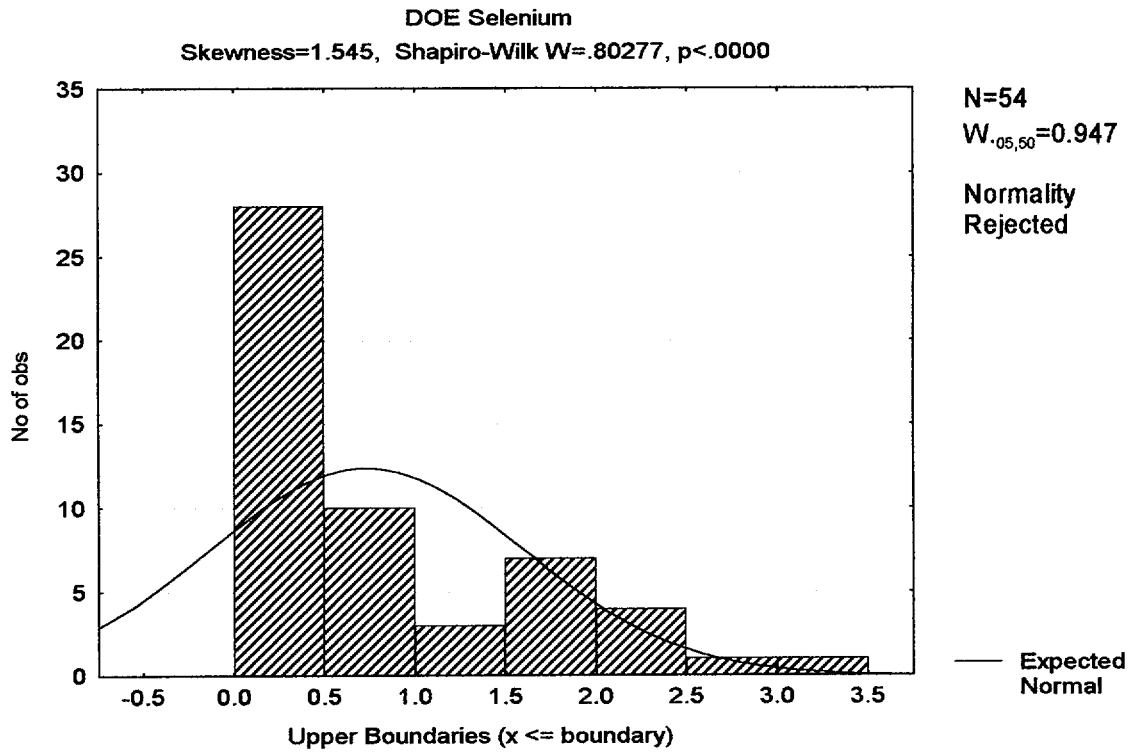

Figure A-5. Test for normal distribution of DOE Selenium data.

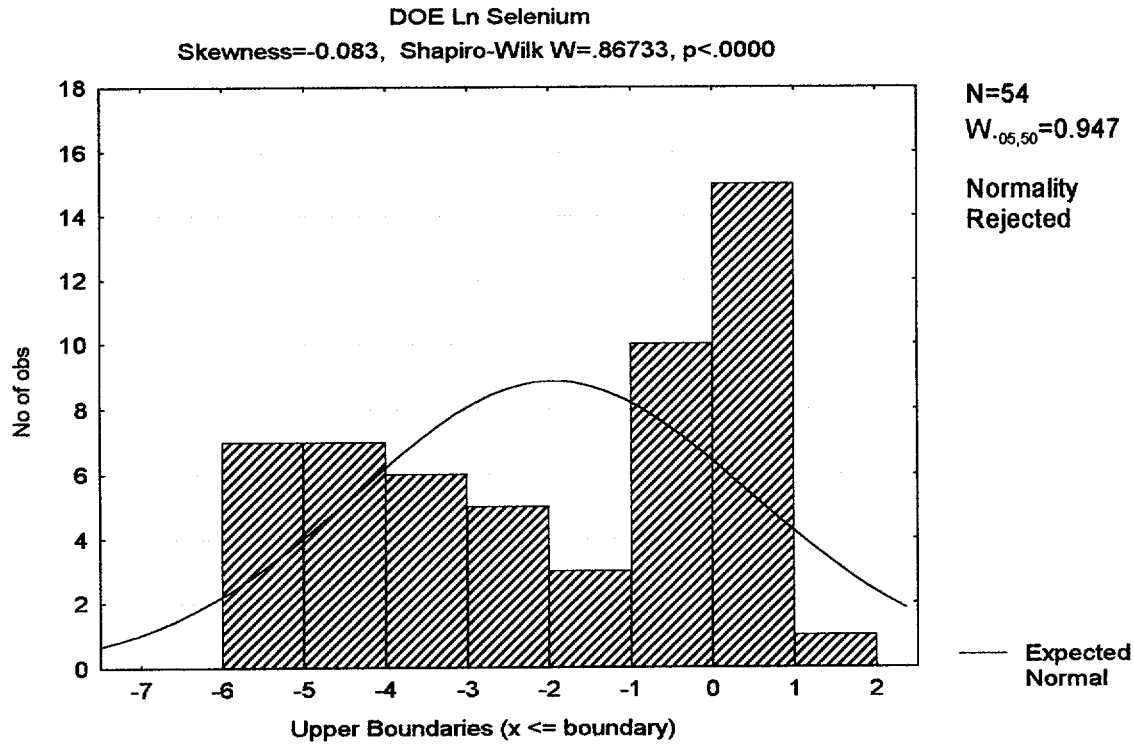

Figure A-6. Test for normal distribution of the natural log of DOE Selenium data.

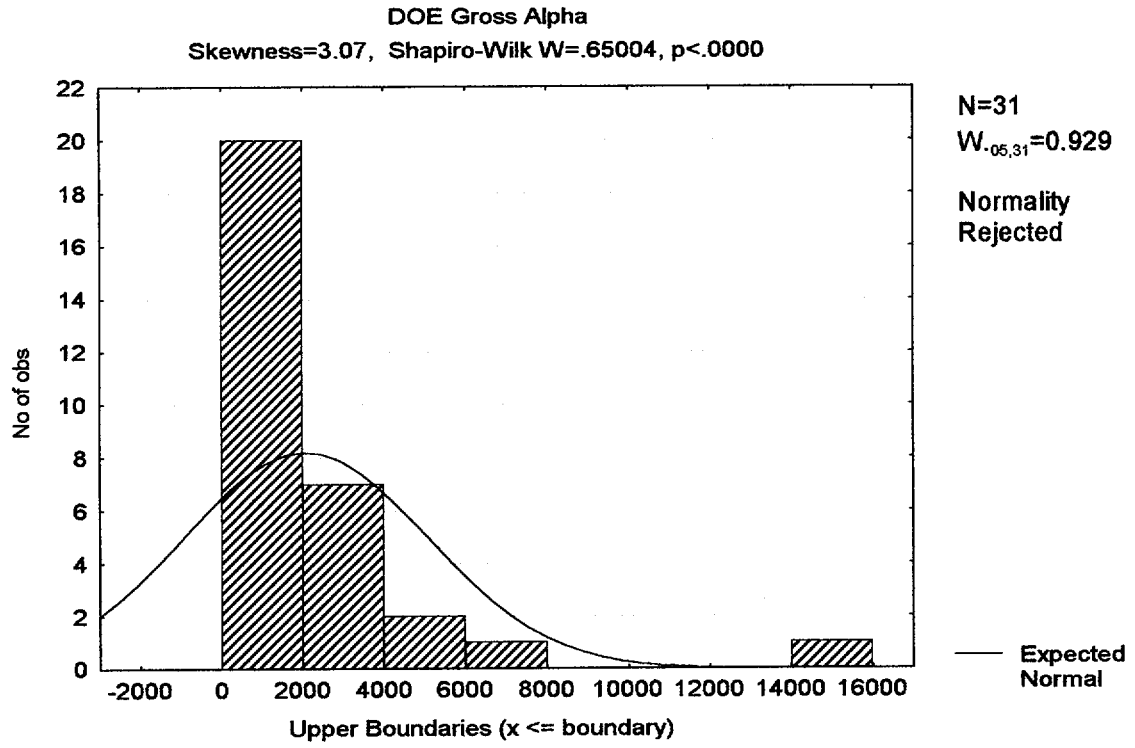

Figure A-7. Test for normal distribution of DOE Gross Alpha data.

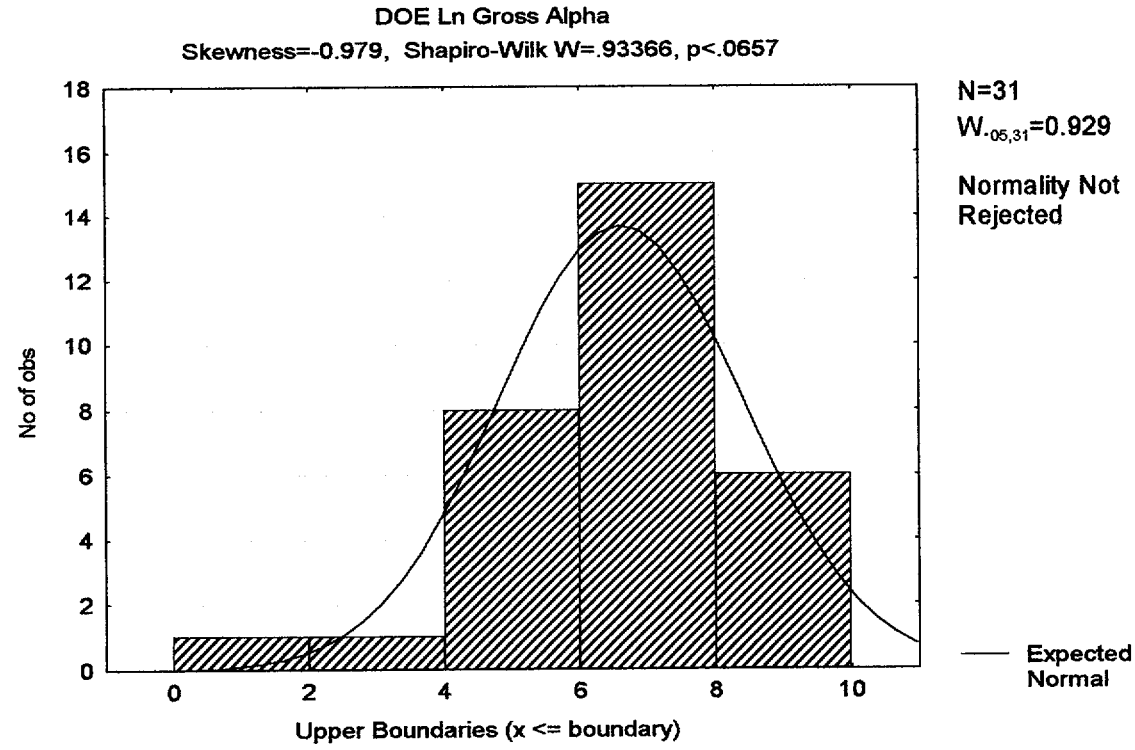

Figure A-8. Test for normal distribution of the natural log of DOE Gross Alpha data.

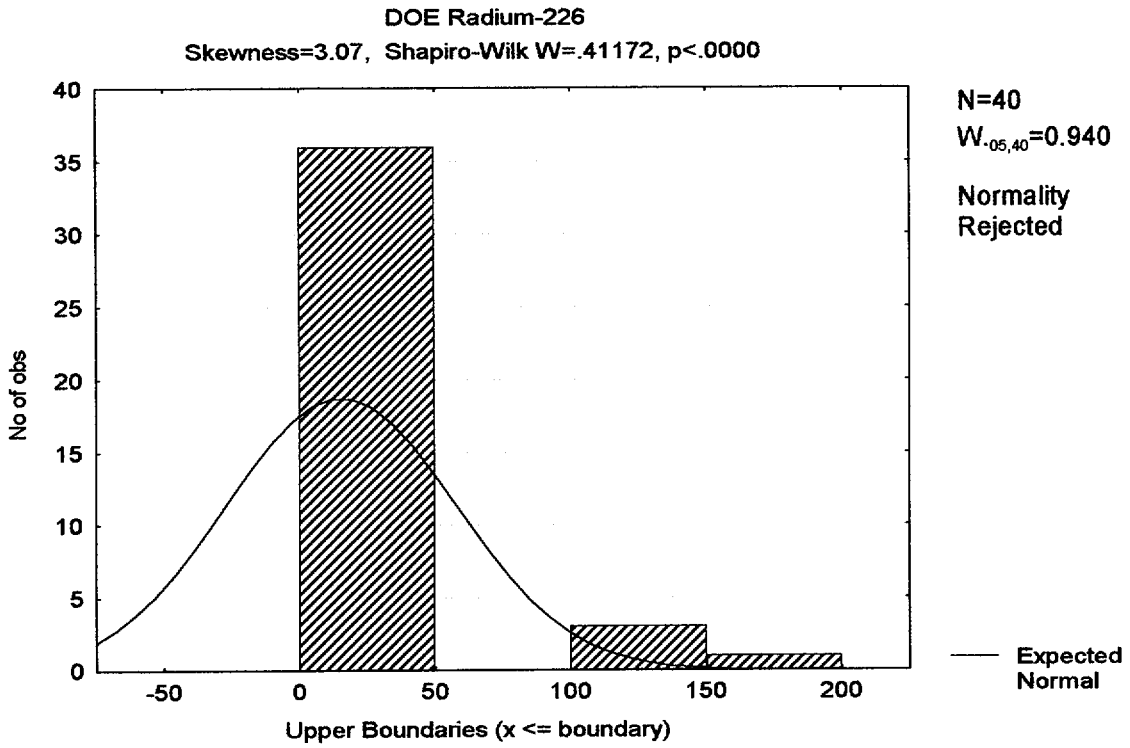

Figure A-9. Test for normal distribution of DOE Radium-226 data.

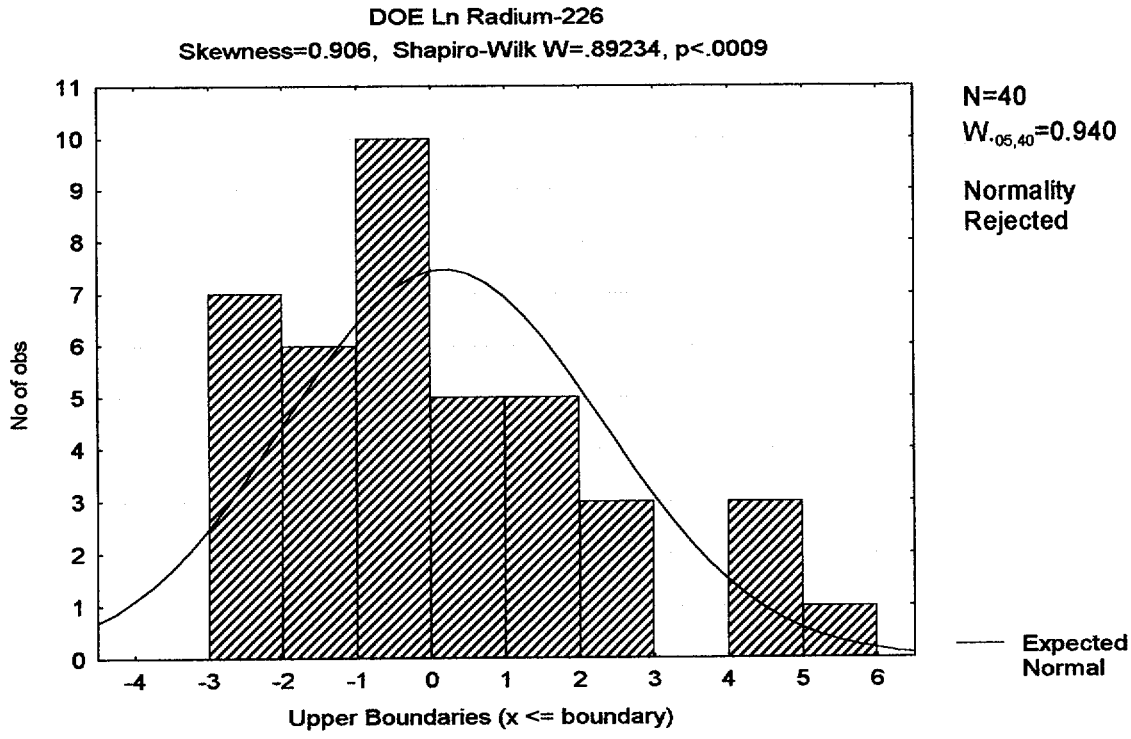

Figure A-10. Test for normal distribution of the natural log of DOE Radium-226 data.

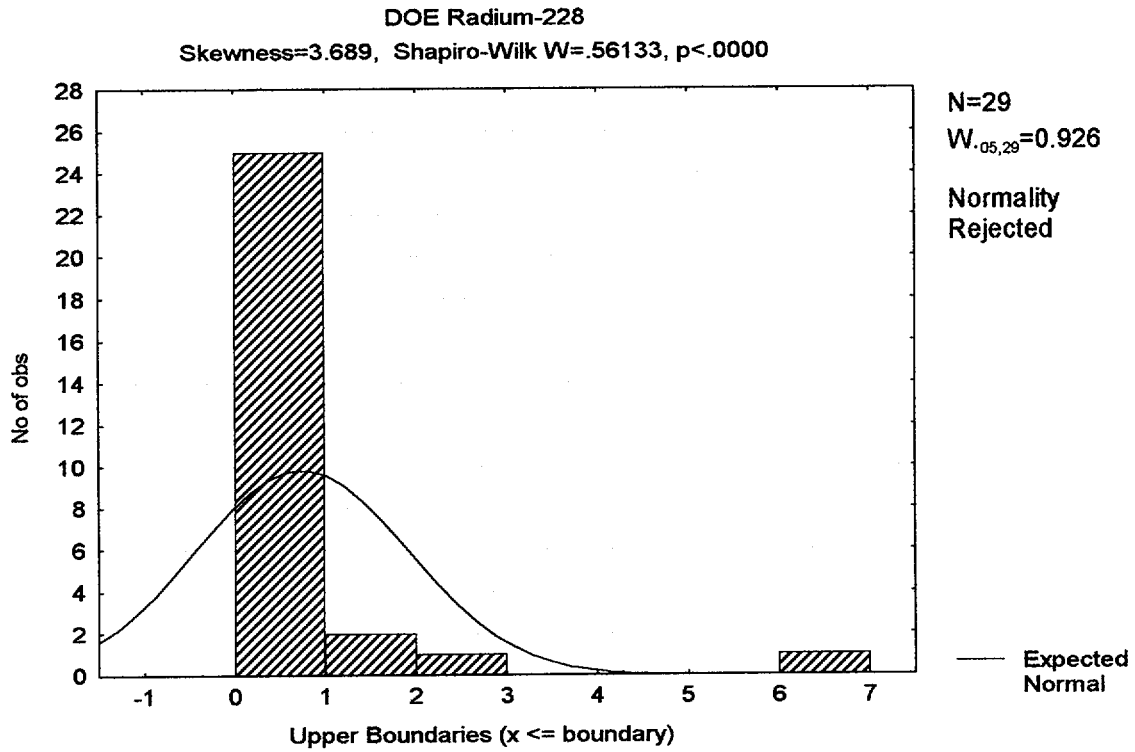

Figure A-11. Test for normal distribution of DOE Radium-228 data.

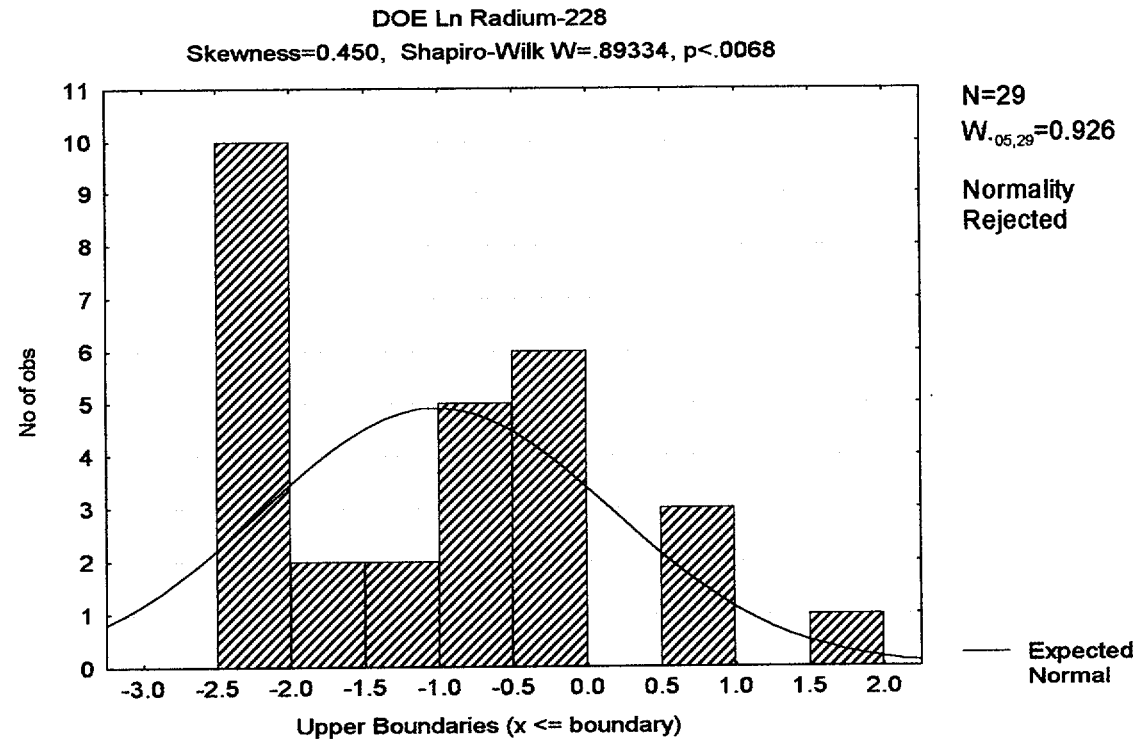

Figure A-12. Test for normal distribution of the natural log of DOE Radium-228 data.

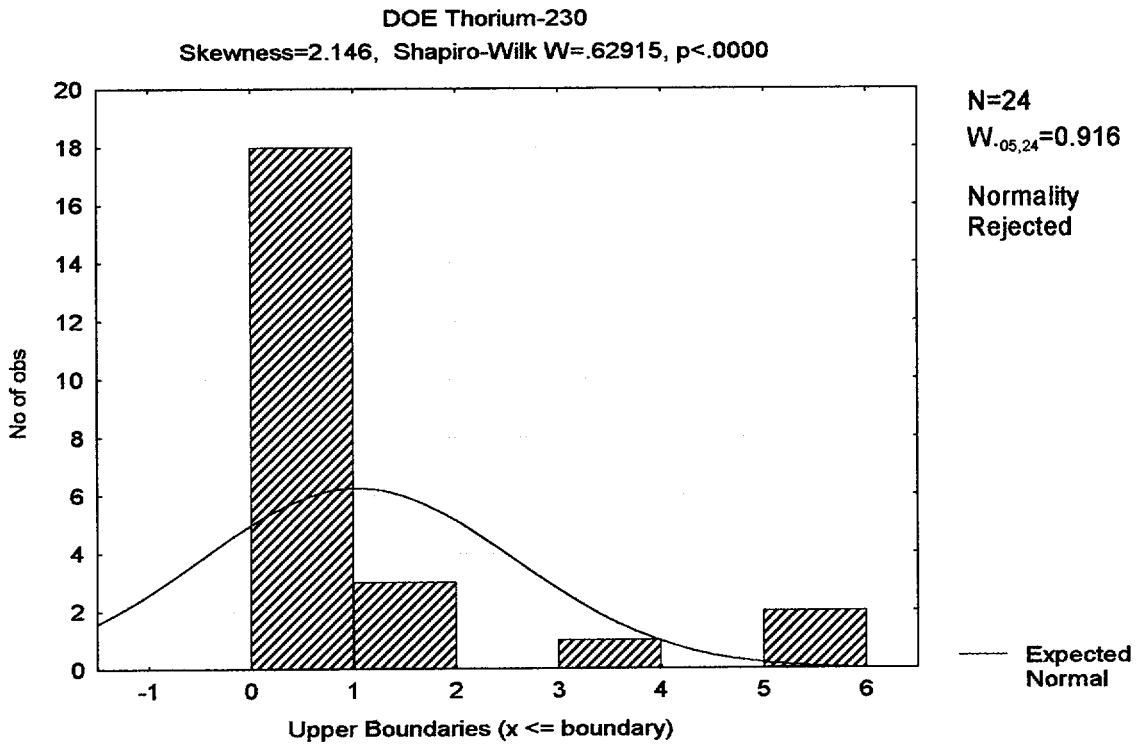

Figure A-13. Test for normal distribution of DOE Thoriium-230 data.

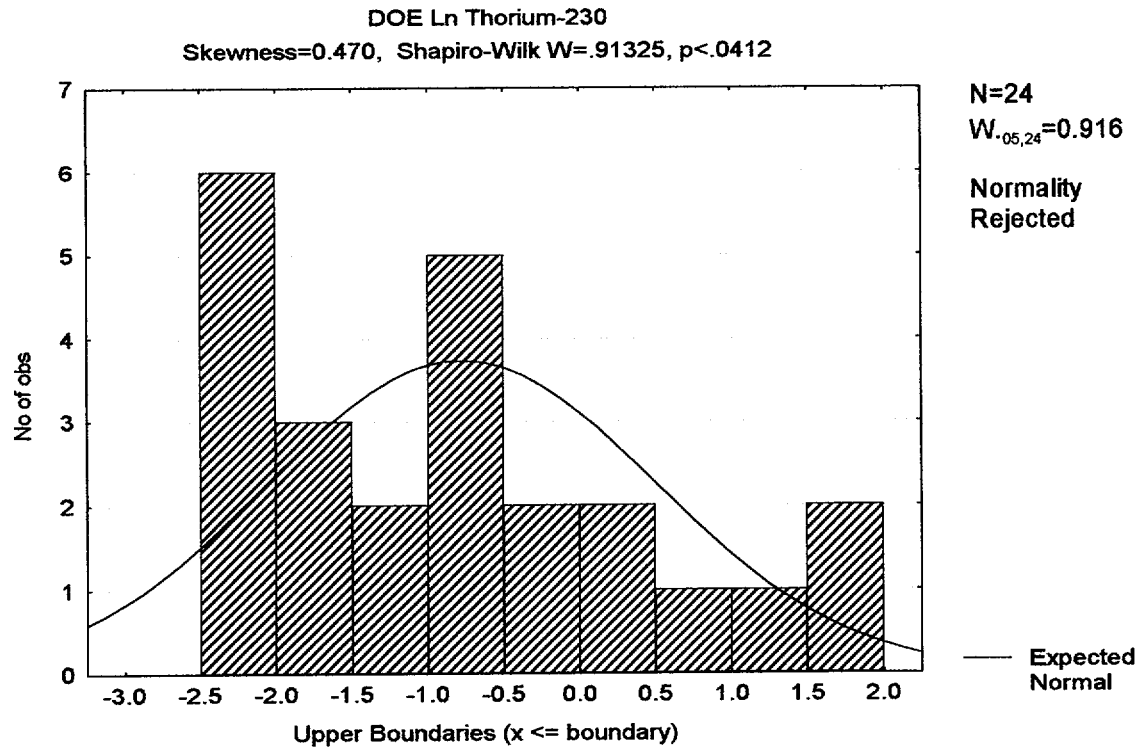

Figure A-14. Test for normal distribution of the natural log of DOE Thoriium-230 data.

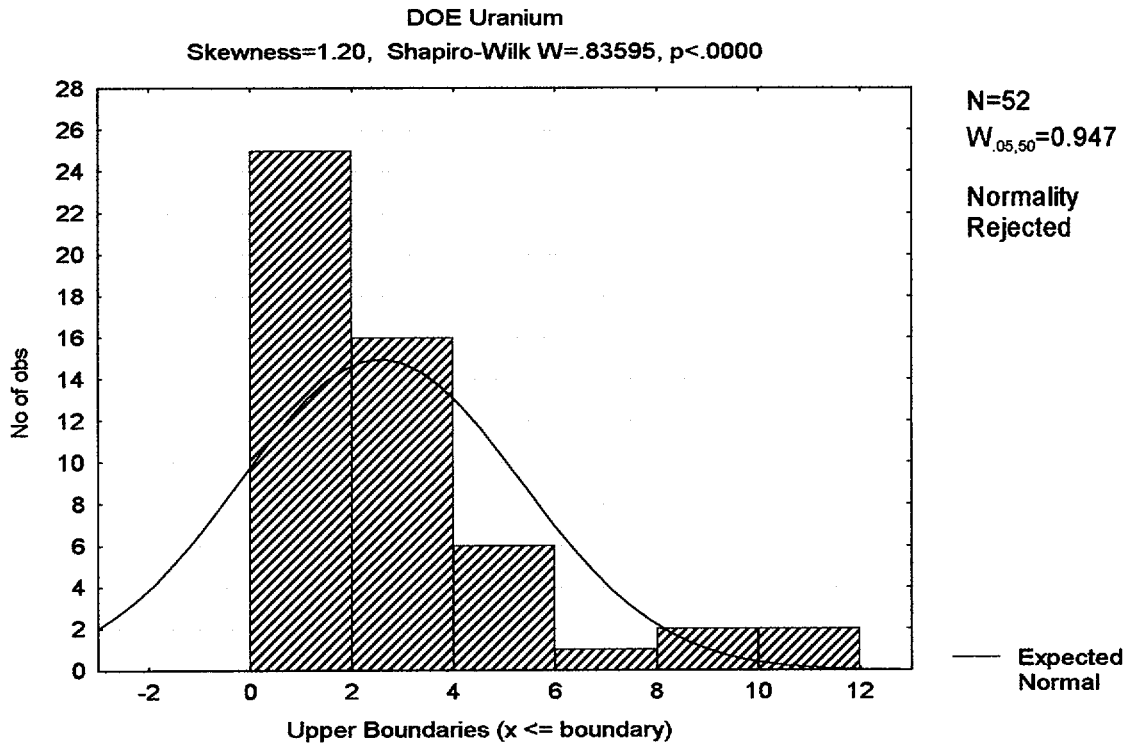

Figure A-15. Test for normal distribution of DOE Uranium data.

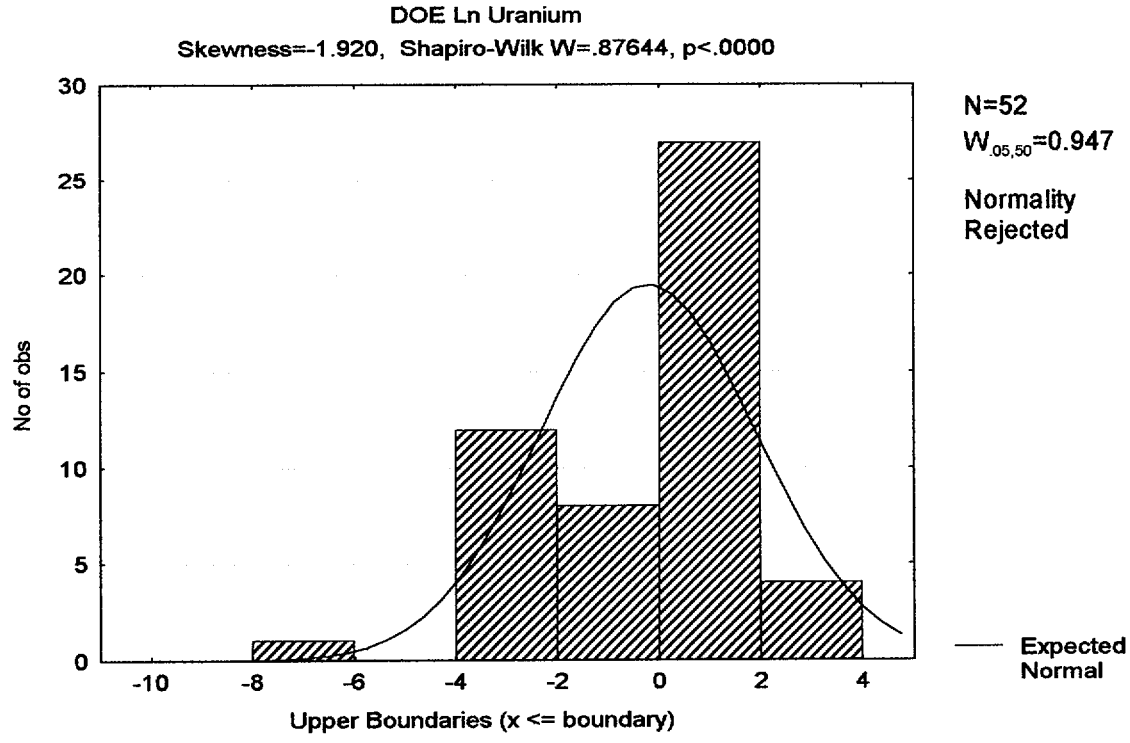

Figure A-16. Test for normal distribution of the natural log of DOE Uranium data.

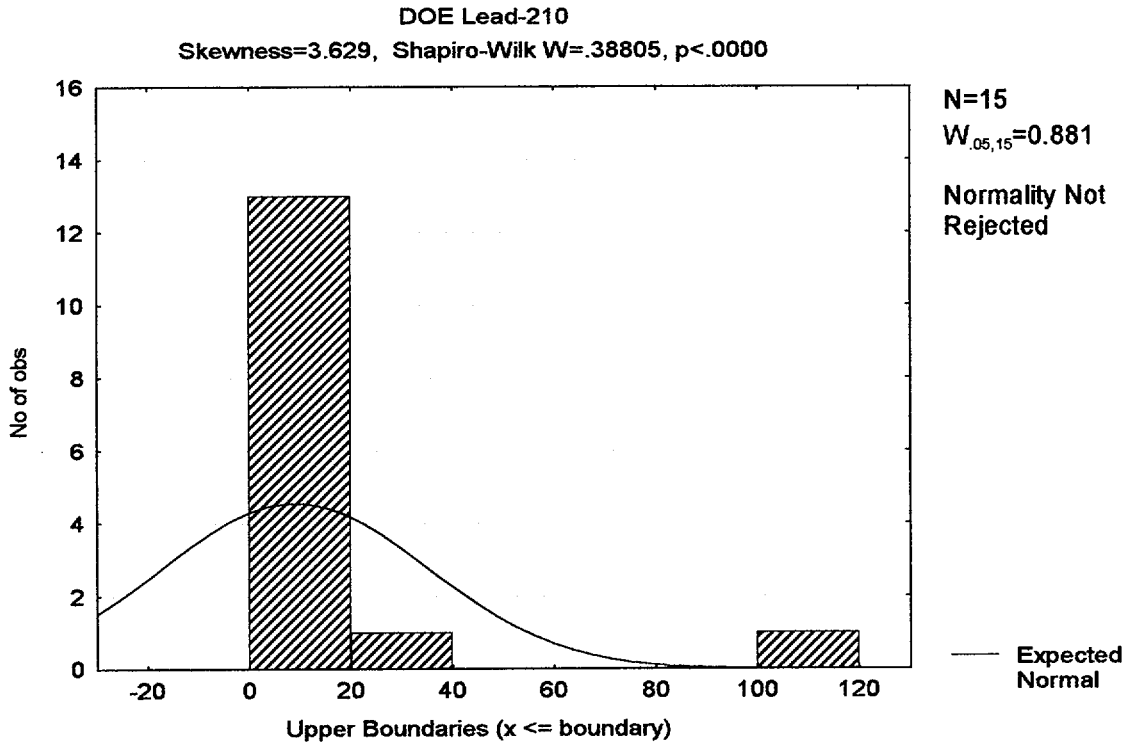

Figure A-17. Test for normal distribution of DOE Lead-210 data.

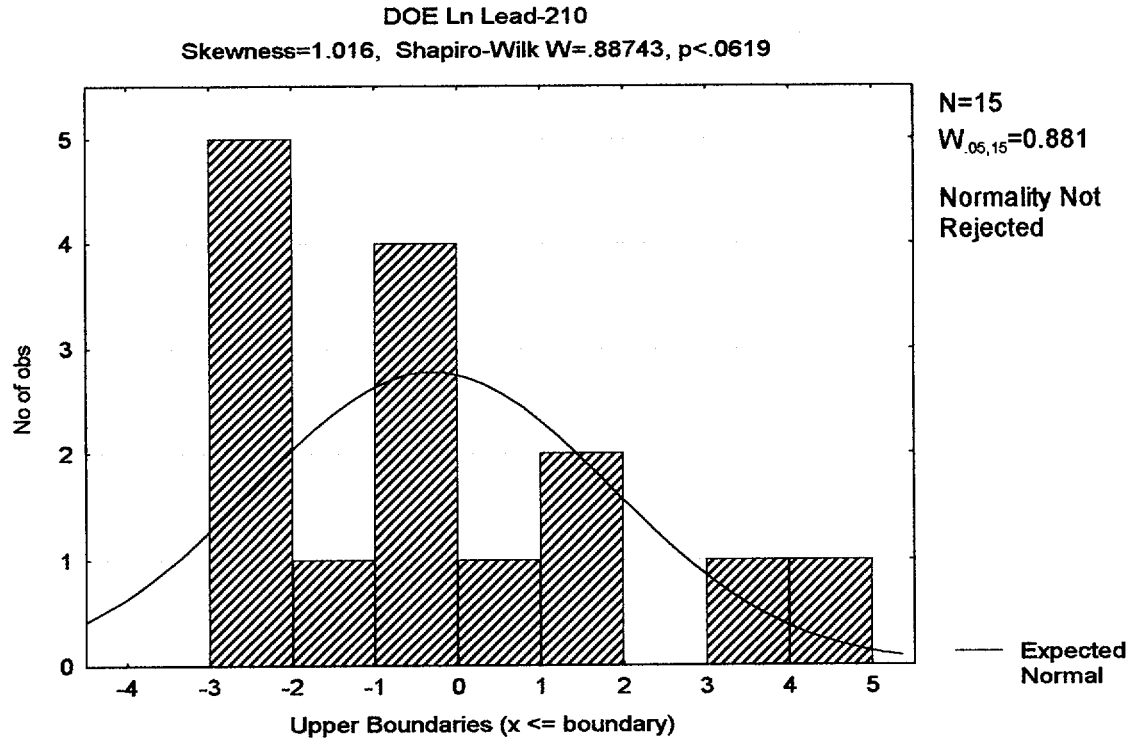

Figure A-18. Test for normal distribution of the natural log of DOE Lead-210 data.

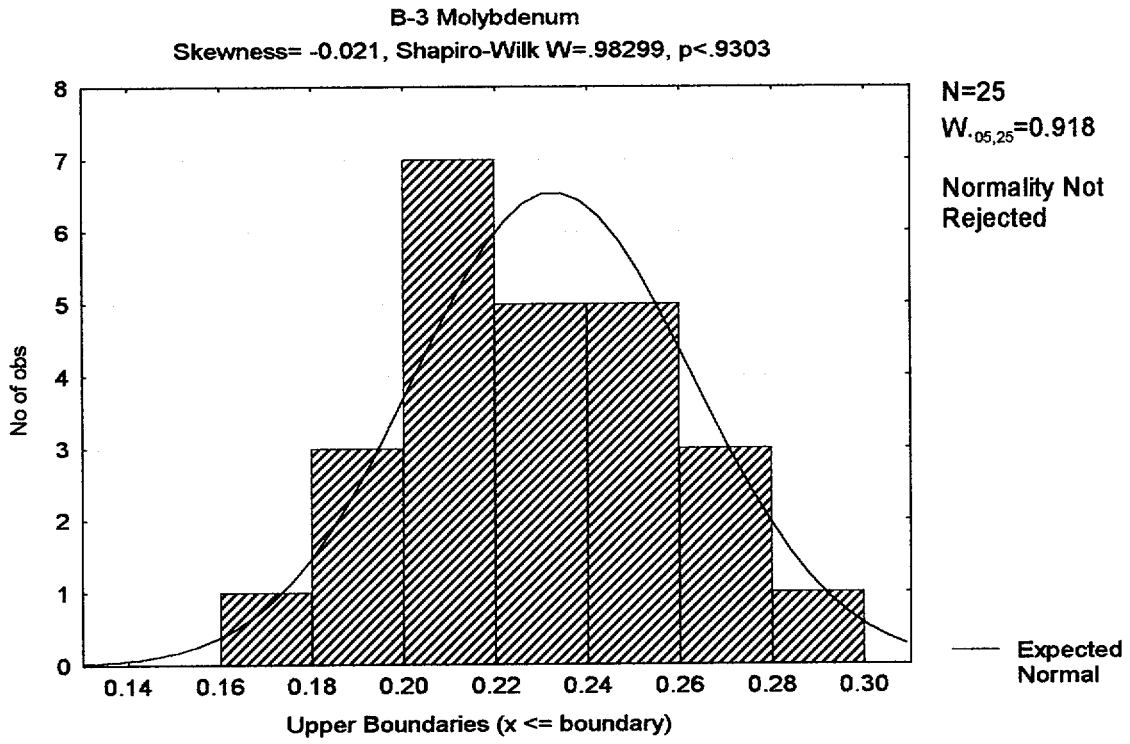

Figure A-19. Test for normal distribution of B-3 Molybdenum data.

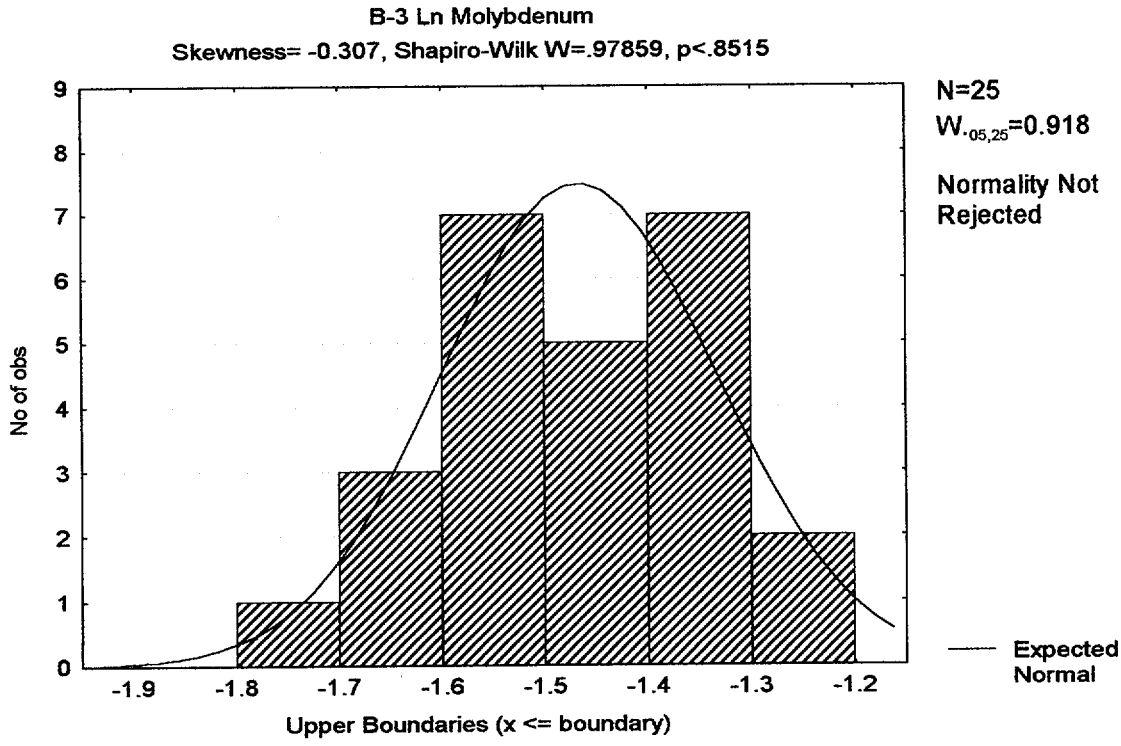

Figure A-20. Test for normal distribution of the natural log of B-3 Molybdenum data.

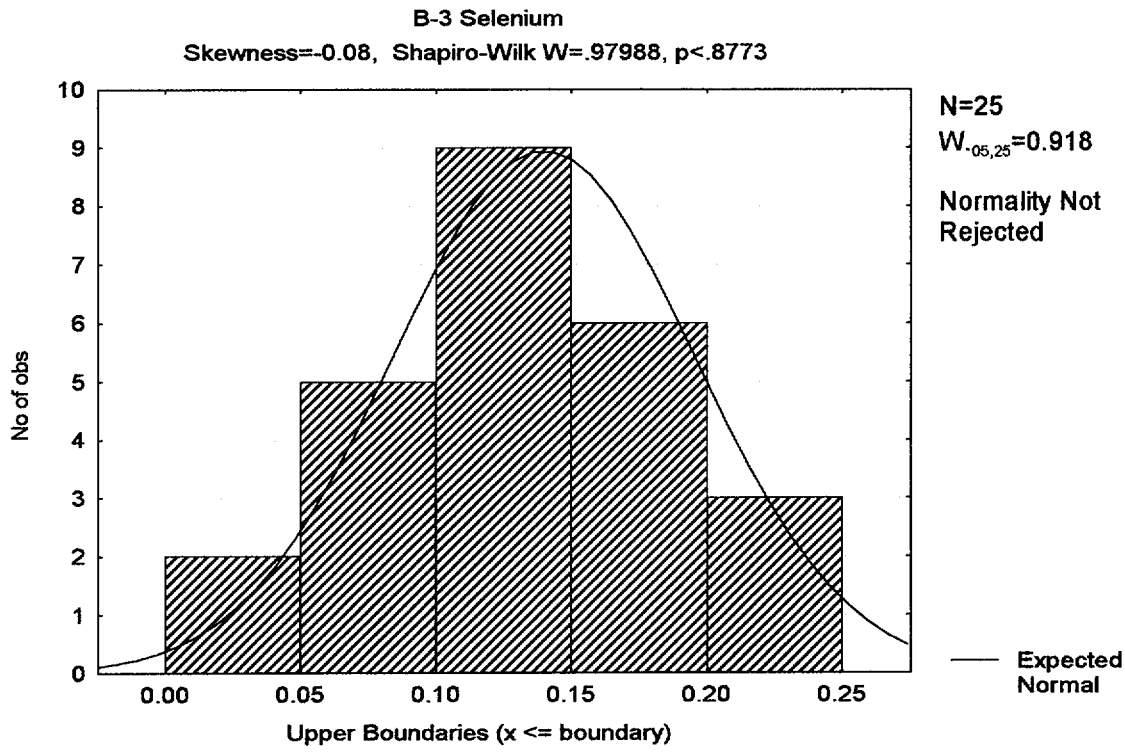

Figure A-21. Test for normal distribution of B-3 Selenium data.

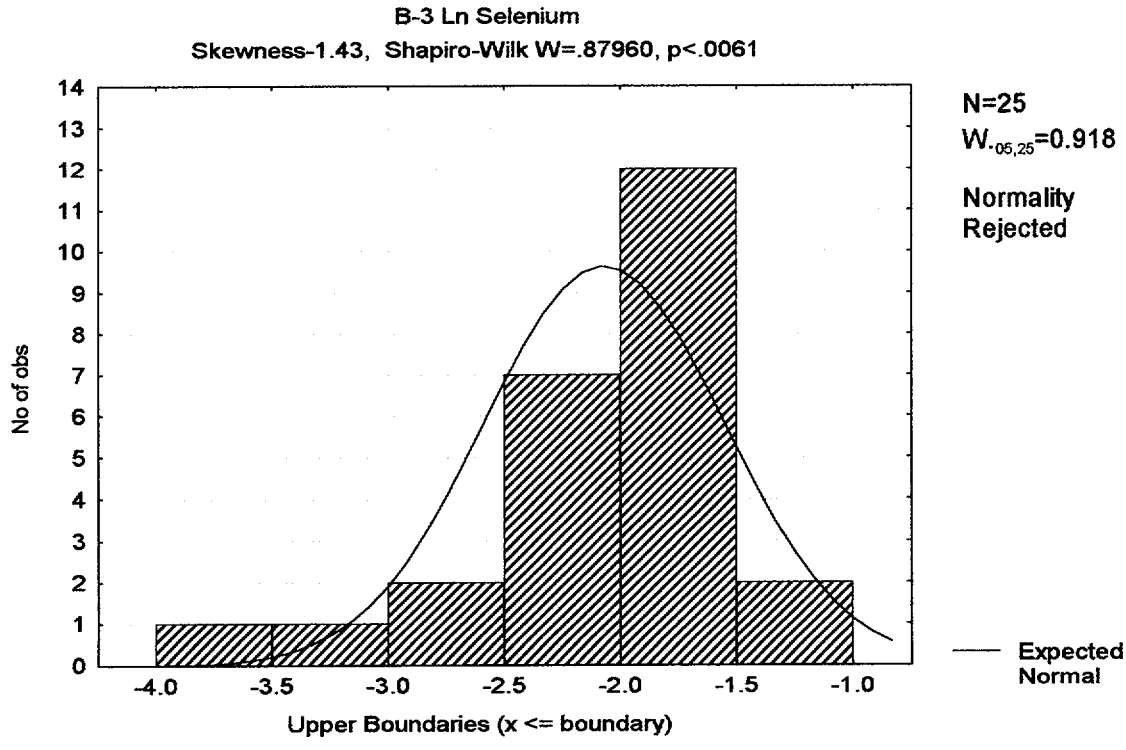

Figure A-22. Test for normal distribution of the natural log of B-3 Selenium data.

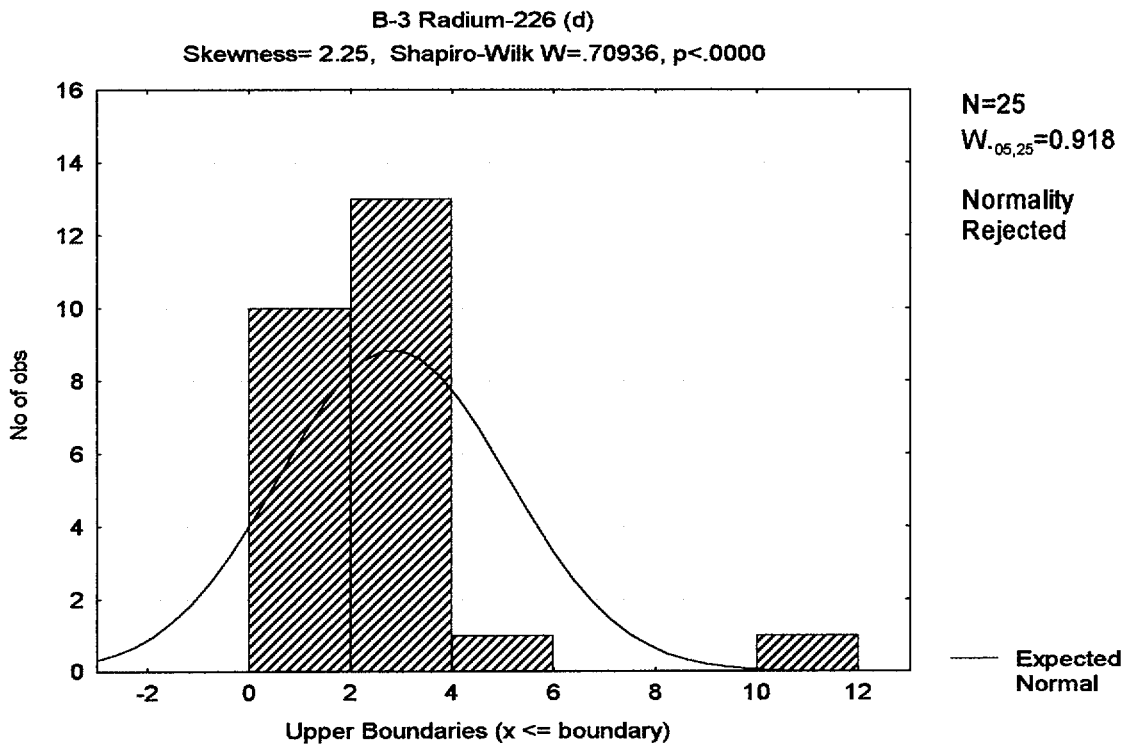

Figure A-23. Test for normal distribution of DOE Radium-226 9 (dissolved) data.

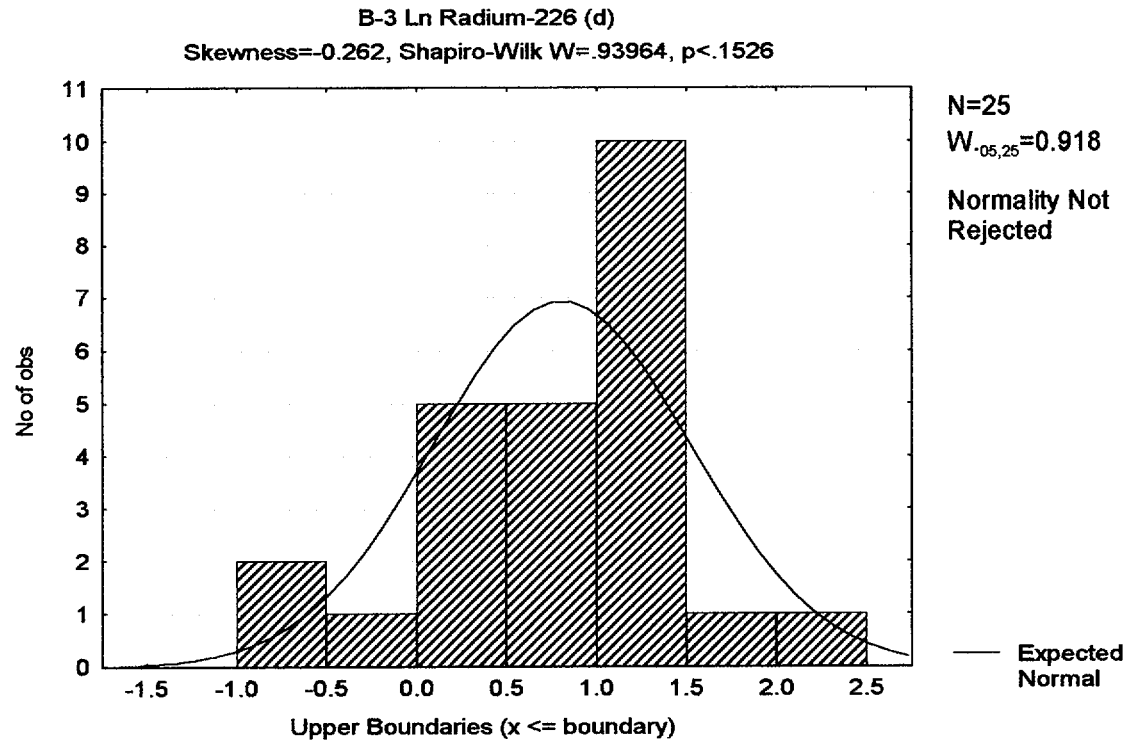

Figure A-24. Test for normal distribution of the natural log of DOE Radium-226 (dissolved) data

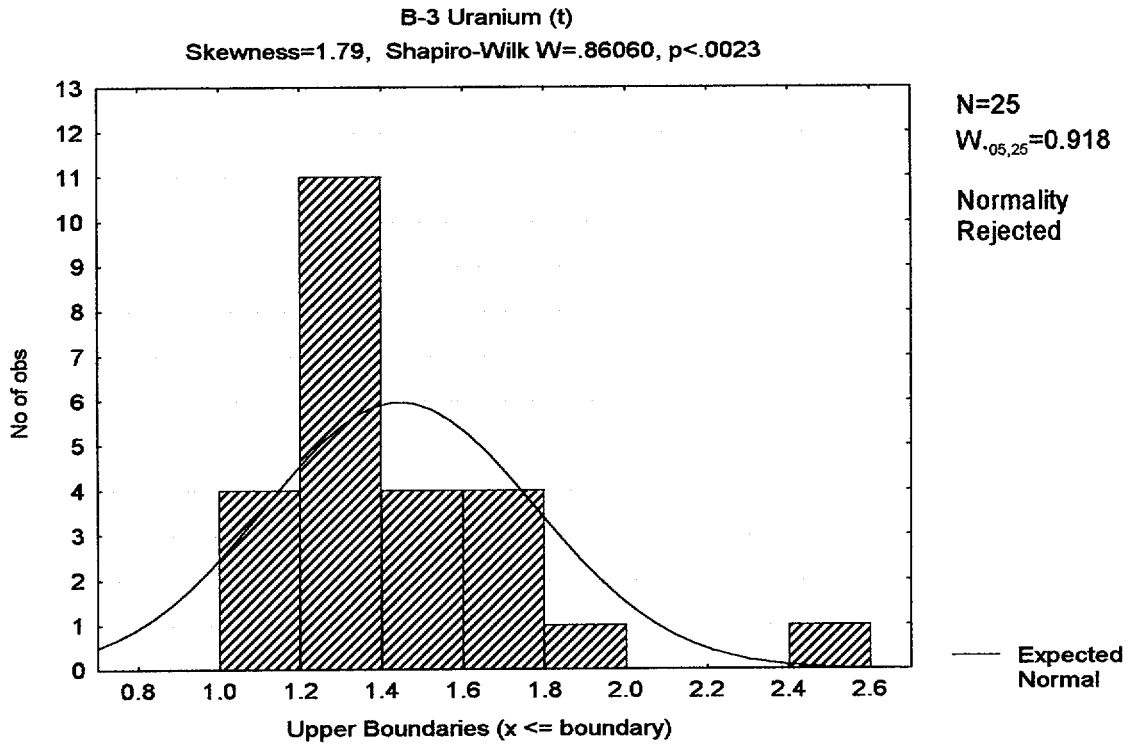

Figure A-25. Test for normal distribution of B-3 Uranium (total) data.

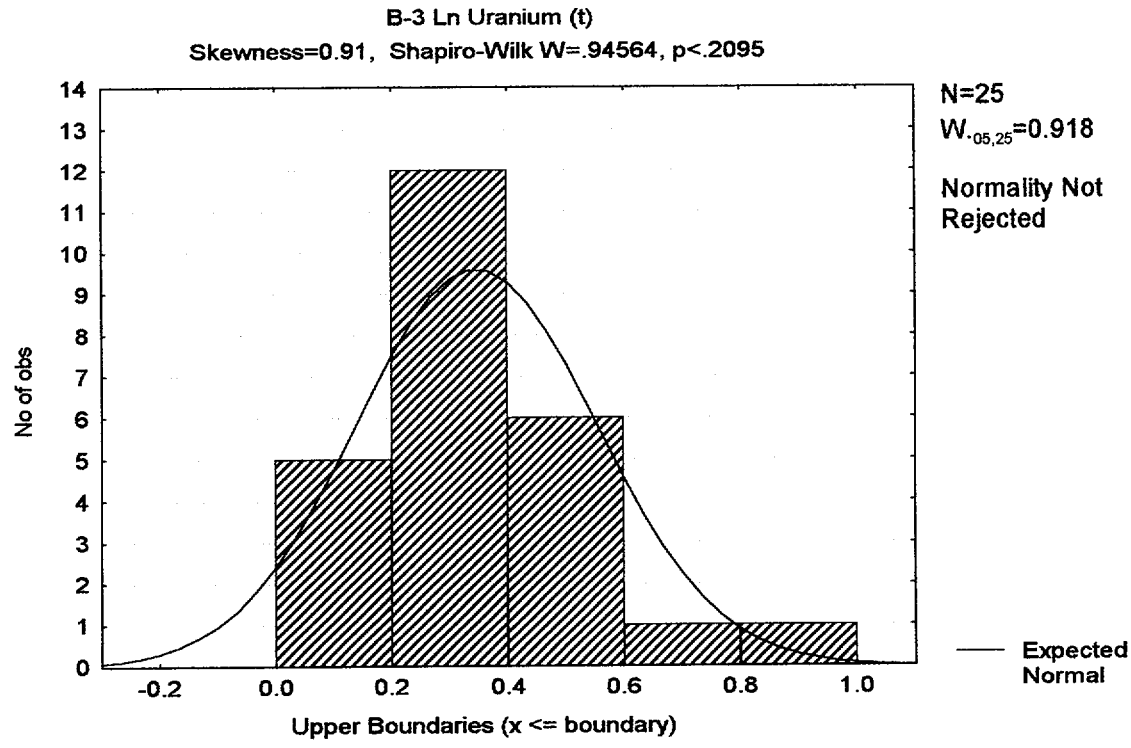

Figure A-26. Test for normal distribution of the natural log of B-3 Uranium (total) data.

APPENDIX B

GEOCHEMICAL MODELING OF CONSTITUENTS IN GROUNDWATER AT THE QUIVIRA MINING COMPANY URANIUM MILL FACILITY, AMBROSIA LAKE, NEW MEXICO

January 2001

Prepared for

Rio Algom Mining Company

Prepared by

Maxim Technologies, Inc.

10601 Lomas NE

Albuquerque, New Mexico 87112

GEOCHEMICAL MODELING OF CONSTITUENTS IN GROUNDWATER AT THE QUIVIRA MING COMPANY URANIUM MILL FACILITY, AMBROSIA LAKE, NEW MEXICO

TABLE OF CONTENTS

List of Tables

List of Figures

GEOCHEMICAL MODELING OF CONSTITUENTS IN ALLUVIAL GROUNDWATER AT THE QUIVIRA MINING COMPANY URANIUM MILL FACILITY, AMBROSIA LAKE, NEW MEXICO

1. INTRODUCTION

The purpose of geochemical modeling of groundwater in the vicinity of the Quivia Mining Company (QMC) Facility was to investigate the geochemical environment for attenuation capacity and constituent behavior. These investigations are useful in helping to establish possible cleanup strategies and to help understand processes that affect constituents moving from one geochemical environment to another. Results from the geochemical model will be used in concert with the groundwater flow model Modflow to demonstrate reduction in constituent concentrations in groundwater over time and over distance from the source.

2. CONCEPTUAL MODEL

Activities at the Facility started in 1957. A water storage reservoir was constructed to contain mine water for mill use. Unlined evaporation Ponds 4, 5, and 6 were constructed for evaporative treatment of mine water and mill effluents. Tailings Impoundments 1 and 2 were built in late 1958. Pond 3, also built in 1958, was located at the eastern toe of Tailings Impoundment 1 for decant of the tailings impoundments. The tailings were first produced in November 1958. The solid portions of the process were disposed through a slurry transfer system to the tailings impoundments, while the liquid fraction was transferred to evaporation ponds. Evaporation pond residues from Ponds 4, 5, 6, 7, and 8 were placed in Tailings Impoundments 1 and 2 prior to final reclamation.

The alluvial materials were unsaturated before mining began in the Ambrosia Lake Valley (Bostick, 1985). Mine-dewatering discharges from underlying geologic units created saturated conditions in the Alluvium during the development of numerous mines in the vicinity. The quality of mine discharge water is dependent on site-specific mine conditions, and mining processes. Mine discharge is not regulated by the NRC and is unrelated to regulated milling activities.

A number of sources, specifically mine pumping and discharge, seepage from the nearby DOE Facility and runoff/erosion from abandoned mine spoils and ore piles, have contributed constituents to the alluvial groundwater. As a result ambient groundwater in the alluvial materials is of low quality and, therefore, of limited use. QMC's current GPS, based on water quality from a single monitor well completed in the Alluvium, are unrealistic due to high ambient concentrations of constituents present in the Alluvium due to other sources in the vicinity of the Facility.

2.1 GROUNDWATER FLOW SYSTEM

Flow directions in the Alluvium are toward and along a paleochannel incised into older bedrock units. The axis of the paleochannel is roughly parallel to the current axis of the Arroyo del Puerto (Figure 1) but is located to the east of that feature, near the current location of Highway 509. QMC employed a hydrologic barrier between tailings seepage and the paleochannel since mining began, and a seepage collection system since 1983. Any flow from the QMC Facility is first to the east toward the bottom of the paleochannel and then south along the axis of the paleochannel. Flow from the DOE Facility, which has never employed a barrier or seepage collection system, is west toward the paleochannel, where it joins with flow from the QMC Facility and moves south into the QMC land withdrawal area.

2.2 MINERALOGY OF ALLUVIAL MATERIAL

Samples of alluvial material were collected in Section 30, up gradient of the QMC Facility in November 2000. A backhoe was employed to dig a ten-foot deep trench. Samples were collected at the bottom of the trench, above the water table. All samples were friable, yellow-brown, silty clay soils that contained visible plant roots. Samples were taken to Gold Hill Geologic Research in Albuquerque, New Mexico for mineral identification by thin section analysis (Attachment 1).

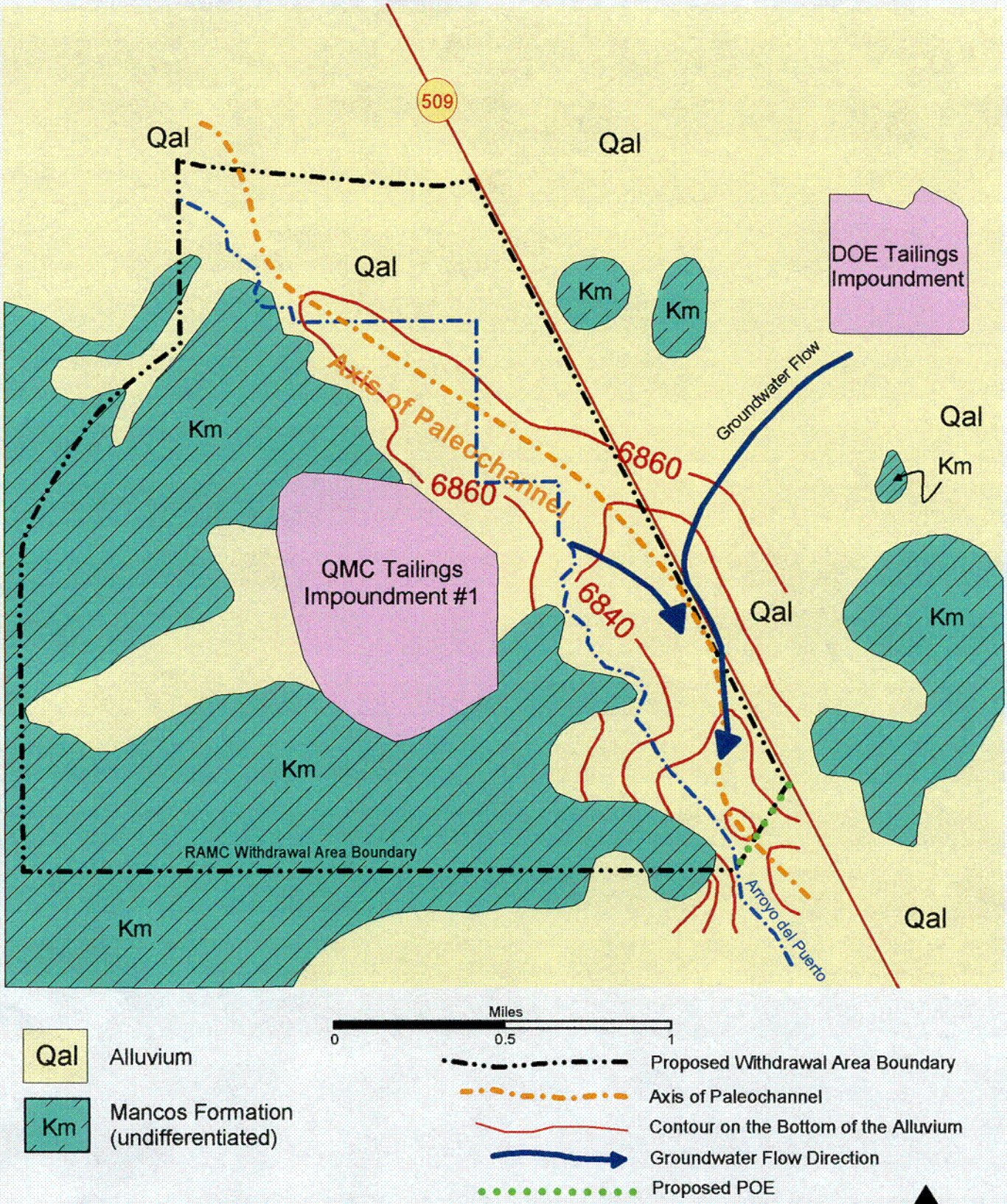

Figure 1. Simplified geologic map of the QMC Facility showing contours on the bottom of the alluvium and the trace of the axis of the paleochannel, Ambrosia Lake, New Mexico.

C05

Samples were found to contain abundant clay, quartz, and chalcedony in limonite and calcite cement. Chalcedony is a slightly more reactive form of SiO_2 than quartz and is typically present in the samples at close to 20 percent by volume. Both limonite and calcite typically exceeded 10 percent of each sample by volume. Gypsum grains were present in each sample (1-2 percent by volume) and very fine-grained magnetite was present in trace amounts.

2.3 Eh CONDITIONS

During November 2000, field measurements of oxidation reduction potential were made in 12 monitor wells in order to determine actual redox conditions in the Alluvium. Table 1 shows results of measurements corrected to the silver-silver chloride electrode. Figure 2 shows the distribution of Eh conditions near Tailings Impoundment 1.

Table 1. Eh measurements in monitor wells at the QMC Facility corrected to the silver-silver chloride electrode.

Location Code	Eh (millivolts)
31-61	429
E-5	291
S-12	287
32-72	419
S-9	26
32-58	327
32-59	332
5-03	-82
5-08	46
5-01	38
5-73	321
5-02	-102

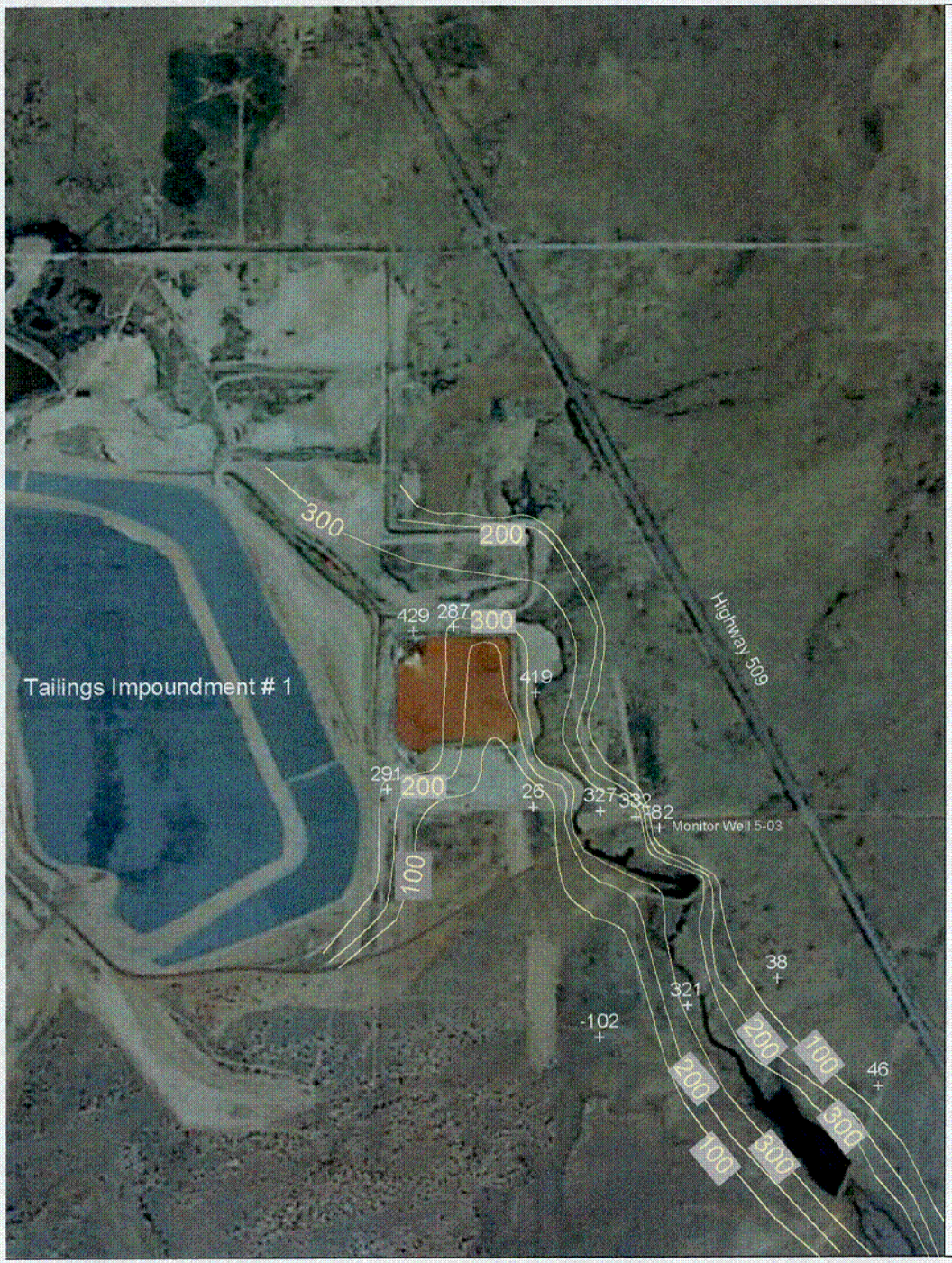

FEET

0 2000 4000

300 Line of equal Eh (millivolts)

-82 Monitor well with Eh measurement

MAXIM TECHNOLOGIES INC®

Figure 2. Contours of Eh measurements (milliVolts) in groundwater from monitor wells completed in the Alluvium, QMC Facility, Ambrosia Lake, New Mexico.

In general, Eh conditions are oxidizing in a narrow band along the flowing portion of Arroyo del Puerto, and immediately downgradient of Tailing Impoundment # 1. Conditions become more reducing in areas away from these features. The Arroyo del Puerto stream flow is a source of oxidized water to the alluvial materials, accounting for the narrow band of oxidizing groundwater adjacent to this feature. Merritt (1971) indicates that sodium chlorate ($NaClO_3$), was added to the milling process as an oxidizer to bring the solution to an Eh of between 0.400 and 0.425 volts. These values are consistent with Eh values measured in groundwater immediately downgradient of Tailings Impoundment # 1.

The sparse distribution of oxidizing conditions at the Facility, after more than 40 years of oxidizing flow in Arroyo del Puerto and seepage from Tailings Impoundment # 1 is testament to the reductive capacity of alluvial materials. Monitor well 5-03 (Figure 2) is approximately 450 feet from Arroyo del Puerto by the shortest possible pathway and has a measured Eh value of –0.082 millivolts (reducing). A quick calculation (450 feet/40 years = 11.25 feet/year) reveals that the oxidizing front, from the infiltration of Arroyo del Puerto surface water into alluvial materials, can be traveling at a ***maximum*** rate of less than 12 feet per year. This indicates that a high reductive capacity still exists in alluvial materials a short distance from features that supply oxidizing waters.

2.4 TAILINGS CONSTITUENT MOVEMENT

High concentrations of calcite in the alluvial materials have caused neutralization of tailings solutions within a few hundred feet of the tailings pile, attenuating many constituents of concern in the solution. Thus, neutralization capacity in the rest of the alluvial materials remains high.

There is no evidence that constituents of concern have reached monitor well 5-03. There is evidence that the redox front in the vicinity of monitor well 5-03 is moving at less than 12 feet per year. Monitor well 5-03 is more than 3200 feet upgradient of the QMC withdrawal area boundary (Point of Exposure). The above observations suggest that it

would take at least 260 years for the redox front (the depletion in redox capacity) to reach the withdrawal area boundary from monitor well 5-03 ((3200 feet)/12 feet/year = 267 years).

3. GEOCHEMICAL MODEL

Groundwater in the alluvium occurs in a variety of geochemical environments, therefore, it is necessary to be able to predict changes in constituent speciation and changes in mineral solubility as groundwater moves from one environment to another. Accordingly, the code selected had to be capable of chemical speciation and mass transfer (dissolution/precipitation, ion exchange/adsorption, mixing, etc.). The computer code PHREEQC (Parkhurst, 1995) was chosen for this study because it has these capabilities, it is based on the long established and well accepted PHREEQE model (Parkhurst, et al, 1980), and thermodynamic data from a variety of sources can easily be incorporated into the model.

3.1 CODE DESCRIPTION

PHREEQC is written in the C programming language and is designed to perform a variety of aqueous geochemical calculations. It is derived from the Fortran PHREEQE but has been completely rewritten to include new capabilities such as the use of redox couples to distribute redox elements among their valance states, and the ability to model ion exchange and surface complexation reactions.

The program's free-format data entry allows changes to the model to be made quickly and easily and the ability to work with a number of different databases. Three different database files are included in the model package, the PHREEQE database (Parkhurst, et al, 1980), the MINTEQ database (Allison et al, 1991), and the WATEQ4F database (Ball and Nordstrom, 1991). The MINTEQ database was used for this study because it contains several uranium species and phases. Thermodynamic data for molybdenum was taken from a summary by Rai and Zachara (1984), thorium was imported from the EQ3/6 database (Wolery, 1992), and radium data was taken from Langmuir and Riese (1985).

PHREEQC uses ion-association and Debye Huckel expressions to account for the non-ideality of aqueous solutions. The ion-exchange model assumes that the thermodynamic activity of an exchange species is equal to its equivalent fraction. The surface complexation module uses the diffuse double layer (Dzombak and Morel, 1990) and the non-electrostatic surface complexation (Davis and Kent, 1990) models.

3.2 PARAMETER SELECTION

The model takes a solution that is representative of solutions coming out of the toe of Tailings Impoundment 1 and equilibrates it with the composition of aquifer materials that have been defined through thin section analysis described above. The aquifer materials represent conditions found in the vicinity of the POE. The model input file is included as Attachment 2 of this report.

3.2.1 Initial Solution

By far, the bulk of attenuation capacity of alluvial materials is used up by neutralization of the low pH that characterizes acid leach tailings solutions and reaction of the aquifer matrix materials with major constituents of tailings solutions (sodium, sulfate, iron, and magnesium). Meanwhile, chemical interaction between the aquifer matrix and minor and trace constituents (molybdenum, nickel, selenium, radium, thorium, uranium, and lead) use little of the attenuation capacity. Therefore, to obtain conservative results, the initial model solution incorporates major element and pH data from a 1980 sampling of monitor well D-4. Sampling occurred before the 1983 installation of the interceptor trench that is a component of the approved CAP for collection of tailings seepage.

Minor and trace element concentrations for the initial model solution are taken from the highest observed concentrations in groundwater from monitor well 31-63 during the period from 1994 to the present. This well is immediately downgradient of Tailings Impoundment 1 and currently is considered to be the most contaminated well at the Facility.

3.2.2 Reactive Minerals

There are three different basic attenuation mechanisms for metals and metalloids in alluvial groundwater. Adsorption of constituents on material in the aquifer matrix is one mechanism (discussed below in the section on adsorption surface). In addition, neutralization of low pH solutions causes many metals to be removed from groundwater by precipitation of a variety of mineral phases, and reductive processes cause Eh sensitive constituents to be removed as oxide minerals (for example, uranium) or sulfide minerals (pyrite, etc.).

The model assumes the presence of the minerals calcite ($CaCO_3$), chalcedony (SiO_2), and gypsum ($CaSO_4$) in the aquifer matrix that are available to react with constituents in groundwater. The amount of each of these minerals present initially is consistent with their abundance in the matrix and their solubility in water. For example, chalcedony is the most abundant of the reactive minerals in the aquifer matrix but is the least soluble; therefore the model assumes that 0.001 moles of chalcedony are available to react with the initial solution. By contrast, calcite is only half as abundant as chalcedony but is many times more soluble. Therefore, the model assumes that 0.05 moles of calcite are available to react with the initial solution.

Magnetite is present in the aquifer matrix in trace amounts and may be an authigenic phase. Therefore it was allowed to precipitate if it came to saturation. Pyrite was also allowed to precipitate to keep the system from becoming unrealistically reducing. In addition, the following minerals were allowed to precipitate if they came to saturation: molybdenite, RaSO4, Th(OH)4(am), uraninite, and NiSe.

3.2.3 Adsorption Surface

Both clays and limonite have been observed to be abundant in the alluvial material. Both are strong adsorptive materials and serve to attenuate constituents in groundwater. Clay types are both numerous and complex and were not specifically identified in petrographic

analysis. Therefore, in spite of their adsorptive capacity, clays were not included in the model.

Limonite is a generic term for amorphous iron oxyhydroxide. More specific iron oxide phases include goethite, and hematite. Most iron oxides precipitate as amorphous iron oxyhydroxides and then, over geologic time, evolve into the more crystalline iron oxides. The common iron oxyhydroxide, ferrihydrite was chosen to represent these minerals in the model because data exist on sorbent properties of this mineral.

The model assumes that amorphous iron oxyhydroxides comprise ten percent of the alluvial material by weight. The model further assumes that only 0.1 percent of that amount is available as a sorbant surface. Therefore, each cell of the model contains 0.1 percent ferrihydrite, by weight, as an adsorption surface.

Adsorption parameters that have to be chosen for the model are surface area per amount of ferrihydrite (S_A) and surface site density (N_S) on that surface area. Langmuir (1997) gives a compilation of the range of values that has been measured for these parameters. S_A ranges from 250-600 m2/g and N_S ranges from 0.1-0.9 moles per mole of Fe. Therefore, in order to ensure that the model makes conservative predictions of attenuation due to adsorption, it was assigned S_A=250 m^2/g and N_S = 0.1 moles per mole of Fe. Ten percent of these sites were assigned as strongly binding sites and 90 percent were assigned as weakly binding sites.

3.3 Predictive Simulation

The model takes a solution that comes out of the toe of Tailings Impoundment # 1 and equilibrates it with the composition of aquifer materials that has been defined through thin section analysis described above. Results are shown in Table 2 and the model output file is included as Attachment 3 of this report.

Table 2. Concentrations of constituents at the downgradient edge of Tailings Impoundment 1(model input) and at the Point of Exposure (model output).

Constituents	mg/L In	mg/L Out	pCi/L In	pCi/L Out
Bicarbonate	0	51.0		
Calcium	1005	1061		
Chloride	2574	2574		
Iron	44	0.018		
Potassium	8.6	8.6		
Magnesium	342	342		
Molybdenum	0.201	0.00001		
Sodium	191	191		
Nickel	0.2	0.0004		
Lead	7.7E-10	1.8E-16	58	0.00001
Radium	3.6E-08	1.7E-08	35	17
Sulfate	781	785		
Selenium	0.05	7.4E-12		
Thorium	4.9E-07	4.2E-21	10	8.6E-14
Uranium	2.92	5.0E-06		

Table 3 compares modeled values of constituents of concern with concentrations of constituents in March 1999 groundwater samples from Monitor Wells 5-08 and 5-04, which contain no component of QMC tailings seepage. These wells are near the proposed POE (Figure 1) and represent current groundwater quality at the POE. Current groundwater concentrations in these wells are at or below detection levels for molybdenum, nickel and selenium in good agreement with modeled values. Modeled values for lead, thorium, and uranium are lower than observed values. The modeled value for radium closely matches the observed value.

Radionuclide concentrations can be due to local concentrations of uranium ore materials in contact with aquifer materials at that point. Uranium atoms decay to daughter product atoms (thorium-230, radium-226, and lead-210), that are unstable in the uranium mineral lattice. These atoms tend to be released from uranium minerals into groundwater because

they have different chemical properties and sizes than the original uranium atom. Thus, the concentration of these daughter products in groundwater at a location that has uranium minerals in the aquifer matrix is a balance between the rate of release to groundwater and the rate of removal by attenuation mechanisms.

Table 3. Comparison of concentrations of constituents in wells near the proposed POE boundary to modeled values.

Constituent	Modeled Concentrations	MW 5-08*	MW 5-04**
Molybdenum (mg/L)	0.00001	0.01	0.003
Nickel (mg/L)	0.0004	<0.001	<0.001
Lead-210 (pCi/L)	0.00001	4.8	2
Radium-226 (pCi/L)	17	20	0.89
Selenium (mg/L)	7.4E-12	<0.001	0.002
Thorium-230 (pCi/L)	8.6E-14	2.1	1.2
Uranium (mg/L)	5.0E-06	0.0066	0.0275

*Concentrations of constituents in March 1999 groundwater samples from Monitor Well 5-08.

**Concentrations of constituents in March 1999 groundwater samples from Monitor Well 5-04.

Radium distributions at the Facility present evidence that lead, radium, thorium, and uranium concentrations in groundwater in the vicinity of the POE are from localized sources unrelated to QMC tailings seepage. Radium is present above 5 pCi/L in three isolated areas in the alluvium (Figure 3). Two areas in the northern portion of the Facility are directly adjacent to sources. The third, at the southern end of the Facility centered on Monitor Well 5-08, is completely isolated from the other two. This isolation and the very low solubility of radium sulfate suggest a local source that is unrelated to other sources at the QMC Facility.

Monitor Well 5-08 is directly adjacent to the former haul road leading from the Coppin Mine. QMC has documented one incident in 1997 when a storm mobilized stockpiled uranium ore and spoils at the Coppin Mine (QMC, 1997). Storm runoff transported this

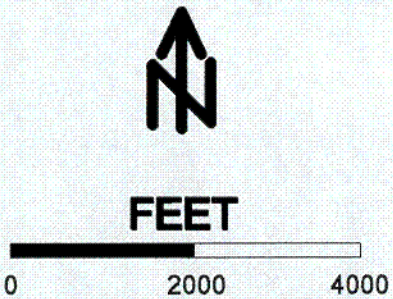

Line of equal Radium-226 concentration (pCi/L).

Monitor well with Radium-226 measurement (pCi/L).

Proposed Point of Exposure (POE).

MAXIM TECHNOLOGIES INC®

Figure 3. Contours of Radium-226 concentrations in groundwater from monitor wells completed in the Alluvium, QMC Facility, Ambrosia Lake, New Mexico.

C07

material to the stock pond between Monitor Wells 5-08 and 5-04, resulting in a discharge at the NPDES Outfall.

The good agreement between modeled constituent concentrations and constituent concentrations observed in groundwater near the proposed POE provides confidence that the model is a good predictive tool. Modeled radionuclide concentrations are lower than observed concentrations due to the presence of uranium ore materials in the aquifer that are unrelated to milling activities. Even so, observed concentrations of radioniclide constituents are far lower than concentrations observed in Monitor Wells adjacent to Tailings Impoundment 1 (model input), in accordance with model predictions. Therefore, the model is considered to be validated.

3.4 Model Assumptions And Limitations

Primary model assumptions and limitations that were considered before drawing conclusions based on geochemical modeling are:

- Only equilibrium precipitation and adsorption are modeled. Mixing with other sources of water in the alluvium and dilution and dispersion effects would result in lowering the concentrations of most, if not all, constituents of concern. Mixing and dilution and dispersion are not taken into account in this model.
- Major element data were from 1980 while concentrations of all constituents in tailings seepage have declined for the last 20 years. This feature of the model allows high confidence in predictions that risks to human health and the environment at the POE will not increase over time.
- Minor and trace element data were taken from the highest observed concentration during the period between 1994-2000. A more realistic approach would model the mean concentration. Modeling the higher concentration is more conservative.
- Gross alpha could not be included explicitly in the model because it is not an elemental parameter.

4. CONCLUSIONS

Geochemical modeling indicates that there will be a reduction in constituent concentrations in groundwater over time and over distance from the source due to natural attenuation by alluvial material. Under the current flow regime, it would take at least 260 years for the redox front (the depletion in redox capacity) to reach the withdrawal area boundary from Monitor Well 5-03. In the mean time, dilution, dispersion and mixing processes would be acting to reduce concentrations of constituents of concern along the flowpath. Hence, it would be considerably more than 260 years before the modeled concentrations in Table 3 were exceeded at the Point of Exposure.

Hydrogeologic modeling (Appendix C of the ACL Document) indicates that the alluvium will return to its premining unsaturated state in less than half that time if mine dewatering ends and flow in the Arroyo del Puerto ceases to provide current levels of recharge. The bulk of the Alluvium will be dewatered within 65 years. Therefore, all constituents that are derived from QMC milling processes will be contained within the proposed land withdrawal area as a result of geochemical and hydrogeologic processes.

5. REFERENCES

Allison, J.D., Brown, D.S., and Novo-Gradac, K.J., 1991, MINTEQA2/PRODEFA2, A geochemical assessment model for environmental systems, version 3.0 users manual, Environmental Research Laboratory, Office of Research and Development, U.S. Environmental Protection Agency, Athens Georgia, 106p.

Ball, J.W., and Nordstrom, D.K., 1991, WATEQ4F, Users manual with revised thermodynamic database and test cases for calculating speciation of major, trace and redox elements in natural waters, U.S. Geological Survey Open-File Report 90-129, 185 p.

Bostick, K., 1985, Ground-Water Discharge Plan Analysis for Kerr-McGee Nuclear Corporation Ambrosia Lake Uranium Mill, Quivira Mining Company. New Mexico Environmental Improvement Division Unpublished Report, 86p.

Davis, J.A., and Kent, D.B., 1990, Surface complexation modeling in aqueous geochemistry, in Hochella, M.F., and White, A.F., eds., *Mineral-Water Interface Geochemistry,* Washinton, D.C., Mineralogical Society of America, Reviews in Mineralogy, v. 23, p.177-260.

Dzombak, D.A., and Morel, F.M.M., 1990, *Surface complexation modeling: Hydrous ferric oxide,* New York, John Wiley, 393 p.

Langmuir , D., 1997, *Aqueous Environmental Geochemistry,* Upper Saddle River , New Jersey, Prentice Hall, 600p.

Langmuir, D., and Riese, A.C., 1985, The thermodynamic properties of radium, Geochimica et Cosmochimica Acta, v. 49, p. 1593-1601.

Merritt, R.C. 1971. *The Extractive Metallurgy of Uranium.* Prepared Under Contract with the U.S. Atomic Energy Commission by the Colorado School of Mines Research Institute.

Parkhurst, D.L., 1995, Users guide to PHREEQC, A computer program for speciation, reaction-path, advective-transport, and inverse geochemical calculations, U.S. Geological Survey, Water Resources Investigations Report 95-4227, Lakewood, Colorado, 143 p.

Parkhurst, D.L., Thorstenson, C., and Plummer, L.N., 1980. PHREEQE: A Computer Program for Geochemical Calculations. U.S. Geological Survey Report No. PB81-167801

QMC (Quivira Mining Company). 1997. NPDES Permit No. NM0020532 Outfall 001Report. Submitted to USEPA October 21, 1997.

Rai, D., and J.M. Zachara. 1984. *Chemical Attentuation Rates, Coefficients, and Constants in Leachate Migration, Volume I: A Critical Review.* EPRI, EA-3356, Research Project 2188-1.

Wolery, T.J., 1992, EQ3/6, A software package for geochemical modeling of aqueous systems: Package overview and installation guide (Ver. 7), UCRL-MA-110662 Pt.I, Lawrence Livermore National Lab.

ATTACHMENT 1: ALLUVIAL MATERIAL MINERALOGY REPORT

GOLD HILL GEOLOGICAL RESEARCH

Post Office Box 3883
Albuquerque, New Mexico 87190 U.S.A.

Telephone
(505) 899-8039

November 6, 2000

Dr. Daniel W. Erskine
Maxim Technologies, Inc.
10601 Lomas, N.E., Suite 106
Albuquerque, NM 87112

Dear Dan:

I have completed four 27x45 mm thin sections with cover glass from one of the two samples in bag No. 3. The friable rock samples required two treatments with clear epoxy. One-half of the thin sections were tested for calcite by Alizarin Red S. The petrographic report about them is presented below:

Thin Section: M. Sh.-A

Quartz - 41% of rock (0.2-0.5mm) colorless, angular to round, poorly sorted, most grains are in contact with each other, but a few appear to be floating in the rock cement. Moderate amounts of fluid inclusions are present.

Chalcedony- 24% of rock (0.1-0.2mm) pale brown, bluish white in reflected light, sub-angular to round, poorly sorted, most grains are in contact with each other, but some appear to be floating with the cement of the rock.

Limonite - 23% of rock (less than 0.05mm) brown in reflected light, appears to be an incomplete cement between the grains of the rock.

Calcite - 10% of rock (less than 0.05mm) colorless, as a cement which appears to have selectively cemented some grains and not others. Stained red by Alizarin Red S.

Gypsum - 2% of rock (0.1-0.2mm) colorless, sub-angular to round, cleavage in one direction {010}, low relief, a few grains display polysynthetic twinning.

Magnetite - Trace amount (0.05-0.1mm) black with metallic luster in reflected light, appear to be an octahedra shape.

Chalcedony- Chal
Quartz - qtz
Gypsum - gyp
Void - V
Limonite - blue ink
Calcite - red ink

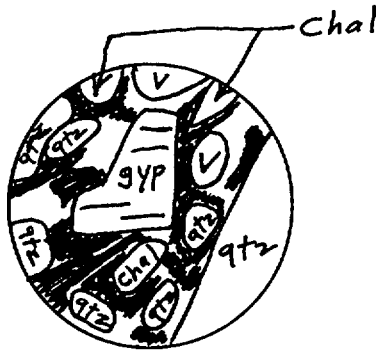

400 x
Ordinary light

Thin Section: M. Sh.-B

Quartz - 45% of rock (0.1-0.6mm) colorless, angular to round, poorly sorted, most grains are in contact with each other, but some are floating within cement of rock. Moderate amounts of fluid inclusions are present.

Chalcedony - 22% of rock (0.1-0.2mm) pale brown, bluish white in reflected light, sub-angular to round, poorly sorted, most grains are in contact with another grain, but some appear to be floating in cement.

Limonite - 20% of rock (less than 0.05mm) brown in reflected light. Appears to be an incomplete cement between grains of the rock.

Calcite - 11% of rock (less than 0.05mm) colorless, as a cement which appears to have selectively cemented some grains and not others. Stained red by Alizarin Red S.

Gypsum - 1% of rock (0.1-0.3mm) colorless, sub-angular to round, cleavage in one direction {010}, low relief, a few grains display polysynthetic twinning.

Magnetite - 1% of rock (0.05-0.1mm) black with metallic luster in reflected light, appears as an octahedral shape and triangles.

Chalcedony- Chal or C
Quartz - qtz or q
Gypsum - gyp
Void - v
Limonite - blue ink
Calcite - red ink

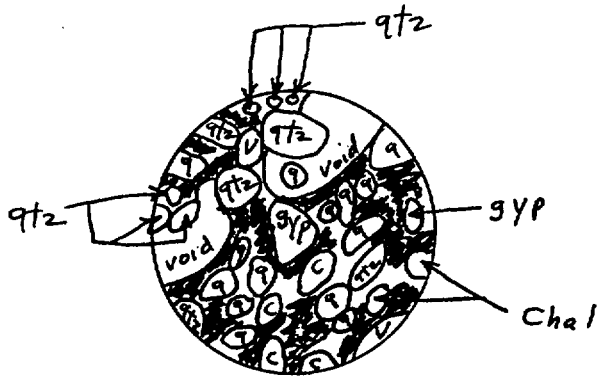

100x
Ordinary light

Thin Section: M. Sh.-C

Quartz - 48% of rock (0.1-0.3mm) colorless, angular to round, poorly sorted, most grains are in contact, but some are floating within the cement of the rock. Moderate amount of fluid inclusions are present.

Chalcedony - 25% of rock (0.1-0.2mm) pale brown, bluish white in reflected light, sub-angular to round, poorly sorted, most grains are in contact with each other but some appear to be floating within cement of rock.

Limonite - 14% of rock (less than 0.05mm) brown, in reflected light, appears to be an incomplete cement of grains and has replaced all of the magnetite (trace amount) grains present.

Calcite - 12% of rock (less than 0.05mm) colorless, as a cement which appears to have selectively cemented some grains and not others. Stained red by Alizarin Red S.

Gypsum - 1% of rock (0.1-0.5mm) colorless, subangular to round, cleavage in one direction {010}, low relief, a few grains display polysynthetic twinning.

Chalcedony - Chal
Quartz - qtz
Gypsum - gyp
Void - V
Limonite - blue ink
Calcite - red ink

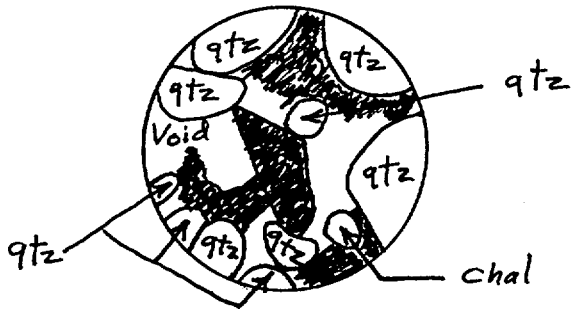

400 x
Ordinary light

Thin Section: M. Sh.-D

Quartz - 44% of rock (0.1-0.4mm) colorless, angular to round, poorly sorted, most grains are in contact with each other, but some are floating within cement of rock. Moderate amounts of fluid inclusions are present.

Chalcedony - 23% of rock (0.1-0.2mm) pale brown, bluish white in reflected light, sub-angular to round, poorly sorted, most grains are in contact with each other, but some appear to be floating in cement.

Limonite - 20% of rock (less than 0.05mm) brown in reflected light, appears to be an incomplete cement for the grains in the rock.

Calcite - 12% of rock (less than 0.05mm) colorless, as a cement which appears to have selectively cemented some grains and not others. Stained red by Alizarin Red S.

Gypsum - 1% of rock (0.1-0.2mm) colorless, sub-angular to round, cleavage in one direction {010}, low relief, a few grains display polysynthetic twinning.

Magnetite - Trace amount (0.05-0.1mm) black with metallic luster in reflected light, appears as an octahedral shape and triangle.

Chalcedony- chal
Quartz - qtz
Gypsum - gyp
Void - v
Limonite - blue ink
Calcite - red ink

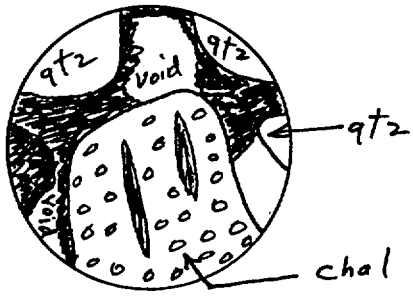

400x
Ordinary light

DISCUSSION

A. The abbreviations used in this report are as follows:

Mancos Shale M. Sh.

B. The G.S.A. color chart was used to obtain the color description of the fresh cut rock that was glued to the glass slide. The four rock samples were the same color which was a moderate yellowish brown on the fresh surface.

C. Dr. Daniel W. Erskine delivered three bags of soil samples derived from the Mancos Shale near the Quivira Mining Company's uranium mill which is located north of Grants, New Mexico. All of the samples were friable and in some cases contained a visible plant root. Dr. Erskine requested that I select one sample and make four thin sections from it which have different orientations. Sample bag 3 was chosen for the work because it appeared to have a lesser amount of clay which made vacuum impregnation with clear epoxy a more sure process. The bag contained two potato shaped samples from which the largest was chosen for the thin sections. The diagram of the orientation of the four thin sections is shown below:

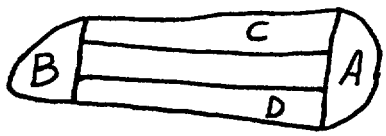

D. The element selenium is found in some water sources north of Grants, New Mexico and the question is what minerals contain selenium? According to Amstutz (1971), Selenium is found in pyrite (traces), sphalerite (traces) and selenides. A selenide is defined as a compound of selenium with one other more positive element or radical. It is clear that selenides cannot be classified as minerals. The 49th Ed. of the Handbook of Chemistry and Physics states that "selenium is found in a few rare minerals such as crook(e)site (Cu_7TISe) and Clausthalite (PbSe)." It should be noted that Northrop (1959) did not list any occurrences of Crookesite or Clausthalite in New Mexico which means that they have never been found in this state. No pyrites or sphalerite were observed in any of the four thin sections.

E. The three bags of samples were classified in the field as soils by Dr. Erskine. The petrographic analysis indicate that the calcite is very fine grained and the quartz has no overgrowths which suggests that this material should be classified as a soil. The other samples contain more clay and plant roots which is common in some soil horizons. The author of this report has not visited the sample location to measure the thickness of the outcrop and its extent in order to make a positive classification of this rock sample.

If you have any questions, please feel free to call me.

Sincerely yours,

Thomas A. Parkhill

Thomas A. Parkhill, M.S.
Geologist - Petrographer

TAP/ejm

ATTACHMENT 2: MODEL INPUT FILE

```
Input file: C:\My Documents\Rio Algom\Geochemical Modeling\POE Model D-
4 Data and 31-63 COCs Minimal Phases 2

SOLUTION 1
    temp      12
    pH        3.5
    pe        7
    units     mg/l
    redox     pe
    density   1

    Alkalinity      0
    Ca           1000
    Cl           2560
    Fe             44
    K               8.6
    Mg            340
    Mo              0.2
    Na            190
    Ni              0.2
    Pb              7.69e-010
    Ra              3.56e-008
    S(6)         1070          charge
    Se              0.05
    Th              6.25e-007
    U               2.9

 -water    1 # kg



EQUILIBRIUM_PHASES 1
    Calcite     0       0.05
    Chalcedony  0       0.001
    Gypsum      0       0.02
    Magnetite   0       0
    Molybdenite 0       0
    Pyrite      0       0
    RaSO4       0       0
    Th(OH)4(am) 0       0
    Uraninite   0       0
    NiSe        0       0

SURFACE 1
      Hfo_sOH     0.01  250   1.35
      Hfo_wOH     0.09
```

ATTACHMENT 3: MODEL OUTPUT FILE

```
Input file: C:\My Documents\Rio Algom\Geochemical Modeling\POE Model D-4 Data
and 31-63 COCs Minimal Phases 2
Output file: C:\My Documents\Rio Algom\Geochemical Modeling\POE Model D-4
Data and 31-63 COCs Minimal Phases 2.out
Database file: C:\Program Files\USGS\PhreeqcI2.2\MinteqM.dat

------------------
Reading data base.
------------------

      SOLUTION_MASTER_SPECIES
      SOLUTION_SPECIES
      SOLUTION_SPECIES
      PHASES
      SURFACE_MASTER_SPECIES
      SURFACE_SPECIES
      END
-----------------------------------
Reading input data for simulation 1.
-----------------------------------

      SOLUTION 1
          temp      12
          pH        3.5
          pe        7
          units     mg/l
          redox     pe
          density   1
          Alkalinity      0
          Ca           1000
          Cl           2560
          Fe             44
          K               8.6
          Mg            340
          Mo              0.2
          Na            190
          Ni              0.2
          Pb              7.69e-010
          Ra              3.56e-008
          S(6)         1070          charge
          Se              0.05
          Th              6.25e-007
          U               2.9
       water    1 # kg
      EQUILIBRIUM_PHASES 1
          Calcite     0       0.05
          Chalcedony  0       0.001
          Gypsum      0       0.02
          Magnetite   0       0
          Molybdenite 0       0
          Pyrite      0       0
          RaSO4       0       0
          Th(OH)4(am) 0       0
          Uraninite   0       0
          NiSe        0       0
      SURFACE 1
            Hfo_sOH     0.01  250   1.35
```

```
            Hfo_wOH      0.09
-----------------------------------------
Beginning of initial solution calculations.
-----------------------------------------

Initial solution 1.

-----------------------------Solution composition------------------------------
--

      Elements            Molality        Moles

      Ca                2.508e-002   2.508e-002
      Cl                7.259e-002   7.259e-002
      Fe                7.920e-004   7.920e-004
      K                 2.211e-004   2.211e-004
      Mg                1.406e-002   1.406e-002
      Mo                2.096e-006   2.096e-006
      Na                8.308e-003   8.308e-003
      Ni                3.424e-006   3.424e-006
      Pb                3.731e-015   3.731e-015
      Ra                1.583e-013   1.583e-013
      S(6)              8.130e-003   8.130e-003   Charge balance
      Se                6.366e-007   6.366e-007
      Th                2.094e-012   2.094e-012
      U                 1.225e-005   1.225e-005

----------------------------Description of solution----------------------------
--

                                     pH  =   3.500
                                     pe  =   7.000
                        Activity of water  =   0.998
                           Ionic strength  =  1.222e-001
                        Mass of water (kg)  =  1.000e+000
                Total alkalinity (eq/kg)  = -4.314e-004
                   Total carbon (mol/kg)  =  0.000e+000
                      Total CO2 (mol/kg)  =  0.000e+000
                     Temperature (deg C)  =  12.000
                  Electrical balance (eq)  = -2.097e-016
 Percent error, 100*(Cat-|An|)/(Cat+|An|)  =  -0.00
                                Iterations  =   8
                                   Total H  = 1.110129e+002
                                   Total O  = 5.553877e+001

----------------------------Distribution of species----------------------------
--

                                                  Log         Log         Log
      Species            Molality    Activity  Molality    Activity       Gamma

      H+               3.855e-004  3.162e-004    -3.414      -3.500      -0.086
      OH-              1.513e-011  1.135e-011   -10.820     -10.945      -0.125
      H2O              5.551e+001  9.979e-001    -0.001      -0.001       0.000
Ca              2.508e-002
      Ca+2             2.273e-002  9.174e-003    -1.643      -2.037      -0.394
      CaSO4            2.349e-003  2.416e-003    -2.629      -2.617       0.012
```

	CaOH+	3.030e-012	2.387e-012	-11.519	-11.622	-0.104
Cl		7.259e-002				
	Cl-	7.259e-002	5.404e-002	-1.139	-1.267	-0.128
	UO2Cl+	3.748e-007	2.903e-007	-6.426	-6.537	-0.111
	NiCl+	1.857e-007	1.439e-007	-6.731	-6.842	-0.111
	NiCl2	2.751e-008	2.829e-008	-7.561	-7.548	0.012
	FeCl+2	3.604e-010	1.295e-010	-9.443	-9.888	-0.444
	FeCl2+	6.214e-011	4.811e-011	-10.207	-10.318	-0.111
	FeCl3	2.528e-013	2.600e-013	-12.597	-12.585	0.012
	PbCl+	1.288e-015	9.976e-016	-14.890	-15.001	-0.111
	PbCl2	1.071e-016	1.101e-016	-15.970	-15.958	0.012
	PbCl3-	5.600e-018	4.337e-018	-17.252	-17.363	-0.111
	PbCl4-2	2.814e-019	1.013e-019	-18.551	-18.994	-0.444
	UCl+3	4.541e-023	4.555e-024	-22.343	-23.341	-0.999
Fe(2)		7.920e-004				
	Fe+2	7.366e-004	2.838e-004	-3.133	-3.547	-0.414
	FeSO4	5.540e-005	5.698e-005	-4.257	-4.244	0.012
	FeOH+	1.325e-010	1.026e-010	-9.878	-9.989	-0.111
	Fe(OH)2	8.210e-019	8.445e-019	-18.086	-18.073	0.012
	Fe(OH)3-	1.119e-025	8.663e-026	-24.951	-25.062	-0.111
Fe(3)		9.060e-009				
	Fe(OH)2+	3.334e-009	2.600e-009	-8.477	-8.585	-0.108
	FeOH+2	3.110e-009	1.118e-009	-8.507	-8.952	-0.444
	FeSO4+	1.406e-009	1.088e-009	-8.852	-8.963	-0.111
	Fe+3	7.269e-010	1.221e-010	-9.139	-9.913	-0.775
	FeCl+2	3.604e-010	1.295e-010	-9.443	-9.888	-0.444
	FeCl2+	6.214e-011	4.811e-011	-10.207	-10.318	-0.111
	Fe(SO4)2-	6.101e-011	4.725e-011	-10.215	-10.326	-0.111
	FeHSeO3+2	6.234e-013	2.243e-013	-12.205	-12.649	-0.444
	FeCl3	2.528e-013	2.600e-013	-12.597	-12.585	0.012
	Fe(OH)3	9.371e-014	9.639e-014	-13.028	-13.016	0.012
	Fe2(OH)2+4	3.516e-015	5.897e-017	-14.454	-16.229	-1.775
	Fe(OH)4-	3.900e-018	3.042e-018	-17.409	-17.517	-0.108
	Fe3(OH)4+5	1.790e-020	3.012e-023	-19.747	-22.521	-2.774
H(0)		1.576e-024				
	H2	7.881e-025	8.106e-025	-24.103	-24.091	0.012
K		2.211e-004				
	K+	2.194e-004	1.634e-004	-3.659	-3.787	-0.128
	KSO4-	1.681e-006	1.311e-006	-5.775	-5.882	-0.108
Mg		1.406e-002				
	Mg+2	1.284e-002	5.401e-003	-1.891	-2.268	-0.376
	MgSO4	1.214e-003	1.249e-003	-2.916	-2.904	0.012
	MgOH+	1.083e-011	8.597e-012	-10.966	-11.066	-0.100
Mo		2.096e-006				
	H2MoO4	1.322e-006	1.360e-006	-5.879	-5.866	0.012
	HMoO4-	5.553e-007	4.301e-007	-6.255	-6.366	-0.111
	MoO4-2	2.175e-007	7.826e-008	-6.663	-7.106	-0.444
	MoO2(OH)+	5.075e-010	3.931e-010	-9.295	-9.406	-0.111
	MoO2+2	9.756e-013	3.511e-013	-12.011	-12.455	-0.444
Na		8.308e-003				
	Na+	8.253e-003	6.397e-003	-2.083	-2.194	-0.111
	NaSO4-	5.460e-005	4.258e-005	-4.263	-4.371	-0.108
Ni		3.424e-006				
	Ni+2	2.952e-006	1.062e-006	-5.530	-5.974	-0.444
	NiSO4	2.593e-007	2.667e-007	-6.586	-6.574	0.012
	NiCl+	1.857e-007	1.439e-007	-6.731	-6.842	-0.111
	NiCl2	2.751e-008	2.829e-008	-7.561	-7.548	0.012

	Ni(SO4)2-2	6.477e-011	2.331e-011	-10.189	-10.632	-0.444
	NiOH+	2.297e-013	1.779e-013	-12.639	-12.750	-0.111
	Ni(OH)2	1.028e-018	1.058e-018	-17.988	-17.976	0.012
	NiSeO4	5.791e-024	5.956e-024	-23.237	-23.225	0.012
	Ni(OH)3-	4.309e-026	3.338e-026	-25.366	-25.477	-0.111
O(0)	0.000e+000					
	O2	0.000e+000	0.000e+000	-48.598	-48.586	0.012
Pb	3.731e-015					
	Pb+2	1.805e-015	6.495e-016	-14.744	-15.187	-0.444
	PbCl+	1.288e-015	9.976e-016	-14.890	-15.001	-0.111
	PbSO4	5.141e-016	5.287e-016	-15.289	-15.277	0.012
	PbCl2	1.071e-016	1.101e-016	-15.970	-15.958	0.012
	Pb(SO4)2-2	1.116e-017	4.017e-018	-16.952	-17.396	-0.444
	PbCl3-	5.600e-018	4.337e-018	-17.252	-17.363	-0.111
	PbCl4-2	2.814e-019	1.013e-019	-18.551	-18.994	-0.444
	PbOH+	5.160e-020	3.996e-020	-19.287	-19.398	-0.111
	Pb(OH)2	4.770e-026	4.906e-026	-25.321	-25.309	0.012
	Pb2OH+3	5.793e-033	5.811e-034	-32.237	-33.236	-0.999
	Pb(OH)3-	2.295e-033	1.777e-033	-32.639	-32.750	-0.111
	Pb(OH)4-2	0.000e+000	0.000e+000	-40.446	-40.890	-0.444
	Pb3(OH)4+2	0.000e+000	0.000e+000	-55.888	-56.332	-0.444
Ra	1.583e-013					
	Ra+2	1.583e-013	5.698e-014	-12.800	-13.244	-0.444
	RaOH+	7.512e-024	5.818e-024	-23.124	-23.235	-0.111
S(6)	8.130e-003					
	SO4-2	4.413e-003	1.448e-003	-2.355	-2.839	-0.484
	CaSO4	2.349e-003	2.416e-003	-2.629	-2.617	0.012
	MgSO4	1.214e-003	1.249e-003	-2.916	-2.904	0.012
	FeSO4	5.540e-005	5.698e-005	-4.257	-4.244	0.012
	NaSO4-	5.460e-005	4.258e-005	-4.263	-4.371	-0.108
	HSO4-	4.070e-005	3.122e-005	-4.390	-4.506	-0.115
	UO2SO4	1.731e-006	1.780e-006	-5.762	-5.749	0.012
	KSO4-	1.681e-006	1.311e-006	-5.775	-5.882	-0.108
	NiSO4	2.593e-007	2.667e-007	-6.586	-6.574	0.012
	UO2(SO4)2-2	1.975e-007	7.108e-008	-6.704	-7.148	-0.444
	FeSO4+	1.406e-009	1.088e-009	-8.852	-8.963	-0.111
	Ni(SO4)2-2	6.477e-011	2.331e-011	-10.189	-10.632	-0.444
	Fe(SO4)2-	6.101e-011	4.725e-011	-10.215	-10.326	-0.111
	PbSO4	5.141e-016	5.287e-016	-15.289	-15.277	0.012
	Pb(SO4)2-2	1.116e-017	4.017e-018	-16.952	-17.396	-0.444
	U(SO4)2	5.295e-020	5.446e-020	-19.276	-19.264	0.012
	USO4+2	7.271e-021	2.617e-021	-20.138	-20.582	-0.444
Se(-2)	1.410e-031					
	H2Se	8.348e-032	8.587e-032	-31.078	-31.066	0.012
	HSe-	5.755e-032	4.457e-032	-31.240	-31.351	-0.111
	Se-2	0.000e+000	0.000e+000	-42.744	-43.188	-0.444
Se(4)	1.189e-011					
	SeO3-2	1.189e-011	4.279e-012	-10.925	-11.369	-0.444
Se(6)	6.365e-007					
	HSeO3-	5.822e-007	4.509e-007	-6.235	-6.346	-0.111
	H2SeO3	5.437e-008	5.593e-008	-7.265	-7.252	0.012
	FeHSeO3+2	6.234e-013	2.243e-013	-12.205	-12.649	-0.444
	SeO4-2	5.083e-020	1.686e-020	-19.294	-19.773	-0.479
	HSeO4-	4.012e-022	3.108e-022	-21.397	-21.508	-0.111
	NiSeO4	5.791e-024	5.956e-024	-23.237	-23.225	0.012
Th	2.094e-012					

Th+4	2.094e-012	3.512e-014	-11.679	-13.454	-1.775
U(3)	2.028e-039				
U+3	2.028e-039	2.034e-040	-38.693	-39.692	-0.999
U(4)	1.496e-018				
U(OH)3+	6.857e-019	5.311e-019	-18.164	-18.275	-0.111
U(OH)4	3.788e-019	3.896e-019	-18.422	-18.409	0.012
U(OH)2+2	3.157e-019	1.136e-019	-18.501	-18.945	-0.444
U(SO4)2	5.295e-020	5.446e-020	-19.276	-19.264	0.012
U(OH)5-	3.052e-020	2.364e-020	-19.515	-19.626	-0.111
UOH+3	2.422e-020	2.430e-021	-19.616	-20.614	-0.999
USO4+2	7.271e-021	2.617e-021	-20.138	-20.582	-0.444
U+4	4.956e-022	8.312e-024	-21.305	-23.080	-1.775
UCl+3	4.541e-023	4.555e-024	-22.343	-23.341	-0.999
U6(OH)15+9	0.000e+000	0.000e+000	-94.237	-103.225	-8.988
U(5)	3.610e-010				
UO2+	3.610e-010	2.796e-010	-9.442	-9.553	-0.111
U(6)	1.225e-005				
UO2+2	9.889e-006	3.559e-006	-5.005	-5.449	-0.444
UO2SO4	1.731e-006	1.780e-006	-5.762	-5.749	0.012
UO2Cl+	3.748e-007	2.903e-007	-6.426	-6.537	-0.111
UO2(SO4)2-2	1.975e-007	7.108e-008	-6.704	-7.148	-0.444
UO2OH+	5.370e-008	4.159e-008	-7.270	-7.381	-0.111
(UO2)2(OH)2+2	3.612e-010	1.300e-010	-9.442	-9.886	-0.444
(UO2)3(OH)5+	6.750e-016	5.228e-016	-15.171	-15.282	-0.111

----------Saturation indices----------
--

Phase	SI	log IAP	log KT	
Anglesite	-10.16	-18.03	-7.86	PbSO4
Anhydrite	-0.37	-4.88	-4.51	CaSO4
B_UO2(OH)2	-4.45	1.55	6.00	UO2(OH)2
Brucite	-12.92	4.73	17.66	Mg(OH)2
Bunsenite	-12.22	1.03	13.25	NiO
CaMoO4(c)	-1.20	-9.14	-7.94	CaMoO4
CaSeO3:2H2O	-7.85	-42.81	-34.96	CaSeO3:2H2O
CaSeO4:2H2O	-18.84	-21.81	-2.98	CaSeO4:2H2O
Clausthalite	-20.89	-118.96	-98.07	PbSe
Cotunnite	-12.76	-17.72	-4.96	PbCl2
Epsomite	-2.88	-5.11	-2.23	MgSO4:7H2O
Fe(OH)2.7Cl0.3	2.19	-0.85	-3.04	Fe(OH)2.7Cl0.3
Fe2(MoO4)3	-2.33	-41.15	-38.82	Fe2(MoO4)3
Fe2(OH)4SeO3	-10.23	-46.60	-36.37	Fe2(OH)4SeO3
Fe2(SeO3)3:2H2O	-7.74	-142.14	-134.40	Fe2(SeO3)3:2H2O
Fe2(SO4)3	-33.90	-28.34	5.56	Fe2(SO4)3
Fe3(OH)8	-15.60	-8.75	6.86	Fe3(OH)8
FeMoO4(c)	-2.95	-24.02	-21.07	FeMoO4
Ferrihydrite	-4.31	0.58	4.89	Fe(OH)3
Ferroselite	-26.28	-210.45	-184.18	FeSe2
FeSe	-24.23	-120.68	-96.45	FeSe
Goethite	-0.40	0.58	0.98	FeOOH
Gummite	-9.62	1.55	11.17	UO3
Gypsum	-0.02	-4.88	-4.86	CaSO4:2H2O
H2MoO4(c)	-0.74	-14.11	-13.37	H2MoO4
Halite	-5.01	-3.46	1.55	NaCl

Hematite	4.15	1.17	-2.98	Fe2O3
Jarosite-H	-7.67	-17.92	-10.26	(H3O)Fe3(SO4)2(OH)6
Jarosite-K	-4.46	-18.21	-13.75	KFe3(SO4)2(OH)6
Jarosite-Na	-6.63	-16.62	-9.99	NaFe3(SO4)2(OH)6
Larnakite	-26.15	-26.22	-0.06	PbO:PbSO4
Laurionite	-13.58	-12.96	0.62	PbOHCl
Lepidocrocite	-0.79	0.58	1.37	FeOOH
Lime	-29.38	4.96	34.34	CaO
Litharge	-21.46	-8.19	13.27	PbO
Maghemite	-5.22	1.17	6.39	Fe2O3
Magnetite	-0.80	-8.74	-7.94	Fe3O4
Massicot	-21.66	-8.19	13.47	PbO
Melanterite	-3.83	-19.76	-15.93	FeSO4:7H2O
Mg-Ferrite	-13.09	5.90	18.99	MgFe2O4
MgMoO4(c)	-8.75	-9.37	-0.62	MgMoO4
MgSeO3:6H2O	-9.11	-43.05	-33.94	MgSeO3:6H2O
Minium	-80.69	-3.57	77.12	Pb3O4
Mirabilite	-5.49	-7.24	-1.75	Na2SO4:10H2O
Mo(c)	-47.08	-77.10	-30.02	Mo
Molybdite	-2.01	-14.11	-12.10	MoO3
MoO2(c)	-5.08	-35.10	-30.02	MoO2
Morenosite	-6.36	-8.82	-2.46	NiSO4:7H2O
Ni(OH)2	-8.76	1.02	9.78	Ni(OH)2
Ni4(OH)6SO4	-37.74	-5.74	32.00	Ni4(OH)6SO4
NiSe	-16.09	-109.74	-93.66	NiSe
NiSeO3:2H2O	-11.88	-46.75	-34.86	NiSeO3:2H2O
O2(g)	-45.59	42.00	87.59	O2
Pb(OH)2(C)	-16.81	-8.19	8.62	Pb(OH)2
Pb2(OH)3Cl	-29.94	-21.14	8.79	Pb2(OH)3Cl
Pb2O(OH)2	-42.58	-16.38	26.20	Pb2O(OH)2
Pb2O3	-56.42	4.62	61.04	Pb2O3
Pb3O2SO4	-45.50	-34.40	11.09	Pb3O2SO4
Pb4(OH)6SO4	-63.69	-42.59	21.10	Pb4(OH)6SO4
Pb4O3SO4	-65.86	-42.59	23.27	Pb4O3SO4
PbMetal	-33.44	-29.19	4.26	Pb
PbO:0.3H2O	-21.17	-8.19	12.98	PbO:0.33H2O
PbSeO4	-27.99	-34.96	-6.97	PbSeO4
Periclase	-17.99	4.73	22.72	MgO
Plattnerite	-38.85	12.81	51.66	PbO2
Portlandite	-18.74	4.96	23.70	Ca(OH)2
RaSO4	-5.51	-16.08	-10.57	RaSO4
Retgersite	-6.74	-8.82	-2.08	NiSO4:6H2O
Schoepite	-4.26	1.55	5.81	UO2(OH)2:H2O
Se(A)	-6.65	-89.77	-83.12	Se
Se(hex)	-6.03	-89.77	-83.74	Se
SeO2	-9.96	-47.77	-37.81	SeO2
SeO3	-48.99	-26.77	22.21	SeO3
Th(OH)4(am)	-1.27	0.54	1.81	Th(OH)4
Thenardite	-7.07	-7.23	-0.16	Na2SO4
U3O8(C)	-10.23	-16.35	-6.12	U3O8
U4O9(C)	-15.33	-56.80	-41.47	U4O9
UO2(am)	-10.89	-19.45	-8.56	UO2
UO3(C)	-6.81	1.55	8.36	UO3
Uraninite	-5.00	-19.45	-14.44	UO2

Beginning of batch-reaction calculations.

Reaction step 1.

Using solution 1.
Using surface 1.
Using pure phase assemblage 1.

----------Phase assemblage----------

Phase	SI	log IAP	log KT	Moles in assemblage Initial	Final	Delta
Calcite	0.00	-8.41	-8.41	5.000e-002	4.916e-002	-8.366e-004
Chalcedony	0.00	-3.68	-3.68	1.000e-003	7.960e-004	-2.040e-004
Gypsum	0.00	-4.86	-4.86	2.000e-002	6.506e-003	-1.349e-002
Magnetite	0.00	32.16	32.16	0.000e+000	2.534e-004	2.534e-004
Molybdenite	-0.00	-141.18	-141.18	0.000e+000	2.096e-006	2.096e-006
NiSe	0.00	-17.74	-17.74	0.000e+000	6.366e-007	6.366e-007
Pyrite	0.00	-90.20	-90.20	0.000e+000	3.148e-005	3.148e-005
RaSO4	-5.83	-16.41	-10.57	0.000e+000		0.000e+000
Th(OH)4(am)	0.00	1.81	1.81	0.000e+000	2.094e-012	2.094e-012
Uraninite	0.00	-14.44	-14.44	0.000e+000	1.225e-005	1.225e-005

----------Surface composition----------

Hfo

1.249e-004	Surface charge, eq
3.572e-002	sigma, C/m**2
3.924e-002	psi, V
-1.597e+000	-F*psi/RT
2.025e-001	exp(-F*psi/RT)
2.500e+002	specific area, m**2/g
3.375e+002	m**2 for 1.350e+000 g

Hfo_s

1.000e-002 moles

Species	Moles	Mole Fraction	Molality	Log Molality
Hfo_sOHCa+2	9.596e-003	0.960	9.592e-003	-2.018
Hfo_sOH	2.599e-004	0.026	2.598e-004	-3.585
Hfo_sOHSO4-2	5.660e-005	0.006	5.657e-005	-4.247
Hfo_sOH2+	4.752e-005	0.005	4.750e-005	-4.323
Hfo_sO-	3.257e-005	0.003	3.256e-005	-4.487
Hfo_sSO4-	5.197e-006	0.001	5.195e-006	-5.284
Hfo_sONi+	1.875e-006	0.000	1.874e-006	-5.727
Hfo_sOHRa+2	8.285e-014	0.000	8.281e-014	-13.082
Hfo_sOPb+	3.700e-015	0.000	3.698e-015	-14.432

Hfo_w

9.000e-002 moles

Species	Moles	Mole Fraction	Molality	Log Molality

Hfo_wOH	5.606e-002	0.623	5.603e-002	-1.252
Hfo_wOHSO4-2	1.221e-002	0.136	1.220e-002	-1.914
Hfo_wOH2+	1.025e-002	0.114	1.024e-002	-1.990
Hfo_wO-	7.024e-003	0.078	7.021e-003	-2.154
Hfo_wOCa+	3.341e-003	0.037	3.339e-003	-2.476
Hfo_wSO4-	1.121e-003	0.012	1.120e-003	-2.951
Hfo_wONi+	9.054e-007	0.000	9.049e-007	-6.043
Hfo_wORa+	4.169e-016	0.000	4.167e-016	-15.380
Hfo_wOPb+	3.104e-017	0.000	3.103e-017	-16.508

----------Solution composition----------
--

Elements	Molality	Moles
C	8.362e-004	8.366e-004
Ca	2.646e-002	2.647e-002
Cl	7.255e-002	7.259e-002
Fe	3.179e-007	3.180e-007
K	2.210e-004	2.211e-004
Mg	1.405e-002	1.406e-002
Mo	6.609e-011	6.612e-011
Na	8.304e-003	8.308e-003
Ni	7.238e-009	7.241e-009
Pb	8.548e-022	8.552e-022
Ra	7.503e-014	7.507e-014
S	8.164e-003	8.168e-003
Se	9.363e-017	9.368e-017
Si	2.039e-004	2.040e-004
Th	1.802e-026	1.803e-026
U	2.113e-011	2.114e-011

----------Description of solution----------
--

pH = 7.334 Charge balance
pe = -2.841 Adjusted to redox equilibrium
Activity of water = 0.998
Ionic strength = 1.233e-001
Mass of water (kg) = 1.000e+000
Total alkalinity (eq/kg) = 7.960e-004
Total CO2 (mol/kg) = 8.362e-004
Temperature (deg C) = 12.000
Electrical balance (eq) = -1.249e-004
Percent error, 100*(Cat-|An|)/(Cat+|An|) = -0.08
Iterations = 41
Total H = 1.110681e+002
Total O = 5.556919e+001

----------Distribution of species----------
--

Species	Molality	Activity	Log Molality	Log Activity	Log Gamma

	OH-	1.034e-007	7.755e-008	-6.985	-7.110	-0.125
	H+	5.647e-008	4.630e-008	-7.248	-7.334	-0.086
	H2O	5.551e+001	9.978e-001	-0.001	-0.001	0.000
C(4)		8.362e-004				
	HCO3-	6.941e-004	5.410e-004	-3.159	-3.267	-0.108
	H2CO3	4.768e-005	4.905e-005	-4.322	-4.309	0.012
	CaHCO3+	4.610e-005	3.630e-005	-4.336	-4.440	-0.104
	MgHCO3+	3.987e-005	3.024e-005	-4.399	-4.519	-0.120
	CaCO3	4.234e-006	4.356e-006	-5.373	-5.361	0.012
	MgCO3	1.638e-006	1.685e-006	-5.786	-5.773	0.012
	NaHCO3	1.387e-006	1.427e-006	-5.858	-5.846	0.012
	CO3-2	1.087e-006	4.013e-007	-5.964	-6.397	-0.433
	NaCO3-	3.072e-008	2.394e-008	-7.513	-7.621	-0.108
	NiCO3	3.376e-009	3.473e-009	-8.472	-8.459	0.012
	NiHCO3+	8.269e-011	6.401e-011	-10.083	-10.194	-0.111
	Ni(CO3)2-2	6.746e-012	2.422e-012	-11.171	-11.616	-0.445
	UO2(CO3)2-2	2.533e-016	9.096e-017	-15.596	-16.041	-0.445
	UO2(CO3)3-4	1.386e-016	2.303e-018	-15.858	-17.638	-1.779
	UO2CO3	3.537e-017	3.639e-017	-16.451	-16.439	0.012
	PbCO3	4.301e-022	4.424e-022	-21.366	-21.354	0.012
	PbHCO3+	2.413e-023	1.868e-023	-22.617	-22.729	-0.111
	Pb(CO3)2-2	1.242e-024	4.460e-025	-23.906	-24.351	-0.445
Ca		2.646e-002				
	Ca+2	2.394e-002	9.643e-003	-1.621	-2.016	-0.395
	CaSO4	2.470e-003	2.541e-003	-2.607	-2.595	0.012
	CaHCO3+	4.610e-005	3.630e-005	-4.336	-4.440	-0.104
	CaCO3	4.234e-006	4.356e-006	-5.373	-5.361	0.012
	CaOH+	2.177e-008	1.714e-008	-7.662	-7.766	-0.104
Cl		7.255e-002				
	Cl-	7.255e-002	5.397e-002	-1.139	-1.268	-0.129
	NiCl+	2.040e-010	1.579e-010	-9.690	-9.802	-0.111
	NiCl2	3.014e-011	3.101e-011	-10.521	-10.509	0.012
	UO2Cl+	7.881e-022	6.101e-022	-21.103	-21.215	-0.111
	PbCl+	1.257e-022	9.730e-023	-21.901	-22.012	-0.111
	FeCl+2	2.083e-023	7.466e-024	-22.681	-23.127	-0.446
	PbCl2	1.043e-023	1.073e-023	-22.982	-22.969	0.012
	FeCl2+	3.579e-024	2.769e-024	-23.446	-23.558	-0.111
	PbCl3-	5.450e-025	4.219e-025	-24.264	-24.375	-0.111
	PbCl4-2	2.740e-026	9.838e-027	-25.562	-26.007	-0.445
	FeCl3	1.453e-026	1.494e-026	-25.838	-25.826	0.012
	UCl+3	2.117e-033	2.112e-034	-32.674	-33.675	-1.001
Fe(2)		3.179e-007				
	Fe+2	2.953e-007	1.135e-007	-6.530	-6.945	-0.415
	FeSO4	2.217e-008	2.281e-008	-7.654	-7.642	0.012
	FeOH+	3.622e-010	2.802e-010	-9.441	-9.552	-0.111
	Fe(OH)2	1.532e-014	1.576e-014	-13.815	-13.802	0.012
	Fe(OH)3-	1.427e-017	1.104e-017	-16.846	-16.957	-0.111
	Fe(HS)2	1.241e-019	1.277e-019	-18.906	-18.894	0.012
	Fe(HS)3-	6.379e-028	4.938e-028	-27.195	-27.306	-0.111
Fe(3)		1.120e-014				
	Fe(OH)2+	8.982e-015	7.001e-015	-14.047	-14.155	-0.108
	Fe(OH)3	1.723e-015	1.773e-015	-14.764	-14.751	0.012
	Fe(OH)4-	4.903e-016	3.821e-016	-15.310	-15.418	-0.108
	FeOH+2	1.229e-018	4.407e-019	-17.910	-18.356	-0.446
	FeSO4+	8.124e-023	6.286e-023	-22.090	-22.202	-0.111
	Fe+3	4.211e-023	7.049e-024	-22.376	-23.152	-0.776
	FeCl+2	2.083e-023	7.466e-024	-22.681	-23.127	-0.446

	FeCl2+	3.579e-024	2.769e-024	-23.446	-23.558	-0.111
	Fe(SO4)2-	3.528e-024	2.731e-024	-23.453	-23.564	-0.111
	FeCl3	1.453e-026	1.494e-026	-25.838	-25.826	0.012
	Fe2(OH)2+4	5.514e-034	9.165e-036	-33.259	-35.038	-1.779
	Fe3(OH)4+5	0.000e+000	0.000e+000	-44.119	-46.899	-2.780
	FeHSeO3+2	0.000e+000	0.000e+000	-46.270	-46.715	-0.445
H(0)		1.622e-012				
	H2	8.111e-013	8.345e-013	-12.091	-12.079	0.012
K		2.210e-004				
	K+	2.193e-004	1.631e-004	-3.659	-3.787	-0.129
	KSO4-	1.680e-006	1.310e-006	-5.775	-5.883	-0.108
Mg		1.405e-002				
	Mg+2	1.280e-002	5.374e-003	-1.893	-2.270	-0.377
	MgSO4	1.208e-003	1.243e-003	-2.918	-2.906	0.012
	MgHCO3+	3.987e-005	3.024e-005	-4.399	-4.519	-0.120
	MgCO3	1.638e-006	1.685e-006	-5.786	-5.773	0.012
	MgOH+	7.362e-008	5.842e-008	-7.133	-7.233	-0.100
Mo		6.609e-011				
	MoO4-2	6.607e-011	2.372e-011	-10.180	-10.625	-0.445
	HMoO4-	2.466e-014	1.909e-014	-13.608	-13.719	-0.111
	H2MoO4	8.588e-018	8.836e-018	-17.066	-17.054	0.012
	MoO2(OH)+	4.830e-025	3.739e-025	-24.316	-24.427	-0.111
	MoO2+2	1.362e-031	4.889e-032	-30.866	-31.311	-0.445
Na		8.304e-003				
	Na+	8.248e-003	6.389e-003	-2.084	-2.195	-0.111
	NaSO4-	5.460e-005	4.256e-005	-4.263	-4.371	-0.108
	NaHCO3	1.387e-006	1.427e-006	-5.858	-5.846	0.012
	NaCO3-	3.072e-008	2.394e-008	-7.513	-7.621	-0.108
Ni		7.238e-009				
	NiCO3	3.376e-009	3.473e-009	-8.472	-8.459	0.012
	Ni+2	3.251e-009	1.167e-009	-8.488	-8.933	-0.445
	NiSO4	2.851e-010	2.933e-010	-9.545	-9.533	0.012
	NiCl+	2.040e-010	1.579e-010	-9.690	-9.802	-0.111
	NiHCO3+	8.269e-011	6.401e-011	-10.083	-10.194	-0.111
	NiCl2	3.014e-011	3.101e-011	-10.521	-10.509	0.012
	Ni(CO3)2-2	6.746e-012	2.422e-012	-11.171	-11.616	-0.445
	NiOH+	1.726e-012	1.336e-012	-11.763	-11.874	-0.111
	Ni(SO4)2-2	7.144e-014	2.565e-014	-13.146	-13.591	-0.445
	Ni(OH)2	5.272e-014	5.423e-014	-13.278	-13.266	0.012
	Ni(OH)3-	1.510e-017	1.169e-017	-16.821	-16.932	-0.111
	NiSeO4	0.000e+000	0.000e+000	-55.201	-55.189	0.012
O(0)		0.000e+000				
	O2	0.000e+000	0.000e+000	-72.624	-72.611	0.012
Pb		8.548e-022				
	PbCO3	4.301e-022	4.424e-022	-21.366	-21.354	0.012
	Pb+2	1.767e-022	6.344e-023	-21.753	-22.198	-0.445
	PbCl+	1.257e-022	9.730e-023	-21.901	-22.012	-0.111
	PbSO4	5.023e-023	5.168e-023	-22.299	-22.287	0.012
	PbOH+	3.444e-023	2.666e-023	-22.463	-22.574	-0.111
	PbHCO3+	2.413e-023	1.868e-023	-22.617	-22.729	-0.111
	PbCl2	1.043e-023	1.073e-023	-22.982	-22.969	0.012
	Pb(CO3)2-2	1.242e-024	4.460e-025	-23.906	-24.351	-0.445
	Pb(SO4)2-2	1.094e-024	3.929e-025	-23.961	-24.406	-0.445
	PbCl3-	5.450e-025	4.219e-025	-24.264	-24.375	-0.111
	Pb(OH)2	2.173e-025	2.236e-025	-24.663	-24.651	0.012
	PbCl4-2	2.740e-026	9.838e-027	-25.562	-26.007	-0.445
	Pb(HS)2	1.449e-028	1.490e-028	-27.839	-27.827	0.012

	Pb(OH)3-	7.147e-029	5.532e-029	-28.146	-28.257	-0.111
	Pb(OH)4-2	7.626e-033	2.738e-033	-32.118	-32.563	-0.445
	Pb(HS)3-	1.365e-037	1.056e-037	-36.865	-36.976	-0.111
	Pb2OH+3	0.000e+000	0.000e+000	-42.421	-43.422	-1.001
	Pb3(OH)4+2	0.000e+000	0.000e+000	-61.580	-62.024	-0.445
Ra	7.503e-014					
	Ra+2	7.503e-014	2.694e-014	-13.125	-13.570	-0.445
	RaOH+	2.427e-020	1.879e-020	-19.615	-19.726	-0.111
S(-2)	7.269e-011					
	HS-	4.737e-011	3.552e-011	-10.324	-10.450	-0.125
	H2S	2.171e-011	2.233e-011	-10.663	-10.651	0.012
	S6-2	2.810e-013	1.009e-013	-12.551	-12.996	-0.445
	S5-2	2.655e-013	9.532e-014	-12.576	-13.021	-0.445
	S4-2	1.502e-013	5.393e-014	-12.823	-13.268	-0.445
	S-2	1.019e-016	3.653e-017	-15.992	-16.437	-0.446
	S3-2	5.015e-017	1.801e-017	-16.300	-16.745	-0.445
	S2-2	2.635e-018	9.462e-019	-17.579	-18.024	-0.445
	Fe(HS)2	1.241e-019	1.277e-019	-18.906	-18.894	0.012
	Fe(HS)3-	6.379e-028	4.938e-028	-27.195	-27.306	-0.111
	Pb(HS)2	1.449e-028	1.490e-028	-27.839	-27.827	0.012
	Pb(HS)3-	1.365e-037	1.056e-037	-36.865	-36.976	-0.111
S(6)	8.164e-003					
	SO4-2	4.430e-003	1.449e-003	-2.354	-2.839	-0.485
	CaSO4	2.470e-003	2.541e-003	-2.607	-2.595	0.012
	MgSO4	1.208e-003	1.243e-003	-2.918	-2.906	0.012
	NaSO4-	5.460e-005	4.256e-005	-4.263	-4.371	-0.108
	KSO4-	1.680e-006	1.310e-006	-5.775	-5.883	-0.108
	FeSO4	2.217e-008	2.281e-008	-7.654	-7.642	0.012
	HSO4-	5.967e-009	4.573e-009	-8.224	-8.340	-0.116
	NiSO4	2.851e-010	2.933e-010	-9.545	-9.533	0.012
	Ni(SO4)2-2	7.144e-014	2.565e-014	-13.146	-13.591	-0.445
	UO2SO4	3.645e-021	3.749e-021	-20.438	-20.426	0.012
	UO2(SO4)2-2	4.172e-022	1.498e-022	-21.380	-21.825	-0.445
	FeSO4+	8.124e-023	6.286e-023	-22.090	-22.202	-0.111
	PbSO4	5.023e-023	5.168e-023	-22.299	-22.287	0.012
	Fe(SO4)2-	3.528e-024	2.731e-024	-23.453	-23.564	-0.111
	Pb(SO4)2-2	1.094e-024	3.929e-025	-23.961	-24.406	-0.445
	U(SO4)2	2.461e-030	2.532e-030	-29.609	-29.596	0.012
	USO4+2	3.386e-031	1.216e-031	-30.470	-30.915	-0.445
Se(-2)	9.363e-017					
	HSe-	9.361e-017	7.246e-017	-16.029	-16.140	-0.111
	H2Se	1.987e-020	2.044e-020	-19.702	-19.690	0.012
	Se-2	2.005e-024	7.201e-025	-23.698	-24.143	-0.445
Se(4)	1.213e-028					
	SeO3-2	1.213e-028	4.354e-029	-27.916	-28.361	-0.445
Se(6)	8.678e-028					
	HSeO3-	8.678e-028	6.717e-028	-27.062	-27.173	-0.111
	H2SeO3	1.186e-032	1.220e-032	-31.926	-31.914	0.012
	FeHSeO3+2	0.000e+000	0.000e+000	-46.270	-46.715	-0.445
	SeO4-2	0.000e+000	0.000e+000	-48.298	-48.778	-0.481
	HSeO4-	0.000e+000	0.000e+000	-54.236	-54.347	-0.111
	NiSeO4	0.000e+000	0.000e+000	-55.201	-55.189	0.012
Si	2.039e-004					
	H4SiO4	2.035e-004	2.094e-004	-3.691	-3.679	0.012
	H3SiO4-	3.453e-007	2.619e-007	-6.462	-6.582	-0.120
	H2SiO4-2	5.932e-012	2.189e-012	-11.227	-11.660	-0.433
	UO2H3SiO4+	1.742e-019	1.348e-019	-18.759	-18.870	-0.111

Th		1.802e-026				
	Th+4	1.802e-026	2.995e-028	-25.744	-27.524	-1.779
U(3)		6.560e-040				
	U+3	6.560e-040	0.000e+000	-39.183	-40.184	-1.001
U(4)		2.112e-011				
	U(OH)5-	2.108e-011	1.632e-011	-10.676	-10.787	-0.111
	U(OH)4	3.828e-014	3.938e-014	-13.417	-13.405	0.012
	U(OH)3+	1.015e-017	7.860e-018	-16.993	-17.105	-0.111
	U(OH)2+2	6.855e-022	2.461e-022	-21.164	-21.609	-0.445
	UOH+3	7.723e-027	7.707e-028	-26.112	-27.113	-1.001
	U(SO4)2	2.461e-030	2.532e-030	-29.609	-29.596	0.012
	USO4+2	3.386e-031	1.216e-031	-30.470	-30.915	-0.445
	U+4	2.322e-032	3.860e-034	-31.634	-33.413	-1.779
	UCl+3	2.117e-033	2.112e-034	-32.674	-33.675	-1.001
	U6(OH)15+9	0.000e+000	0.000e+000	-98.699	-107.707	-9.008
U(5)		5.269e-015				
	UO2+	5.269e-015	4.079e-015	-14.278	-14.389	-0.111
U(6)		4.283e-016				
	UO2(CO3)2-2	2.533e-016	9.096e-017	-15.596	-16.041	-0.445
	UO2(CO3)3-4	1.386e-016	2.303e-018	-15.858	-17.638	-1.779
	UO2CO3	3.537e-017	3.639e-017	-16.451	-16.439	0.012
	UO2OH+	7.723e-019	5.978e-019	-18.112	-18.223	-0.111
	UO2H3SiO4+	1.742e-019	1.348e-019	-18.759	-18.870	-0.111
	UO2+2	2.086e-020	7.490e-021	-19.681	-20.126	-0.445
	UO2SO4	3.645e-021	3.749e-021	-20.438	-20.426	0.012
	UO2Cl+	7.881e-022	6.101e-022	-21.103	-21.215	-0.111
	UO2(SO4)2-2	4.172e-022	1.498e-022	-21.380	-21.825	-0.445
	(UO2)2(OH)2+2	7.481e-032	2.686e-032	-31.126	-31.571	-0.445
	(UO2)3(OH)5+	0.000e+000	0.000e+000	-40.029	-40.140	-0.111

----------Saturation indices----------
--

Phase	SI	log IAP	log KT	
Akerminite	-19.68	30.35	50.03	Ca2MgSi2O7
Anglesite	-17.17	-25.04	-7.86	PbSO4
Anhydrite	-0.34	-4.85	-4.51	CaSO4
Aragonite	-0.15	-8.41	-8.26	CaCO3
Artinite	-6.83	3.73	10.56	MgCO3:Mg(OH)2:3H2O
B_UO2(OH)2	-11.46	-5.46	6.00	UO2(OH)2
Brucite	-5.26	12.40	17.66	Mg(OH)2
Bunsenite	-7.51	5.74	13.25	NiO
Ca-Olivine	-17.85	21.63	39.48	Ca2SiO4
Ca3SiO5	-43.14	34.28	77.42	Ca3SiO5
Calcite	0.00	-8.41	-8.41	CaCO3
CaMoO4(c)	-4.70	-12.64	-7.94	CaMoO4
CaSeO3:2H2O	-24.83	16.14	40.96	CaSeO3:2H2O
CaSeO4:2H2O	-47.82	25.12	72.94	CaSeO4:2H2O
Cerrusite	-15.30	-28.59	-13.29	PbCO3
CH4(g)	-14.87	-57.01	-42.14	CH4
Chalcedony	0.00	-3.68	-3.68	SiO2
Chrysotile	-4.10	29.84	33.94	Mg3Si2O5(OH)4
Clausthalite	-8.85	-31.00	-22.15	PbSe
Clinoenstatite	-3.29	8.72	12.01	MgSiO3
CO2(g)	-2.89	-21.06	-18.18	CO2
Cotunnite	-19.78	-24.73	-4.96	PbCl2

Cristobalite	0.09	-3.68	-3.77	SiO2
Diopside	-3.27	17.70	20.96	CaMgSi2O6
Dolomite	-0.36	-17.08	-16.72	CaMg(CO3)2
Epsomite	-2.88	-5.12	-2.23	MgSO4:7H2O
Fe(OH)2.7Cl0.3	-0.69	9.63	10.33	Fe(OH)2.7Cl0.3
Fe2(MoO4)3	-39.36	-51.45	-12.09	Fe2(MoO4)3
Fe2(OH)4SeO3	-38.36	27.92	66.28	Fe2(OH)4SeO3
Fe2(SeO3)3:2H2O	-85.19	34.89	120.08	Fe2(SeO3)3:2H2O
Fe2(SO4)3	-60.38	-28.09	32.29	Fe2(SO4)3
Fe3(OH)8	-14.80	32.15	46.95	Fe3(OH)8
FeMoO4(c)	-9.87	-17.57	-7.70	FeMoO4
Ferrihydrite	-6.04	12.21	18.26	Fe(OH)3
Ferroselite	-11.26	-30.24	-18.97	FeSe2
FeS(ppt)	-6.14	-45.73	-39.58	FeS
FeSe	-8.59	-15.75	-7.16	FeSe
Forsterite	-8.80	21.12	29.92	Mg2SiO4
Galena	-9.53	-60.98	-51.45	PbS
Goethite	-2.13	12.22	14.35	FeOOH
Greenalite	-5.00	15.81	20.81	Fe3Si2O5(OH)4
Greigite	-20.67	-181.66	-160.98	Fe3S4
Gummite	-16.63	-5.46	11.17	UO3
Gypsum	0.00	-4.86	-4.86	CaSO4:2H2O
H2MoO4(c)	-11.92	-25.29	-13.37	H2MoO4
H2S(g)	-9.81	-53.45	-43.65	H2S
Halite	-5.01	-3.46	1.55	NaCl
Hematite	0.68	24.43	23.76	Fe2O3
Huntite	-5.30	-34.41	-29.11	CaMg3(CO3)4
Hydcerrusite	-47.26	-64.72	-17.46	Pb(OH)2:2PbCO3
Hydromagnesite	-15.25	-22.27	-7.02	Mg5(CO3)4(OH)2:4H2O
Jarosite-H	-28.21	1.63	29.84	(H3O)Fe3(SO4)2(OH)6
Jarosite-K	-21.17	5.18	26.34	KFe3(SO4)2(OH)6
Jarosite-Na	-23.34	6.77	30.11	NaFe3(SO4)2(OH)6
Larnakite	-32.50	-32.57	-0.06	PbO:PbSO4
Larnite	-19.43	21.63	41.05	Ca2SiO4
Laurionite	-16.75	-16.13	0.62	PbOHCl
Lepidocrocite	-2.52	12.22	14.74	FeOOH
Lime	-21.69	12.65	34.34	CaO
Litharge	-20.80	-7.53	13.27	PbO
Mackinawite	-5.41	-45.73	-40.32	FeS
Magadiite	-6.31	-20.61	-14.30	NaSi7O13(OH)3:3H2O
Maghemite	-8.69	24.43	33.12	Fe2O3
Magnesite	-0.84	-8.67	-7.82	MgCO3
Magnetite	0.00	32.16	32.16	Fe3O4
Massicot	-21.00	-7.53	13.47	PbO
Melanterite	-7.22	-9.79	-2.57	FeSO4:7H2O
Merwinite	-29.12	43.00	72.12	Ca3MgSi2O8
Mg-Ferrite	-8.89	36.83	45.72	MgFe2O4
MgMoO4(c)	-12.27	-12.89	-0.62	MgMoO4
MgSeO3:6H2O	-26.10	15.88	41.98	MgSeO3:6H2O
Millerite	-3.92	-47.72	-43.80	NiS
Minium	-90.73	-13.60	77.12	Pb3O4
Mirabilite	-5.49	-7.24	-1.75	Na2SO4:10H2O
Mo(c)	-22.23	-52.25	-30.02	Mo
Molybdenite	-0.00	-141.18	-141.18	MoS2
Molybdite	-13.19	-25.29	-12.10	MoO3
Monticellite	-10.55	21.37	31.92	CaMgSiO4
MoO2(c)	-4.26	-34.28	-30.02	MoO2

Morenosite	-9.32	-11.78	-2.46	NiSO4:7H2O
Natron	-8.96	-10.79	-1.84	Na2CO3:10H2O
Nesquehonite	-3.24	-8.67	-5.43	MgCO3:3H2O
Ni(OH)2	-4.05	5.73	9.78	Ni(OH)2
Ni2SiO4	-7.86	7.79	15.65	Ni2SiO4
Ni4(OH)6SO4	-26.57	5.43	32.00	Ni4(OH)6SO4
NiCO3	-8.82	-15.33	-6.51	NiCO3
NiSe	0.00	-17.74	-17.74	NiSe
NiSeO3:2H2O	-31.84	9.22	41.05	NiSeO3:2H2O
O2(g)	-69.62	17.97	87.59	O2
P-Wollstanite	-5.58	8.97	14.55	CaSiO3
Pb(OH)2(C)	-16.15	-7.53	8.62	Pb(OH)2
Pb2(OH)3Cl	-32.46	-23.66	8.79	Pb2(OH)3Cl
Pb2O(OH)2	-41.26	-15.06	26.20	Pb2O(OH)2
Pb2O3	-67.11	-6.07	61.04	Pb2O3
Pb2OCO3	-36.01	-36.12	-0.12	Pb2OCO3
Pb2SiO4	-39.37	-18.74	20.63	Pb2SiO4
Pb3O2CO3	-55.56	-43.65	11.90	Pb3O2CO3
Pb3O2SO4	-51.19	-40.10	11.09	Pb3O2SO4
Pb4(OH)6SO4	-68.73	-47.63	21.10	Pb4(OH)6SO4
Pb4O3SO4	-70.90	-47.63	23.27	Pb4O3SO4
PbMetal	-20.77	-16.52	4.26	Pb
PbO:0.3H2O	-20.51	-7.53	12.98	PbO:0.33H2O
PbSeO4	-64.01	4.94	68.95	PbSeO4
PbSiO3	-18.84	-11.21	7.63	PbSiO3
Periclase	-10.32	12.40	22.72	MgO
Phosgenite	-33.52	-53.33	-19.81	PbCl2:PbCO3
Plattnerite	-50.21	1.46	51.66	PbO2
Portlandite	-11.05	12.65	23.70	Ca(OH)2
Pyrite	0.00	-90.20	-90.20	FeS2
Quartz	0.54	-3.68	-4.21	SiO2
RaCO3	-11.38	-19.97	-8.58	RaCO3
RaSO4	-5.83	-16.41	-10.57	RaSO4
Retgersite	-9.70	-11.78	-2.08	NiSO4:6H2O
Rutherfordine	-12.08	-26.52	-14.45	UO2CO3
Schoepite	-11.27	-5.46	5.81	UO2(OH)2:H2O
Se(A)	-7.29	-14.49	-7.20	Se
Se(hex)	-6.66	-14.49	-7.82	Se
SeO2	-34.62	3.49	38.11	SeO2
SeO3	-85.66	12.47	98.13	SeO3
Sepiolite(a)	-5.02	13.76	18.78	Mg2Si3O7.5OH:3H2O
Sepiolite(c)	-3.06	13.76	16.82	Mg2Si3O7.5OH:3H2O
Siderite	-2.97	-13.34	-10.37	FeCO3
SiO2(a)	-0.51	-3.68	-3.17	SiO2
SiO2(am)	-0.84	-3.68	-2.84	SiO2
SULFUR	-6.83	-44.47	-37.64	S
Talc	-1.74	22.48	24.22	Mg3Si4O10(OH)2
Th(OH)4(am)	0.00	1.81	1.81	Th(OH)4
Thenardite	-7.07	-7.23	-0.16	Na2SO4
Thermonatrite	-11.01	-10.79	0.22	Na2CO3:H2O
Tremolite	-1.90	57.88	59.77	Ca2Mg5Si8O22(OH)2
U3O8(C)	-19.24	-25.36	-6.12	U3O8
U4O9(C)	-7.32	-48.79	-41.47	U4O9
UO2(am)	-5.89	-14.44	-8.56	UO2
UO3(C)	-13.82	-5.46	8.36	UO3
Uraninite	0.00	-14.44	-14.44	UO2
Uranophane	-23.11	-5.62	17.49	Ca(UO2)2(SiO3OH)2

```
      USiO4(C)          -0.62   -18.12   -17.50  USiO4
      Wollastonite      -4.67     8.97    13.65  CaSiO3

------------------
End of simulation.
------------------

------------------------------------
Reading input data for simulation 2.
------------------------------------

-----------
End of run.
-----------
```

APPENDIX C

HYDROGEOLOGIC MODELING OF GROUNDWATER AT THE QUIVIRA MINING COMPANY URANIUM MILL FACILITY, AMBROSIA LAKE, NEW MEXICO

January 2001

Prepared for
Rio Algom Mining Company

Prepared by

Maxim Technologies, Inc.
10601 Lomas NE
Albuquerque, New Mexico 87112

HYDROGEOLOGIC MODELING OF GROUNDWATER AT THE QUIVIRA MINING COMPANY URANIUM MILL FACILITY, AMBROSIA LAKE, NEW MEXICO

TABLE OF CONTENTS

LIST OF FIGURES

LIST OF TABLES

HYDROGEOLOGIC MODELING OF GROUNDWATER AT THE QUIVIRA MINING COMPANY URANIUM MILL FACILITY, AMBROSIA LAKE, NEW MEXICO

1. INTRODUCTION

Maxim developed a numerical groundwater flow model of the alluvial groundwater system to serve as an interpretive tool assessing the effectiveness of the current CAP other corrective actions. Below are sections describing the conceptual model, model design, calibration, particle tracking, transient modeling, and a sensitivity analysis.

2. CONCEPTUAL MODEL

This section presents the conceptualization of the model area including geology, hydrogeology, and a conceptual water budget.

2.1. GEOLOGICAL SETTING

QMC's mill and tailings facility is located north of the Zuni Uplift portion within the San Juan Basin. The basin is characterized by broad areas of relatively flat lying sedimentary rocks, dipping to the northeast, with portions of the basin covered with Alluvium and basalt flows. The QMC mill is within the Ambrosia Lake Valley that extends from the western side of Mount Taylor.

During the recent geological past, erosional forces cut a canyon up to 100 feet deep into the bedrock surface. Wind and water filled the canyon with sediment forming the current alluvial valley. Near surface sediments are described in lithologic logs for wells in the valley as ranging from fine-grained sand with clay up to gravel. Recently weathered shale (saprolite) is present in many locations.

N/projects/quivira/figs/generalXS

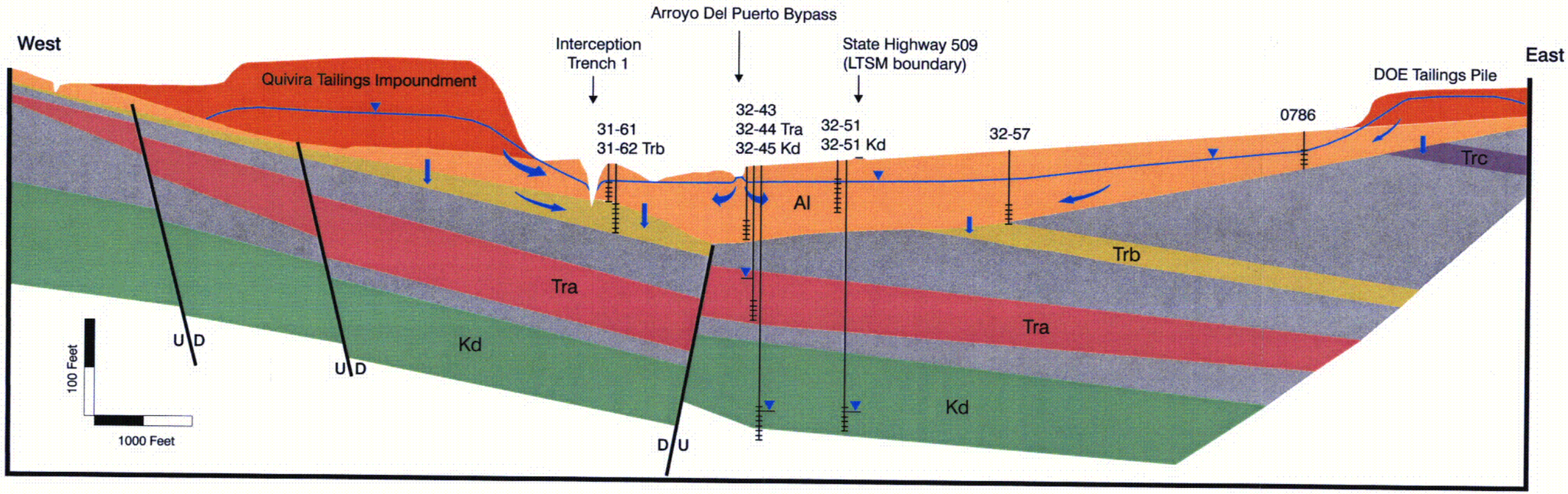

Screened Interval
Groundwater Elevation
Groundwater Flow Direction

Al - Alluvium
Mancos Shale
Trc - Tres Hermanos c Sandstone
Trb - Tres Hermanos b Sandstone
Tra - Tres Hermanos a Sandstone
Kd - Dakota Sandstone

LTSM - DOE Long Term Surveillance and Maintenance

MAXIM 2007209

Generalized Hydrogeologic Cross Section
Ambrosia Lake Facility
Near Grants, New Mexico
FIGURE C-1

C08

Hydrogeologic Setting

Figure C-1 is a generalized hydrogeologic cross section through the Ambrosia Lake Valley. Principal near-surface bedrock hydrogeologic units beneath the valley include the TRA, TRB, TRC and the Dakota Sandstone. Mancos shale serves as aquitards that separate these water-bearing units.

Groundwater flow within bedrock units is generally down-dip, toward the north-northeast. One exception to this is a small portion of TRB in the southwest portion of the study area. Trenches IT-2, IT-3, and IT-4 intercept water flowing in the TRB from the west beneath Tailings Impoundment 1. Groundwater flow in the Alluvium is generally southeast parallel to the Arroyo del Puerto.

Bedrock units are recharged where they crop out or where they are covered by Alluvium. Seepage from Pond 8 (Figure C-2) has recharged the Dakota locally. Most of the seepage from Tailings Impoundments 1 and 2 migrates laterally through the Alluvium and shallow saprolite in the direction of the surface slope to the Alluvium of Arroyo del Puerto where it enters the interception trench. The seepage that enters the unweathered bedrock beneath Tailings Impoundment 1 and 2 slowly migrates through the TRB to the north and northeast of the Facility in the general direction of the dip. The dewatering trench located between Pond 7 and Pond 2 has minimized any tailings seepage to the TRA, which underlies the Alluvium in the general vicinity of Pond 7.

A regional cone of depression has formed within bedrock units beneath the site resulting from the presence of vent holes and mine shafts and the dewatering of mines north and east of the facility (QMC 1986). The bedrock formations above the Westwater Canyon Member of the Morrison Formation have essentially been dewatered within this cone of depression.

Figure C-2 shows the groundwater elevation map for the Alluvium in the valley. Currently, groundwater in the alluvial system flows to the southeast with a gradient of approximately 0.006 ft/ft. A groundwater mound has formed in the northern portion of the study area, caused by

infiltration from the Arroyo del Puerto bypass channel. North of this mound, groundwater flows north toward mine shafts and vent holes located in Section 30. South of the mound groundwater flows toward the northern half of trench IT-1, creating the "groundwater sweep" referred to in the CAP (AVM and AHS 2000). Groundwater seeping from Tailings Impoundment 1 flows east toward trench IT-1. At the southern end of IT-1, tailings solution flows from Tailings Impoundment 1. East of the facility groundwater flow from the DOE Tailings pile and the highlands east of it is to southwest with a gradient of approximately 0.01 ft/ft. Some of the water in the alluvium beneath Tailings Impoundments 1 and 2 leaks into TRB beneath it and flows eastward where is its intercepted by IT-2, IT-3, and IT-4.

Groundwater exits the alluvial system at the northern and eastern margins of the study area where vent holes and mine shafts intersect the water table. Alluvial groundwater also exits the southern end of study area as underflow beneath the Arroyo del Puerto through a narrow gap in bedrock.

Prior to mining in the area, natural sources of recharge to the alluvial system were insufficient to establish saturated conditions within the alluvium (QMC 1986). Any water infiltrating beyond the root zone probably drained into sandstone units below the alluvial system. Two principal sources of recharge to the alluvial system are currently maintaining the saturated condition near the facility:

- Infiltration of water from the Arroyo del Puerto bypass channel, and
- Leakage from Tailings Impoundments 1 and 2.

Hydraulic gradients between the alluvial system and subcropping Tres Hermanos units are generally downward (Figure C-2) indicating some groundwater is probably leaking from the alluvial system into subjacent sandstone units. This idea is supported by the water budget analysis discussed below.

G:\MINES\MISC\QUIVERA\ARCVIEW\DRGPLOT.APR Figure C-2

USGS 7.5 Minute Quadrangle - Ambrosia Lake (reprojected to stateplane NM West feet, NAD27)

0 Feet 1500

MAXIM 2007209-100

- Proposed Withdrawal Area
- Approximate Extent of Saturated Alluvium Boundary
- Interception Trenches (IT-1 to IT-4)
- Bypass Channel
- Dewatering Trench

- DOE Alluvial Wells
- Quivira Alluvial Wells
- NRC Point of Compliance Wells

- Groundwater Elevation Contour

Contour Interval 5 feet

Water table elevation readings based on November/December 1997 readings.

Groundwater Elevation Map
Ambrosia Lake Area
Near Grants, New Mexico
FIGURE C-2

C09

Prior to mining activity, the Arroyo del Puerto was an ephemeral drainage. Flow in the creek occurred only in response to large rainfall or snowmelt events. Currently, the creek is dry until it reaches the B-3 discharge point. An average of 337,000 ft^3/d of treated mine water was discharged to the Arroyo del Puerto channel at the B-3 discharge during 1999. Water is then diverted from the creek for mine injection and irrigation. Most of the remaining water in the channel is pumped into Pond 9 just south of the Puertocito Creek weir. Between the B-3 discharge point and the Puertocito Creek weir water leaks from the creek. This leakage is the primary source of recharge to the alluvial groundwater system in the site.

2.2. ALLUVIAL FLOW SYSTEM CHARACTERISTICS

Lithologies described in alluvial well logs range from sandy clay to sand. Hydraulic conductivity estimates based on these lithologic descriptions range from 10^{-2} to 10^{2} ft/day. Hydraulic conductivity for the alluvium 0.6 feet per day based on pumping tests performed in wells AW-1 and AW-2 was 0.6 feet per day (QMC 1986). The groundwater model developed for the site was calibrated using a hydraulic conductivity of 18 ft/d. Based on the lithology of the alluvium, porosity is estimated to range from 0.15 to 0.25 (Fetter 1989). Specific yield estimates range from 0.10 to 0.20. Estimates of average linear groundwater velocity for the site based on these parameters and a gradient of 0.006 range from 0.014 to 1.2 feet per day.

3. MODEL DESIGN

This section describes design elements needed to simulate groundwater flow using MODFLOW including the development of a finite-difference grid, boundary conditions, and initial aquifer parameters assigned to the model.

3.1. MODEL AREA AND GRID

The model area selected includes roughly the saturated extent of alluvium excluding the area beneath Tailings Impoundment 1 (Figure C-3). A small portion of TRB adjacent to the southeast corner of Tailings Impoundment 1 was included because groundwater collected by trench IT-4

and portions of IT-2 and IT-3 come from saturated TRB in that area. Groundwater flow directions in that area suggest that this wedge of TRB is in direct communication with the alluvial system.

A finite difference grid was fit to the area of interest (Figure C-3). The grid has 119 rows and 124 columns with a uniform grid-spacing of 100 feet. This makes for a total of 14,746 cells with 7,703 of them being active. The model has a single layer that is designated as MODFLOW Type-1 (unconfined).

3.2. WATER BUDGET

In order to estimate model inputs, a water budget was developed for the alluvial groundwater system based on current conditions. This water budget is summarized below.

Current inflows and outflows to the alluvial system were based on 1999 data. Infiltration from Arroyo del Puerto was estimated based on documented water losses from the creek. The influx from Tailings Impoundment 1 and the DOE tailings pond were estimated based on modeling results presented in QMC (1986) and using Darcy's Law. Underflow through the southern end of the model area and drainage to mine shafts vents and was estimated using Darcy's Law. Recovery from trenches IT-1 through IT-4 were based on 1998 and 1999 monthly data. Differences between inflows and outflows were assumed to represent drainage to TRA, TRB and TRC. Flux estimates are summarized in Table C-1.

Table C-1. Estimated Flux for Model Boundaries

	Low (ft^3/d)	High (ft^3/d)	Estimated Flux(ft^3/d)
IN			
Arroyo and Irrigation Infiltration	81,620	163,423	119,850
Influx from Tailings Impoundment 1	3,000	12,000	5,000
Influx from East to the DOE pile	109	8,500	5,000

Total In:	**84,729**	**183,923**	**129,850**
OUT			
Underflow to South	504	25,200	18,000
Trench IT-1	4,000	19,250	8,000
Trench IT-2	96	231	149
Trench IT-3	1,020	2,312	1,328
Trench IT-4	424	2,349	543
Infiltration to mineshafts & vents	20,000	60,000	48,000
Total Out:	**26,044**	**109,342**	**76,020**
Infiltration to Bedrock Units:			**53,830**

3.3. BOUNDARY CONDITIONS

Figure C-3 shows the finite difference grid and various MODFLOW boundary conditions. Infiltration from irrigation is simulated using Recharge cells. Influxes from the Arroyo del Puerto are simulated as constant flux boundaries using Well Package cells. Underflow to the south, drainage to the mine vents, drainage to the TRA, TRB, and TRC, as well as water removed from the infiltration trenches were simulated with Drain Package cells.

Influxes from Tailings Impoundment 1 were estimated using the variably saturated flow model SWMS/HYDRUS-2D. A limited suite of unsaturated hydraulic characteristics for the tailings material were based on values used in previous and similar modeling exercises (for example, Shepherd Miller (SMI, 1998)) and on professional judgement. From this limited suite of information, van Genuchten unsaturated flow characteristic values were estimated assuming that the tailing material behaved like natural soil material. Saturated hydraulic conductivity values for the tailing material were also estimated. Table C-2 presents the estimated hydraulic parameters for the soil material (silty clay loam).

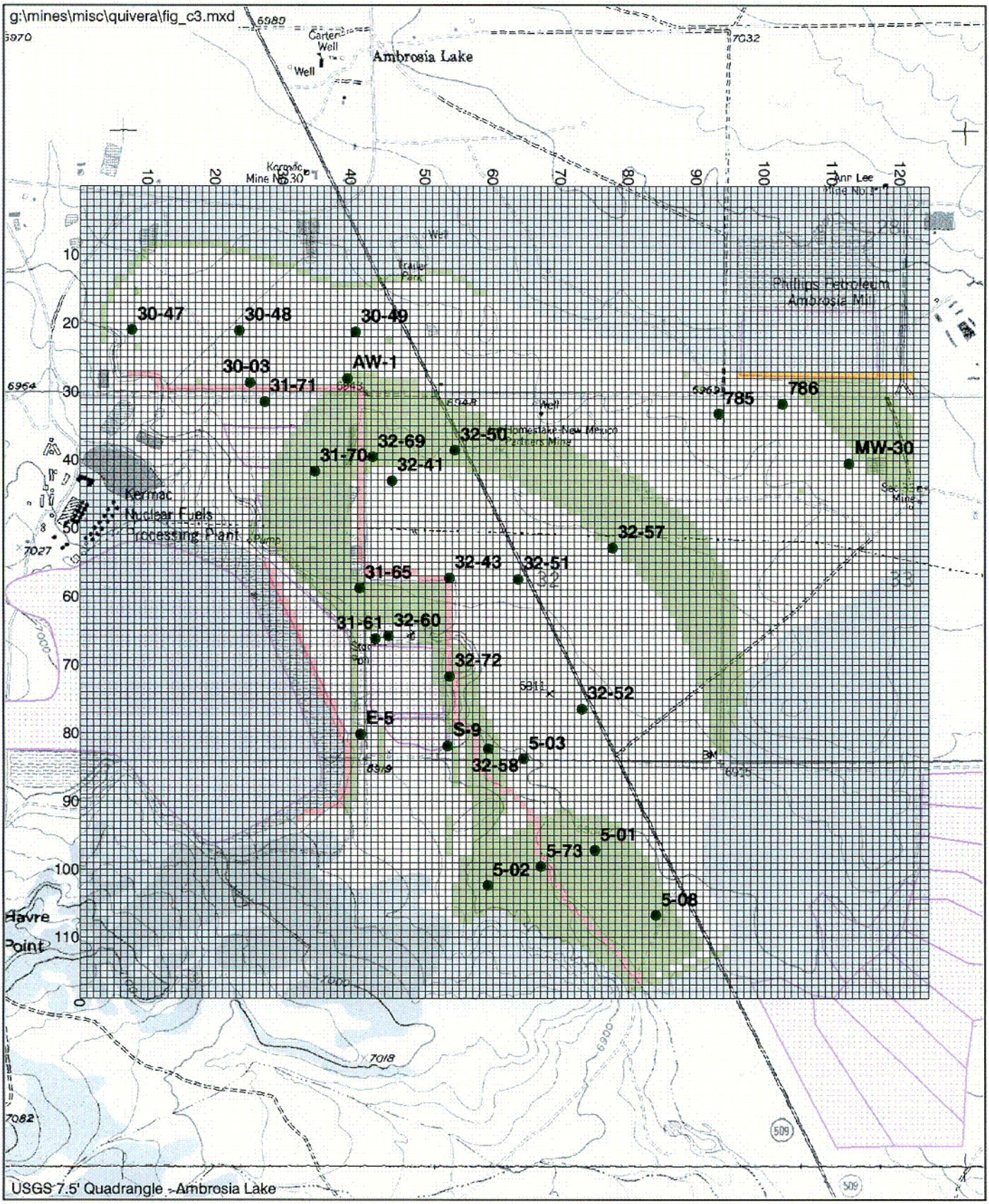

N

2,000 1,000 0 Feet

MAXIM 2007209

- Calibration Target Well
- Drains Cells
- No Flow Cells
- Constant Head Cells
- Constant Flux Cells

Model Boundary Conditions and Grid Layout
Ambrosia Lake Area
Near Grants, New Mexico
FIGURE C-3

C10

Table C-2. Estimated Hydraulic Parameters For partially Saturated Model Estimating Influx From tailing Impoundment 1.

	N	Alpha	Θ_r	Θ_{sat}	K_{sat}
	Dimensionless	Dimensionless	Vol/vol	Vol/vol	Cm/day
Tailings	1.23	0.01	0.089	0.430	1.5

Where Θ_r is the residual volumetric water content, Θ_{sat} is the saturated water content, and K_{sat} is the saturated hydraulic conductivity.

To define the initial conditions for the model, it was assumed that the tailings material was near saturation. Although there is some evidence suggesting that the tailings impoundment contained free water, it was felt that this would make model calibration more difficult. Instead, initial conditions for the model domain used a relatively low suction level (on the order of 100 cm).

The model domain was oriented vertically, over a depth of approximately 50 feet. The domain thickness was estimated based on a review of available maps and cross-sections for the site. The upper boundary was assigned a no flux boundary and the lower boundary was assigned a free drainage condition. The initial time step was set at 1.00E-6 days and a total simulation time of 36,500 days (100 years) was used.

The model results indicate that after a period of rapid drainage at the start of the simulation period, discharge from the pile approaches a quasi-steady-state value near a time of approximately 50 years. From 50 years forward, seepage does not vary significantly.

The estimated seepage rate was converted to a volumetric flow rate by assuming that a tailings impoundment footprint area of 15,000,000 ft^2. Selected data pairs of seepage rate and time were input into a computer curve-fitting routine (Curvefit, a BASIC-based fitting program). Using these points, a power function relating the seepage rate and time (in years) was developed. The power function has the following form:

$$\text{Seepage Rate}_{(ft^3/day)} = 30903 * \text{Time}_{(years)}^{(-0.934)}$$

R^2 =0.98

The results of the fitted curve and the calculated seepage rates through time are presented in Figure C-4.

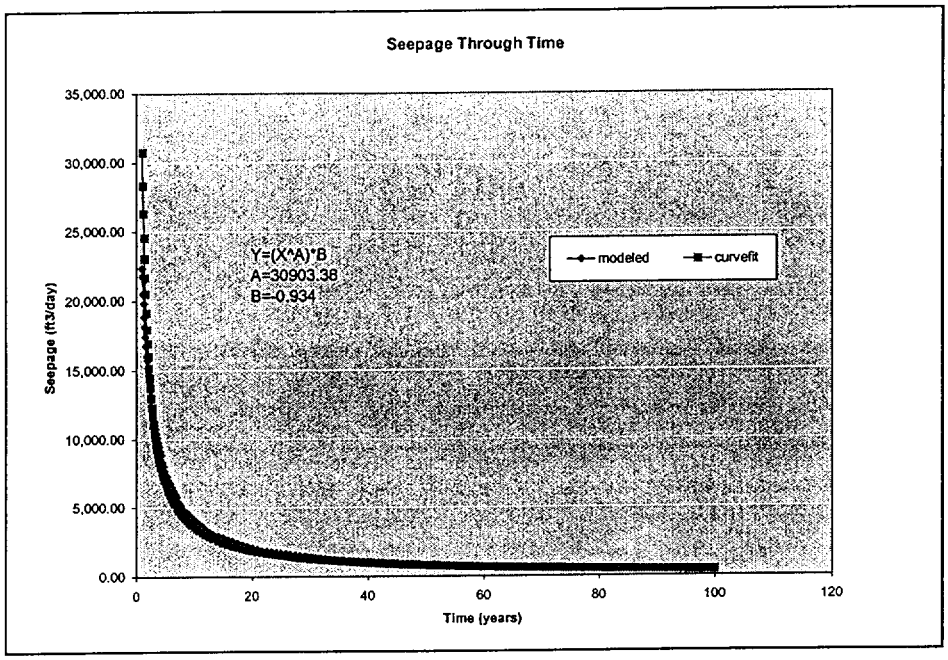

Figure C-4. Predicted Seepage through Time for Tailings Impoundment 1&2.

3.4. INITIAL PARAMETER ASSIGNMENTS

Hydraulic conductivity values were assigned to the alluvial cells uniformly using values of 15 ft/d based on previous modeling at the site. TRB cells were given values of 5 ft/d. Cells within the model domain representing islands of Mancos Shale and Saprolite were given values of 0.1 ft/d.

Initial fluxes for the Arroyo del Puerto and Tailing Impoundment 1 and recharge from infiltration were average or representative values from the Table C-1. Conductance for drains were

estimated based on hydraulic estimates. For transient runs, porosity and specific yield were estimated at 0.2 and 0.14, respectively.

4. CALIBRATION

This section describes methods used to calibrate the numerical model and presents results of the calibration. The model was calibrated to "steady state" conditions based on 1997 groundwater level data. 1997 data were selected because it was the most recent data that included data from the DOE facility east of the QMC Mill. This made calibration somewhat problematic, since the water table has been dropping in many portions of the site for several years and the alluvial groundwater flow system is not in equilibrium.

4.1. METHODS

Both qualitative and quantitative methods were used to judge calibration results of the numerical model. The qualitative method involved visual comparison between contour maps of measured and simulated heads. Quantitative methods used to evaluate model calibration included comparison of simulated heads to measured heads at target locations and comparison of simulated groundwater fluxes to measured and estimated fluxes.

November 1997 head values from QMC and DOE monitoring wells were contoured (Figure C-2) in accordance with the conceptual model and the resulting potentiometric surface was used as the qualitative calibration target. Quantitative calibration targets for head are water table elevations measured in alluvial wells with screens across the water table during second November 1997. Error associated with these targets is estimated to be at least ± 5 feet. Sources of error include measurement error, seasonal variation, interpolation error and scaling effects.

The following calibration objectives were established for the numerical model:

- The model must produce simulated potentiometric contours that generally resemble measured head contours, and

- The model should produce simulated heads and fluxes that generally fall within calibration target ranges.

Model parameters were subsequently adjusted using trial-and-error procedures in an attempt to accomplish the objectives. Hydraulic conductivity values, recharge rates, and conductance of drains were systematically adjusted to produce simulated potentiometric surfaces that resembled potentiometric maps drawn using field-measured heads. After each calibration run, the residual at each target node was calculated. Residual is the difference between the measured heads and simulated heads at target nodes. Residual statistics were used as one criterion to judge the degree to which calibration of the model improved through successive runs.

While calibrating the flow model, parameters with a higher degree of uncertainty (estimates having no field measurements to back them up, e.g. conductance of TRB) were adjusted before adjusting parameters with a lower degree of uncertainty (estimates based on field measured values, leakage from Arroyo del Puerto).

4.2. CALIBRATION RESULTS

Figure C-5 shows the Steady State model calibration results including contours of simulated head elevations and calculated residual at each target well location. Comparison of Figure C-2 to Figure C-5 shows that qualitatively, simulated heads generally match field-measured heads. Table C-3 below presents calibration statistics.

TABLE C-3 Residual Statistics from Steady State Model Calibration.

Residual Mean	-0.685503
Res. Std. Deviation	3.087917
Sum of Squares	290.149241
Absolute Residual Mean	2.637267
Min. Residual	-5.593886
Max. Residual	5.677376
Head Range	75.310000
Std/Head Range	0.041003

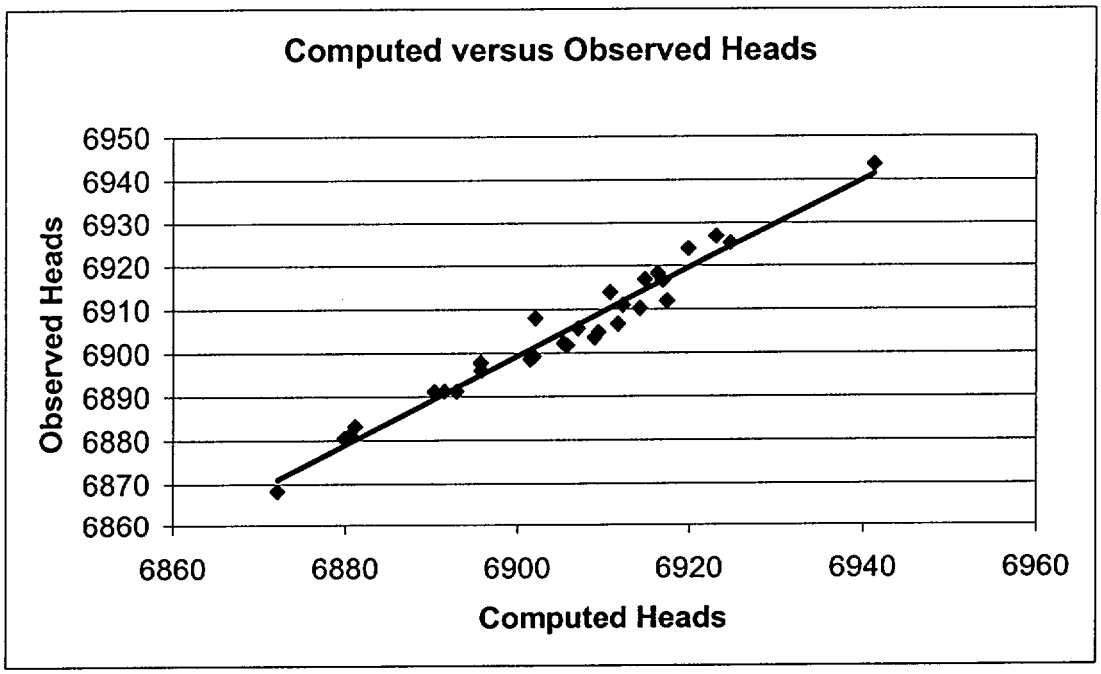

Measured versus simulated heads are plotted in the chart above. The chart shows that measured and simulated heads are randomly distributed on either side of the regression line, indicating the model is relatively well calibrated (Anderson and Woessner 1992).

The chart presented above shows a plot of observed heads compared to those predicted by the steady state groundwater flow model. The distribution of computed versus observed data show little or no bias. Table C-4 shows a comparison of estimated fluxes to calibrated flux values.

TABLE C-4. Estimated Versus calibrated Fluxes for the Groundwater Flow Model.

	Estimated Flux (ft^3/d)	Calibrated Flux (ft^3/d)
IN		
Arroyo infiltration	119,850	119,096
Influx from Tailings Impoundment 1	5,000	4,900
Influx from NE Highlands and DOE pile	5,000	6,159
Total In:	**129,850**	**130,155**
OUT		
Underflow to South	18,000	15,728
Trench IT-1	8,000	6,019
Trench IT-2	149	107
Trench IT-3	1,328	883
Trench IT-4	543	268
Infiltration to mineshafts & vents	48,000	40,816
Infiltration to Bedrock Units	53,830	66,706
Total Out:	**129,850**	**130,527**

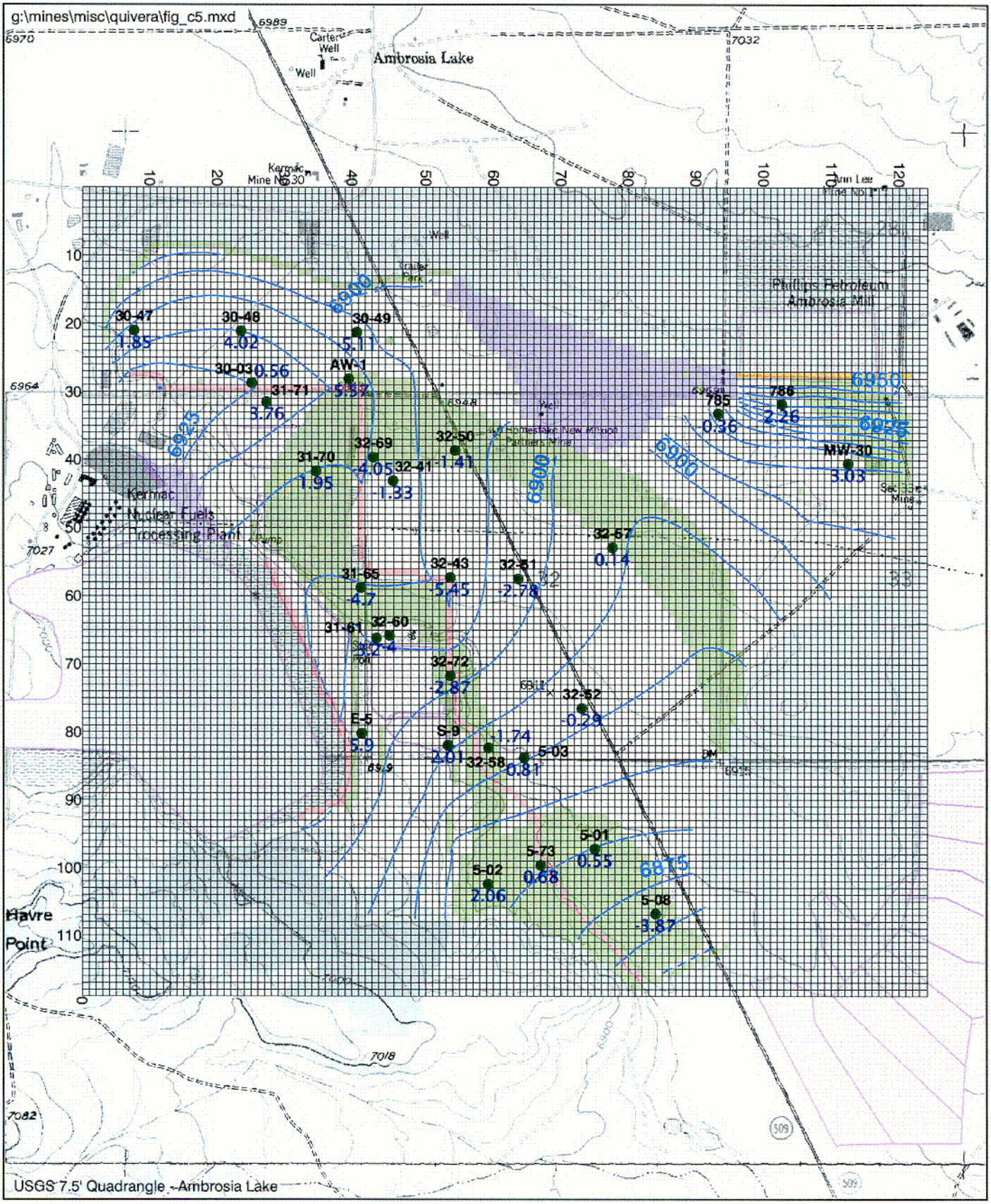

N

2,000 1,000 0 Feet

MAXIM 2007209

Groundwater Elevation Contours
Dry Cells
Calibration Target Well
Well Residual 5-08 -3.87
Drains Cells
No Flow Cells
Constant Head Cells
Constant Flux Cells

Model Calibration Results
Ambrosia Lake Area
Near Grants, New Mexico
FIGURE C-5

5. PARTICLE TRACKING AND TRANSIENT MODELING

This section presents the results of transport analyses using particle tracking methods. It includes transient modeling to assess CAP effectiveness and long-term transport at the site.

5.1. STEADY STATE TRANSPORT

Based on preliminary calibrated model parameters, the average linear groundwater velocity at the site is approximately 0.5 feet per day. Figure C-6 shows particle traces from MODPATH depicting transport directions for the alluvial system under steady state flow conditions. This figure shows that most particles originating in Tailings Impoundment 1 are captured by trench IT-1. Particles from the south end of Tailings Impoundment 1 are transported past the southern end of IT-1 but many of these particles are captured by trench IT-3 or TRB drain cells. Particles north of the Arroyo del Puerto end up in drains representing mine vents and shafts to the north.

Particles south of the west end of the Arroyo del Puerto bypass channel end up in trench IT-1 or TRB drains. Particles south of the first 90-degree bend in the bypass channel end up infiltrating to TRB. Particles originating in the southern half of the model that do not infiltrate to TRA or TRB are transported out of the southern model boundary.

5.2. TRANSIENT FLOW MODELING

In order to assess the effectiveness of the CAP and to estimate the time required to capture contaminant plumes, the calibrated flow model was run in transient mode under two scenarios. The first scenario maintained the fluxes used in the steady state calibration for the Arroyo del Puerto. Decreasing flux from Tailings Impoundment 1 was simulated using the output from SWMS/HYDRUS-2D as presented in section 3.3. The model was then run over 8 stress periods (10 time steps each, with a 1.2 time step multiplier) for a period of 1,000 years.

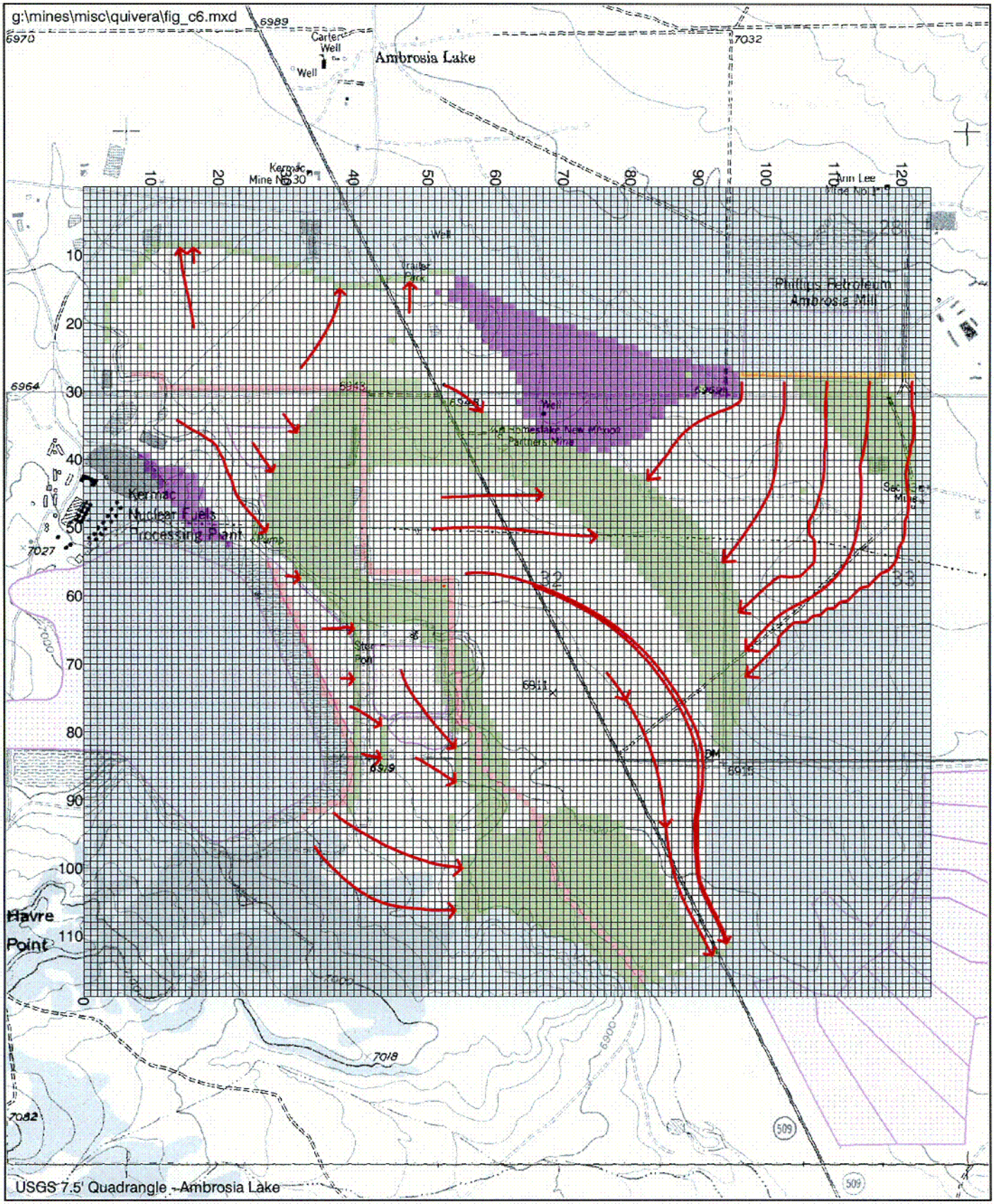

N

2,000 1,000 0 Feet

MAXIM 2007209

- Particle Pathlines
- Dry Cells
- Drains Cells
- Constant Head Cells
- No Flow Cells
- Constant Flux Cells

Steady State Particle Pathlines
Ambrosia Lake Area
Near Grants, New Mexico
FIGURE C-6

C12

A second scenario was simulated to assess the affects of discontinuing the current CAP. Under this scenario, constant flux boundaries representing the Arroyo del Puerto infiltration and drain cell boundaries representing interception trenches were removed from the model. Declining flux from Tailings Impoundment 1 was simulated as described in the paragraph above. The model was again run over 8 stress periods 1,000 years.

Preliminary results of the 1,000 year transient flow model run simulating operation of the current CAP results in a water table that looks very similar to Figure C-2 with the exception that water table elevations southeast of Tailings Impoundment 1 are slightly lower and the area immediately south of DOE Impoundment goes dry.

Figure C-7 shows preliminary results of the discontinued CAP transient scenario after 65 years. This figure indicates that after 65 years most of the alluvial system is dewatered. At 100 years, only 12 feet of saturation remains at well 5-08 and relatively little water is discharging as underflow in the alluvium to the south.

5.2.1. Transient Particle Tracking

The 1984 chloride plume was selected as being representative of the extent of alluvial groundwater affected by mill activities. To estimate the time required for plume capture under the current CAP, particles were input to the model. Particles representing mass in groundwater from Tailings Impoundment 1 were input along the flux boundary representing the impoundment at time = 0 days and at the end of each stress period in which water drained from the impoundment. Particles were tracked over a 1,000-year period.

To estimate the time required to capture the plume under the discontinued CAP scenario, particles were input to the system as described above and particles were also tracked for 1,000 years.

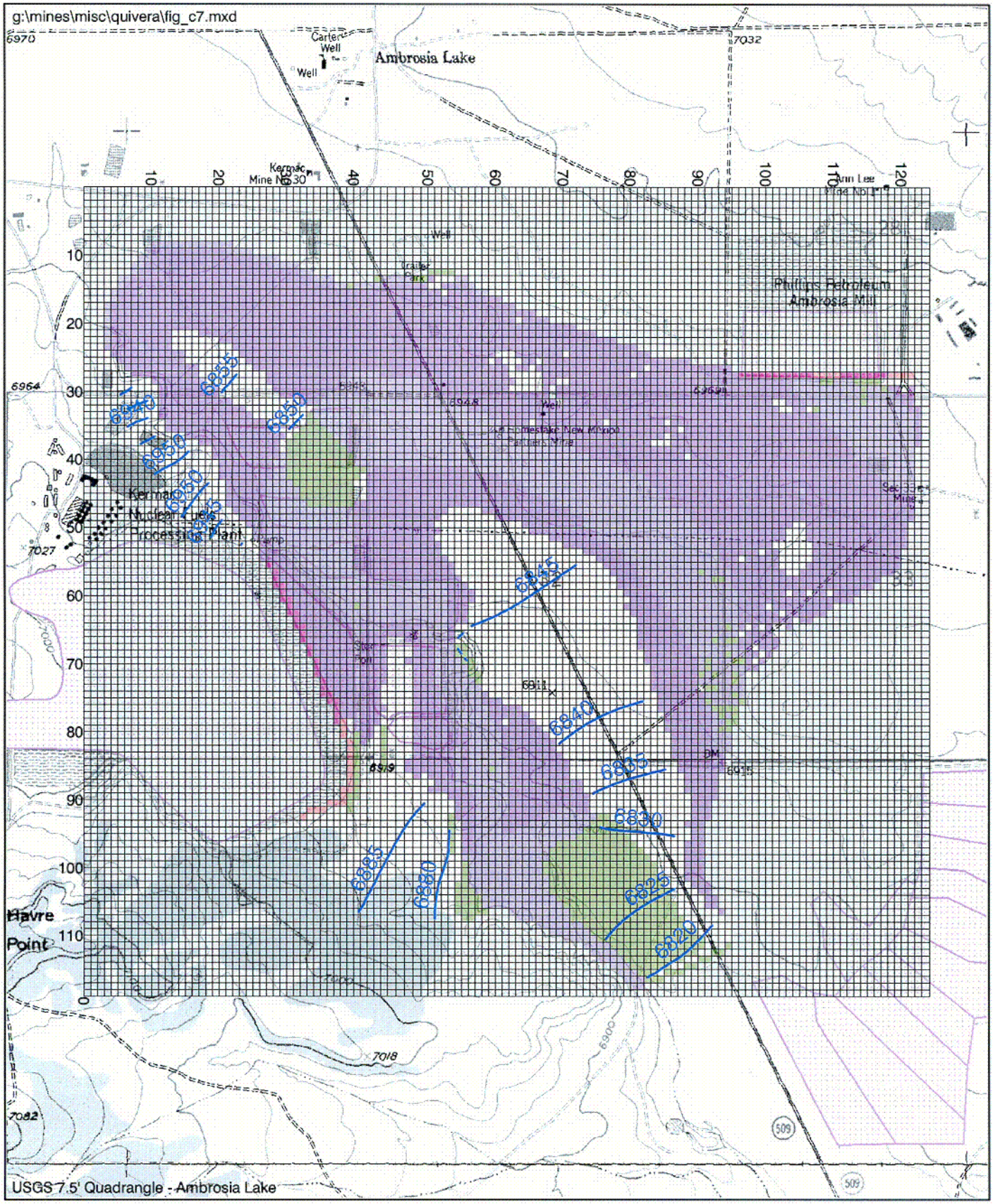

N

2,000 1,000 0 Feet

MAXIM 2007209

- Groundwater Elevation Contours
- Dry Cells
- No Flow Cells
- Drain Cells
- Contant Flux Cells

Water Table Elevations After 65 Years for Discontinued CAP Scenario
Ambrosia Lake Area
Near Grants, New Mexico
FIGURE C-7

C13

Transient pathlines for the current CAP scenario are presented in Figure C-8. MODPATH output indicates that approximately 45 years were required for all the particles representing the current plume in the alluvial system to be captured or removed from the system. More than 100 years were required to capture particles within the TRB included in the southwest portion of the model domain. This assumes advective transport velocities, which would be representative of the least retarded species (chloride). Other more retarded species would require more time. In addition, due to heterogeneities and preferential flow paths present in real systems, practical experience indicates that approximately 4 to10 pore volumes would be required to remove 100 percent of contaminant mass from the system.

It is difficult to assess the time required for complete capture of particles under the discontinued CAP scenario due to numerical issues after 100 years as model cells go dry. MODPATH results show that particles remain in TRB portion of the model domain after 1,000 years. However, this water is stagnant and trapped by dry cells within the model.

6. SENSITIVITY ANALYSIS

A sensitivity analysis was conducted to identify which parameters most influence model results. The sensitivity analysis also helps to quantify the uncertainty in the calibrated model caused by uncertainty in the estimates of model parameters. The parameters included in the sensitivity analysis included hydraulic conductivity, influx from Tailings Impoundment 1, and the porosity of the alluvium.

Calibrated values of hydraulic conductivity and the influx from Tailings Impoundment 1 were increased and decreased by constant multiples and input to the steady state flow model. The resulting standard deviation of head residual, also known as the root mean squared error (RMSE) was noted for each model run. The graph below summarizes the results of this analysis.

Results of the sensitivity analysis show that the model is most sensitive to changes in hydraulic conductivity. Most notably, decreases in hydraulic conductivity values. Varying influx from the Tailings Impoundment 1 had relatively little effect on the calibration of the model.

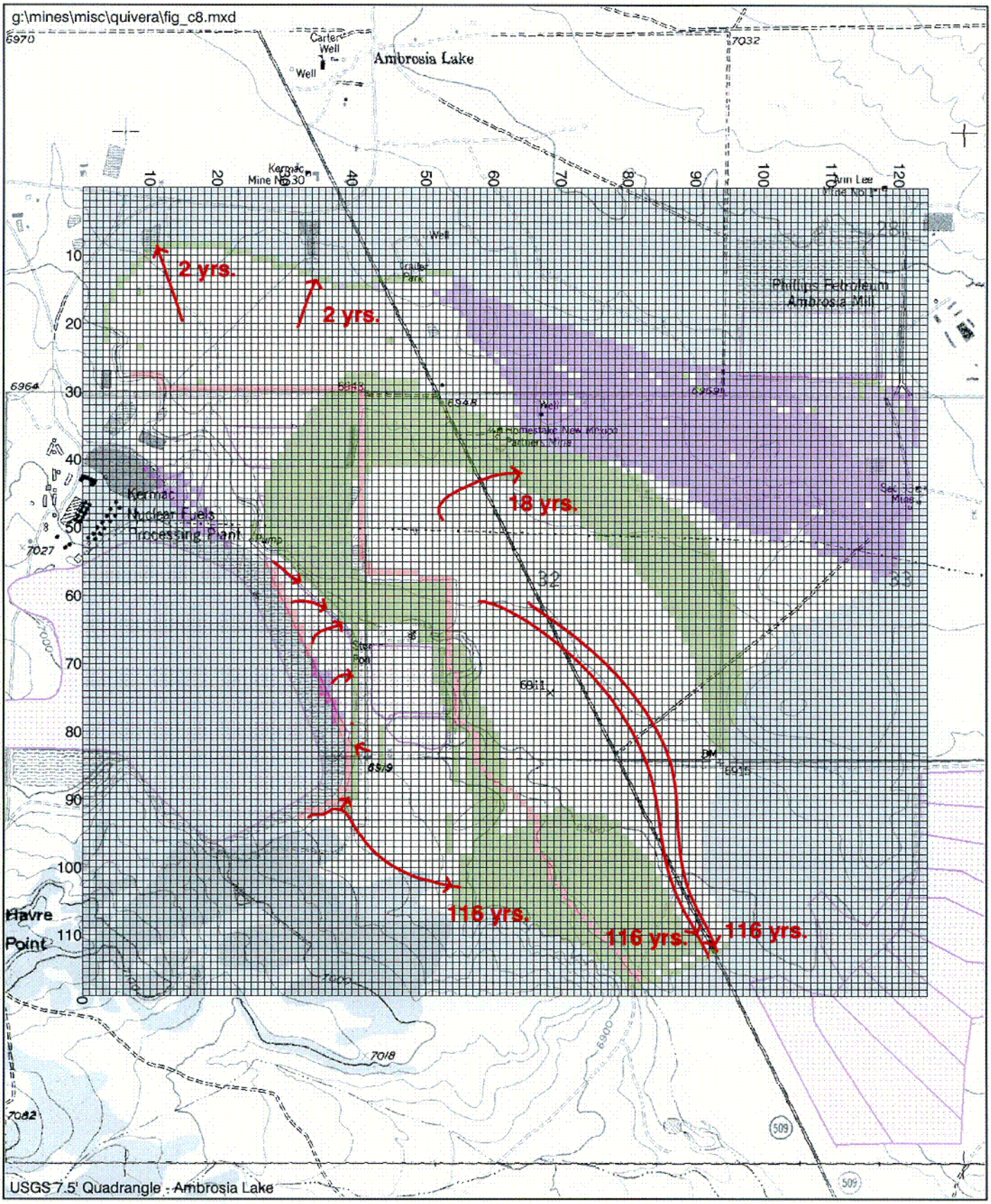

N

2,000 1,000 0 Feet

MAXIM 2007209

- Particle Pathlines
- Dry Cells
- Drain Cells
- No Flow Cells
- Constant Flux Cells

Transient Pathlines for Existing CAP Scenario
Ambrosia Lake Area
Near Grants, New Mexico
FIGURE C-8

C14

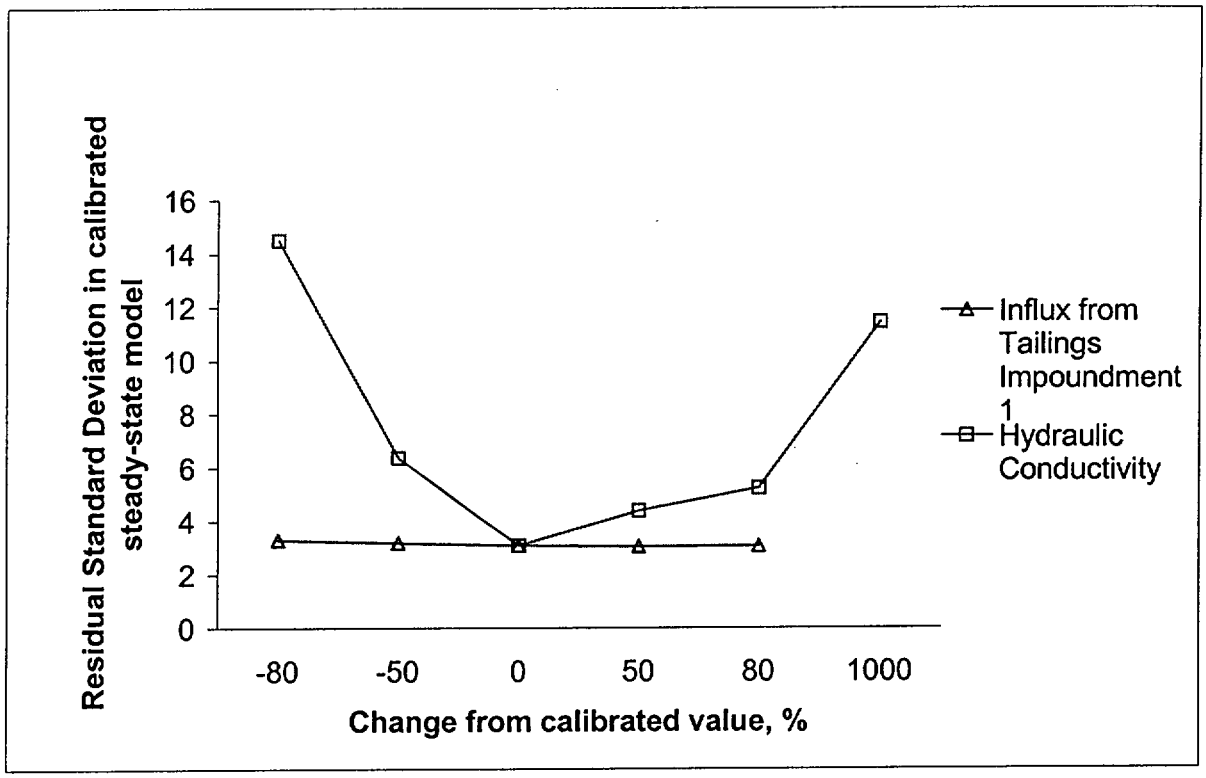

Figure C-9 Sensitivity Analysis for Hydraulic Conductivity and Influx from Tailings Impoundment 1.

Porosity values for the alluvium were varied to demonstrate how porosity effects model results for travel time through the model area. The following is a summary of the results of this analysis.

Table C-5 Approximate Time for Total Particle Capture.

Porosity	Approximate time required for total particle capture from entire model domain
0.10	45 years
0.20 (calibrated value)	100 years
0.30	150 years

Changes in porosity values showed a direct influence on travel times of particles through the system. This is expected because travel time is directly proportional to porosity (Fetter, 1989).

7. MODEL LIMITATIONS

The numerical groundwater model described in this report was developed to serve as an interpretive and predictive tool. The model was generally able to simulate a pre-established set of hydraulic and solute transport conditions, which indicates the calibrated model is reliable.

Limited site-specific data were available regarding aquifer parameters. Attempts to calibrate the model using hydraulic conductivity values from pumping tests performed on alluvial wells were unsuccessful.

Inherent in any modeling effort is a degree of uncertainty. In developing the groundwater model, simplifying assumptions were used such as:

- Groundwater flow is horizontal and isotopic,
- Hydraulic conductivity of alluvium is uniform, and
- Natural recharge from precipitation is negligible.

This work was performed in accordance with the generally accepted practices of other consultants undertaking similar studies at this time. In completing this project, Maxim observed the degree of care and skill generally exercised by other consultants operating under similar circumstances and conditions. Maxim's findings and conclusions must be considered not as scientific certainties, but as opinions based on our professional judgement concerning the significance of the data gathered during the course of the evaluation. Other than this, no warranty is implied or intended.

8. REFERENCES

AMV & AHS, 2000. Corrective Action Program and Alternate Concentration Limits Petition For Upper Most Bedrock Units, Ambrosia Lake Uranium Mill facility Near Grants, New Mexico. Prepared for: Quivira Mining Company. USNRC License No. SUA-1473, Docket No. 40-8905.

Anderson, M. P. and W. W. Woessner. 1992. *Applied Groundwater Modeling.* Academic Press, Inc. San Diego. 381pp.

Curvefit – A public domain program to fit values of X and Y to 25 different equations. Version 1.00, Basic version completed May 21-22 1984.

Fetter, C.W., 1989, Applied Hydrogeology. Macmillian, New York, New York, 592 pp.

HYDRUS-2D/MESHGEN 1999. Simulating Water Flow and Solute Transport in Two-Dimensional Variably Saturated Media by J Simúnkek, M. eja and M. Th van Genuchten; U. S. Salinity Laboratory, USDA/ARS, International Groundwater Modeling Center – TPS 53C Version 2.0.

McDonald and Harbaugh. 1989. A Modular Three-Dimensional Finite-Difference Ground-Water Flow Model (MODFLOW), Techniques of Water-Resources Investigations of the United States Geological Survey (USGS). Book 6, Chapter A-1. U.S. Government Printing Office, Washington D.C.

Pollock, D.W., 1994. User's Guide for MODPATH/MODPATH-PLOT, Version 3: A particle tracking post-processing package for MODFLOW, the U.S. Geological Survey Finite-Difference Ground-Water flow Model. USGS Open-File Report 94-464, 234p.

Quivira Mining Company (QMC). 1986. Tailings Stabilization Report, License SUA-1473, Docket 40-8905, Vol. II. Submitted to NRC October 1, 1986.

Shepherd Miller, Inc. (SMI), 1998. Technical Memorandum from Dan Overton to Tom Gieck (Umerco Minerals Corporation) titled Evaluation of Drainage from the A-9 repository, Gas Hills, Wyoming. SMI # 100039.

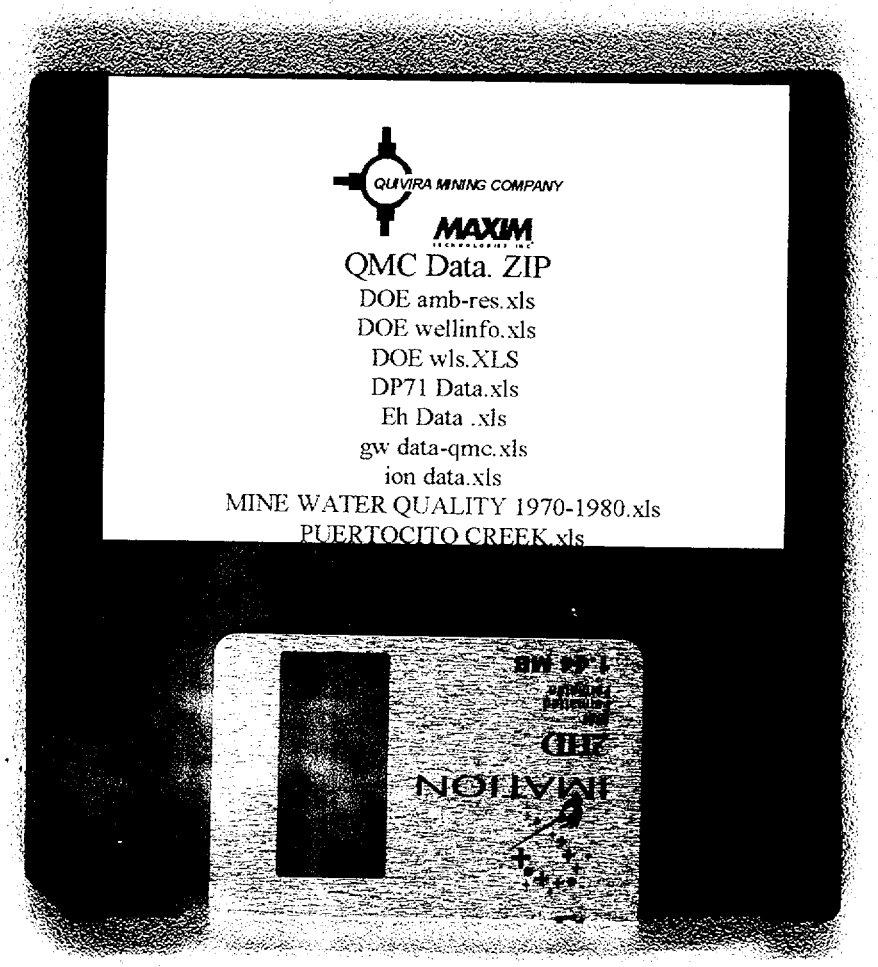
QUIVIRA MINING COMPANY
MAXIM
QMC Data. ZIP
DOE amb-res.xls
DOE wellinfo.xls
DOE wls.XLS
DP71 Data.xls
Eh Data .xls
gw data-qmc.xls
ion data.xls
MINE WATER QUALITY 1970-1980.xls
PUERTOCITO CREEK.xls